[redacted]

CENTRAL RESEARCH LIBRARY
DOCUMENT COLLECTION

ORNL-1506
Progress
4a

MARTIN MARIETTA ENERGY SYSTEMS LIBRARIES
3 4456 0353314 8

DECLASSIFIED
CLASSIFICATION CHANGED TO:
BY AUTHORITY OF: AEC - 7-12-60
BY: A. Bowman 8/24/60

SOLID STATE DIVISION

QUARTERLY PROGRESS REPORT

FOR PERIOD ENDING FEBRUARY 10, 1953

LABORATORY RECORDS
1954

AEC RESEARCH AND DEVELOPMENT REPORT

OAK RIDGE NATIONAL LABORATORY
CENTRAL RESEARCH LIBRARY
CIRCULATION SECTION
4500N ROOM 175
LIBRARY LOAN COPY
DO NOT TRANSFER TO ANOTHER PERSON
If you wish someone else to see this report, send in name with report and the library will arrange a loan.
UCN-7969 (3 9-77)

OAK RIDGE NATIONAL LABORATORY
OPERATED BY
CARBIDE AND CARBON CHEMICALS COMPANY
A DIVISION OF UNION CARBIDE AND CARBON CORPORATION
UCC
POST OFFICE BOX P
OAK RIDGE, TENNESSEE

[redacted]

This document contains Restricted Data as defined in the Atomic Energy Act of 1946. Its transmittal or the disclosure of its contents in any manner to an unauthorized person is prohibited.

[redacted]

[redacted]

ORNL-1506
This document consists of 78 pages
Copy 4 of 154 copies Series A

Contract No W-7405-eng-4

SOLID STATE DIVISION

QUARTERLY PROGRESS REPORT

For Period Ending February 10, 1953

D. S. Billington, Director

EDITED BY

J. T. Howe

DATE ISSUED

MAY 27 1953

OAK RIDGE NATIONAL LABORATORY
Operated by
CARBIDE AND CARBON CHEMICALS COMPANY
A Division of Union Carbide and Carbon Corporation
Post Office Box P
Oak Ridge, Tennessee

[redacted]

MARTIN MARIETTA ENERGY SYSTEMS LIBRARIES

3 4456 0353314 8

[redacted]

INTERNAL DISTRIBUTION

1. C. E. Center
2. Biology Library
3. Health Physics Library
4-5. Central Research Library
6. Reactor Experimental Engineering Library
7-12. Central Files
13. C. E. Larson
14. W. B. Humes (K-25)
15. L. B. Emlet (Y-12)
16. A. M. Weinberg
17. E. H. Taylor
18. E. J. Murphy
19. E. D. Shipley
20. D. S. Billington
21. F. C. Vondergage
22. R. C. Briant
23. J. A. Swartout
24. S. C. Lind
25. F. L. Steahly
26. A. H. Snell
27. A. Hollaender
28. M. T. Kelley
29. G. H. Clewett
30. K. Z. Morgan
31. J. A. Felton
32. A. S. Householder
33. C. S. Harrill
34. C. E. Winters
35. D. W. Cardwell
36. E. M. King
37. C. P. Keim
38. L. K. Jetter
39. E. J. Boyle
40. W. D. Manly
41. C. D. Susano
42. B. S. Borie
43. R. J. Gray
44. J. H. Frye, Jr.
45. E. E. Stansbury
46. G. P. Smith
47. J. E. Cunningham
48. E. C. Miller
49. A. F. Cohen
50. J. O. Betterton, Jr.
51. R. B. Oliver
52. T. H. Blewitt
53. J. H. Crawford, Jr.
54. W. E. Brundage
55. O. Sisman
56. G. W. Keilholtz
57. J. T. Howe
58. R. H. Kernohan
59. S. E. Dismuke
60. J. C. Wilson
61. W. J. Sturm
62. M. T. Robinson
63. J. W. Cleland
64. K. Lark-Horovitz (consultant)
65. M. C. Wittels
66. R. A. Weeks
67. W. W. Parkinson
68. [illegible] D. Bopp
69. C. D. Baumann
70. J. [illegible] Trice
71. J. G. Morgan
72. G. E. Klein
73. R. G. Berggren
74. D. K. Holmes
75. D. K. Stevens
76. A. J. Miller
77. R. S. Livingston
78. R. J. Jones
79. D. D. Cowen

[redacted]

[redacted]

80. P. M. Reyling
81. G. C. Williams
82. D. Binder
83. M. J. Feldman
84. C. C. Webster
85. J. M. Warde
86. W. O. Harms
87. W. R. Willis
88. F. Seitz (consultant)
89. E. P. Wigner (consultant)
90. R. L. Sproull (consultant)

EXTERNAL DISTRIBUTION

91-98. Argonne National Laboratory
99-101. Atomic Energy Commission, Washington
102-105. Brookhaven National Laboratory
106-109. Carbide and Carbon Chemicals Company (Y-12 Plant)
110-112. Mills Atomic Power Laboratory
113-114. General Electric Company, Richland
115. Hanford Operations Office
116-119. Los Alamos Scientific Laboratory
120-121. New York Operations Office
122. Patent Branch, Washington
123-137. Technical Information Service, Oak Ridge
138-141. University of California Radiation Laboratory
142. Massachusetts Institute of Technology (Kaufmann)
143. Battelle Memorial Institute
144-146. North American Aviation, Inc.
147. Westinghouse Electric Corporation
148. Savannah River Operations Office, Wilmington
149-152. Idaho Operations Office (1 copy to Phillips Petroleum)
153-154. Wright Air Development Center (1 copy - Materials Laboratory, Attn. Helen Akerd, 1 copy - Directorate of Research, Attn. Helen Akerd)

[redacted]

[redacted]

Quarterly reports previously issued in this series are as follows

ORNL-1025	Period Ending January 31, 1951
ORNL-1095	Period Ending April 30, 1951
ORNL-1128	Period Ending July 31, 1951
ORNL-1214	Period Ending October 31, 1951
ORNL-1261	Period Ending January 31, 1952
ORNL-1301	Period Ending May 10, 1952
ORNL-1359	Period Ending August 10, 1952
ORNL-1429	Period Ending November 10, 1952

[redacted]

[redacted]

CONTENTS

PAGE

PART I. SECRET PROJECTS

SUMMARY 1

RADIATION METALLURGY 5
- Creep Under Irradiation 5
- MTR Tensile Creep Apparatus 7
- Thermocouples 8
- Extensometers 8
- Impact Tests on Irradiated Metals 9
- High-Temperature Strain Gages 9

NUCLEAR MEASUREMENTS 10
- Neutron-Spectra Measurements in the BSF 10
- Irradiation Facility for the MTR 11

ENGINEERING PROPERTIES 13
- ORNL Graphite Reactor Liquid-Metals Loop 13
- LITR Sodium Stress-Corrosion Loop 15
- Universal Plug for Hole HB-2 of the LITR 17

FUSED SALTS 19
- Liquid Fuels Irradiation in the MTR 19
- Liquid Fuel Tests in the LITR 22
- Physical Properties of Irradiated Salts 22
- Development of LITR Facility C-46 23
- Dynamic Corrosion Tests 23
- Thermodynamic Studies of Sulfate Systems 23

CRYSTAL PHYSICS 26
- ORNL 86-in. Cyclotron Studies 26
- Proton Irradiation of Titanium Impact Specimens 26
- Proton Irradiation of Aluminum 27
- Irradiation of Teflon Cable 27
- Neutron Irradiation of LiF Crystal 30

SPECIAL PROJECTS 30
- Irradiation of Miscellaneous Materials 30
- Annealing of Irradiated Graphite-UO_2 Materials 33

[redacted]

[redacted]

PART II. UNCLASSIFIED PROJECTS

SUMMARY 41

SOLID STATE REACTIONS 43
- Estimation of Effective Fast Flux in Hole 52N 43
- Mobility and Hole Concentration in Bombarded *P*-type Germanium 43
- Low-Temperature Irradiation of Copper-Beryllium Alloy 46
- Transistor Bombardment 46
- Rectifier Measurements 47
- Field Control for the ADL Magnet 49
- Magnetic Susceptibility of Germanium 52
- Radiation Effects in Ionic Crystals 54

ENGINEERING PROPERTIES 56
- Radiation Stability of Plastics and Elastomers 56

CRYSTAL PHYSICS 57
- Deformation of Copper Single Crystals at 300 and 78°K 57

SPECIAL PROJECTS 67
- Hall and Magnetoresistance Effects in Metals 67

[redacted]

[redacted]

PUBLICATIONS

Publications of the Solid State Division during the past quarter were

R. G. Cleland, *Preliminary Title List for Bibliography on Radiation Effects in Solid Materials*, ORNL-1433 (Nov. 14, 1952).

M. C. Wittels, "The Lattice Expansion of Quartz due to Fast Neutron Bombardment," *Phys. Rev* **89**, 656 (1953).

G. T. Murray and W. E. Taylor, *Effect of Neutron Irradiation on Supersaturated Solid Solution Beryllium in Copper*, ORNL-1323 (Jan. 29, 1953).

M. T. Robinson and G. E. Klein, "Unit Cell Constants of α-Copper Phthalocyanine," *J Am Chem Soc* **74**, 6294 (1952).

Publications that were in press at the close of the quarter were

C. D. Bopp, *Gamma Radiation Induced in Engineering Materials*, ORNL-1371.

R. M. Carroll, *A Simple Electromagnetic Flowmeter for Liquid Metals*, ORNL-1461.

[redacted]

Part I

SECRET PROJECTS

SOLID STATE DIVISION QUARTERLY PROGRESS REPORT

SUMMARY

RADIATION METALLURGY

Creep Under Irradiation Cantilever creep tests conducted in the LITR and ORNL graphite reactor on Inconel in air at 1500°F and 3000 and 4000 psi indicate that the creep is not great enough, under these conditions, to necessitate a change in design values of unirradiated material.

A correlation is believed to exist between irradiation hardening and the effects of irradiation on creep. It has been found that type 347 stainless steel hardens under irradiation at temperatures up to 1400°F, the creep rate below this temperature is reduced by irradiation, whereas irradiation increases creep rate in type 347 stainless steel at temperatures above 1400°F. The corresponding critical temperature for Inconel appears to be about 1550°F. Further tests will be made to confirm this postulation.

MTR Tensile-Creep Apparatus The Phillips Petroleum Co. has approved the design of the MTR tensile-creep apparatus and has requested that strength tests be run on the pressurized equipment and that temperature estimates be made on some of the structural parts. Final approval has not been received on the safety circuit as last submitted. Parts have been made for adapting the apparatus to the LITR.

Thermocouples A piece of glass-insulated thermocouple wire was irradiated at room temperature in a helium atmosphere to verify the previous suspicion that irradiation carbonizes the organic binder enough to allow leakage between the wires. Carbonization was found on visual inspection, but the activity has not yet decayed sufficiently to permit leakage to be measured.

Variations in the heating and cooling rates of the sodium chloride, thermocouple-calibration capsules cause apparent changes in the melting point. A motor-driven variac permits reproducibility within ±2°F.

Extensometers Microformer lead-out wires are now being insulated with Sauereisen cement, this has eliminated the failures that occurred when Glyptal was used. Sauereisen cement must be thoroughly cured, however, if it is to produce satisfactory insulation.

The figure-8 Bourdon tube, designed to eliminate zero shift, has failed to come up to expectations. The shift in the zero point is apparently caused by unequal coefficients of thermal expansion that are produced by differential plastic deformation that is introduced in making the part. This effect is markedly diminished by annealing.

Impact Tests on Irradiated Metals. Impact samples of types 304 and 347 stainless steel, Ti 75A, and iodide titanium were exposed to integrated neutron fluxes of 1.3×10^{17} to 9.5×10^{17} nvt. Temperatures during irradiation were 230°F for 36 hr and approximately 60°F (because of heater failure) for the remainder of the irradiation. Impact tests have not yet been run. A new furnace is being designed to operate at 250°F, and impact samples are being fabricated of high-purity iron.

High-Temperature Strain Gages The The search for a high-temperature strain gage that can be used satisfactorily under irradiation has not, as yet, met with success. All the sample wires irradiated to date have shown resistance increases and indications of temperature coefficient-of-resistance changes produced by radiation.

NUCLEAR MEASUREMENTS

Neutron-Spectra Measurements in the BSF Neutron-spectra measurements

were made in the BSF. Both a proton-recoil and nuclear-threshold methods were used so that a comparison of the two methods could be obtained. Threshold-detector methods are not yet capable of high enough resolution to show up the spectral structure, as is possible by proton recoil methods.

Irradiation Facility for the MTR The plug-type irradiation facility for the MTR will allow pneumatic insertion and withdrawal of 18 sample-carrying rabbits. After withdrawal, the irradiated samples can be quickly transferred to nonradioactive containers for immediate counting.

A probe-type fission chamber of only 3/4-in. OD has been designed and fabricated. At first, the chamber will utilize natural uranium, but later, other fissionable materials will be used to obtain various threshold-energy characteristics.

ENGINEERING PROPERTIES

ORNL Graphite Reactor Liquid-Metals Loop. After bench testing the sodium-Inconel loop for about a week, a leak developed in the joint at which the inlet and outlet tubes were welded together and was apparently caused by differential expansion of the two tubes. The internal tubes were replaced with new tubes that were spiraled to provide for thermal expansion, the apparatus was bench tested 84 hr and then inserted in the reactor. The loop contained two sets of samples of Inconel, and types 316, 310, and 347 stainless steels, one set was located in the high-temperature, irradiated zone and the other set was placed in the cooler, out-of-pile portion of the loop. In-pile operation was maintained at 820°C for 218 hr, after which the heaters failed. The loop will be withdrawn for heater replacement and will be reinserted for further operation.

LITR Sodium Stress-Corrosion Loop. The Inconel-sodium loop was operated for 110 hr at 1070°F, then for 49 hr at 1270°F, a tensile specimen, located at the end in the reactor, was maintained under a stress of 1500 psi during the entire operation. Samples were taken from the jacket at regular intervals so that activity measurements could be made to determine relative flux values. The elongation of the tensile specimen will be measured in the hot cells.

The sodium in the out-of-pile portion of the loop contained a very small amount of activity that had half-lives of about 10 days and several months. The activity of out-of-pile tubing is only slightly above background, this indicates that very little radioactive corrosion products were deposited on the walls of the tubing or penetrated into them.

Universal Plug for Hole HB-2 of the LITR. A plug that will be usable for most experiments in hole HB-2 of the LITR has been designed, and fabrication is about 90% complete. The plug consists of sections (8-in. long) axially mounted on a rod. Two spiral grooves are cut on the outside of the assembled plug to permit easy access to experiments. The entire plug is placed in a stainless steel jacket so that experiments may be conducted in any desired atmosphere.

FUSED SALTS

Liquid Fuels Irradiation in the MTR. Thermal-flux measurements were made in position A-38 of the MTR, cobalt foil was used instead of the cobalt wire previously employed. The short-lived activities that result from impurities in the wire were almost entirely eliminated.

A fission analysis was made on a portion of the No. 30 salt in order to check the flux measurements. The fission analysis for 0.39 g of salt that had been irradiated for 145 megawatt-days was $4.61 \pm 0.18 \times 10^{18}$ fissions, the value, computed from flux measurements, was $4.86 \pm 0.49 \times 10^{18}$ fissions.

Metallographic examination of an irradiated, salt-bearing, Inconel capsule showed intergranular corrosion that averaged about 2 mils with subsurface voids 2 to 4 mils deep. At one section of the capsule, corrosion penetration 10 to 12 mils deep and large grain size were observed. A study will be made to determine whether large grain size is caused by excessive temperature rather than by radiation.

An increase in the uranium content above 6.5 mole % of a salt similar to No. 30 was found to cause segregation of the UF_4. Exploration has been initiated of the NaF-rich region of the UF_4-ZrF_4-NaF system adjacent to the pseudo-binary system in order to establish composition limits for the system such that UF_4 will not separate as the primary phase upon cooling.

Liquid Fuel Tests in the LITR A series of Inconel capsules containing 0.7 g of No. 30 salt was irradiated in the LITR at a thermal flux of 2.3×10^{13} neutrons/cm^2·sec. Studies of the capsules and of the composition of the salt will be made.

Additional irradiations that parallel MTR conditions are being conducted in the LITR to permit a comparison of the damage produced by lower fluxes and lower fission heat with the damage produced in the MTR.

Physical Properties of Irradiated Salts Melting points were determined for ANP salts irradiated in the MTR and the LITR and comparisons were made with nonirradiated control samples. No definite conclusion can yet be drawn as to what effect radiation has on the melting points of the fuels under study. The program will be continued in the LITR because it is possible to irradiate larger capsules that have thermocouple wells, whereas the MTR capsules are too small to permit a well and the thermocouples must be attached to the outside.

Development of LITR Facility C-46 A new irradiation facility has been completed in position C-46 of the LITR. Furnace controls and recording instruments are located in Building 3006.

Dynamic Corrosion Tests. The dynamic-corrosion, rocking-capsule apparatus was bench tested with natural uranium salt at a hot-zone temperature of 1500°F and a cold-zone temperature of 1150°F. After 15,400 cycles, the bellows failed, it was replaced with an angular-displacement mechanism that is now ready for operation.

Thermodynamic Studies of Sulfate Systems. Salt systems such as sulfates, phosphates, fluorophosphates, silicates, and borates may be potential reactor fuels or coolants. Except for the sulfates, thermodynamic data are limited. Free energies of reaction at 1000°K (727°C) were computed for several possible sulfate reactions, and one reaction was examined experimentally. The studies indicate that the sulfates cannot be used in reactor fuels containing UF_4.

CRYSTAL PHYSICS

ORNL 86-in. Cyclotron Studies. Bombardment and analyses of ANP eutectics in the 86-in. cyclotron have been completed. Detailed discussion and conclusions will be presented in a forthcoming report.[1] The capsules were heated by the cyclotron beam, and water was used in most of the experiments to prevent overheating and to maintain the capsule at a constant temperature. Calculations indicated that a greater amount of heat could have been removed if a refrigerated stream of helium gas had been used, but attempts to operate gas-cooled targets were unsuccessful.

Proton Irradiation of Titanium Impact Specimens. Titanium impact specimens of the substandard Izod type were bombarded with 20-Mev protons for 200 to 1000 amp-hr and will be compared with unirradiated and reactor-irradiated specimens. An added variable

[1] W J Sturm *et al*, *The Stability of Several Inconel-UF4 Eutectic Fuel Systems under Proton Bombardment*, ORNL-1530 (to be published)

will be the relative angle between the incident-proton direction during the bombardment and the direction of the impact-machine striker. After fracture, the specimens will be subjected to vacuum-fusion analysis to determine the residual hydrogen content.

Proton Irradiation of Aluminum Experiments were conducted to determine whether hydrogen could be introduced into aluminum by proton bombardment at temperatures below 450°C and whether the hydrogen so introduced would be retained by the metal. Hardness measurements indicated that the bombarded area had increased approximately 12 Tukon DPH numbers, this increase could have been caused by knock-on atoms produced by the protons, or it could have been caused by retention of the protons as trapped atoms, a mechanism similar to hydrogen-embrittlement in other metals.

Metallurgical examination revealed that a striated precipitate or that locally melted spots were formed in the region of the intense knock-ons, also, the grain boundaries had widened in this band. It was noted that the precipitate formed in a direction parallel to that in which the sheet was rolled.

Vacuum-fusion analysis revealed that more than 50% of the bombarding hydrogen was retained in the aluminum. Further studies will be made to distinguish between hydrogen-embrittlement and work-hardening and to determine the nature of the precipitate.

Irradiation of Teflon Cable Three tests were made of the effects of radiation on the quarter-wave frequency of Teflon, high-voltage, coaxial cable. The first test was the exposure of a coiled quarter-wave line to the gamma-ray source in the water canal of the Physics of Solids Building. The signal was brought to the instruments by an additional half-wave line. The second test was the same as the first except that exposure occurred in hole 1867 of the ORNL graphite reactor and instrumentation was somewhat improved. A third test was made in hole 1867, in this test the half-wave line previously used to lead from the radiation source was eliminated, and a short length of the quarter-wave line itself lead to the instruments. In all instances, there was a decrease in quarter-wave frequency (that is, an increase in dielectric constant) that was gradual and reached a saturation. A thermocouple will be added to the line, and experiments will be conducted to determine whether the changes noted are produced by radiation or temperature.

Neutron Irradiation of LiF Crystal Because of the high cross section for the (n,α) reaction in Li^6, neutron irradiation would be expected to produce defects in the LiF crystal more rapidly than in the other alkali halides. Irradiation of a LiF crystal in hole 12 of the ORNL graphite reactor for five days made the crystal too opaque for optical measurements. Density and lattice parameter measurements indicate a density decrease of 0.45 and 0.66%, respectively.

Simultaneous irradiation of KCl and LiF crystals produced a much deeper color in the LiF.

SPECIAL PROJECTS

Irradiation of Miscellaneous Materials The density change of diamonds is being investigated as a possible neutron monitor capable of rapid, qualitative measurements. Density change in diamonds as a function of vertical position in the LITR has been established, and the rate of change diminished rapidly when the integrated neutron flux reached a level of approximately 7×10^{19} nvt.

The total flux, as well as the fast flux, is important to the expansion properties of diamond.

X-ray diffraction studies of quartz that had been disordered by an exposure to 6.6×10^{19} nvt and then annealed at 900°C show a reordering of the structure insofar as normal lattice parameters are concerned. However, a residual disorder or strain exists in the crystal structure despite the high-temperature treatment. The density change of quartz exposed to 1.35×10^{20} nvt was found to be -12.4% by the hydrostatic method. X-ray and thermal studies are in progress.

Annealing of Irradiated Graphite-UO_2 Materials Studies of graphite-UO_2 bars, before and after irradiation, indicate that resistivity changes induced by neutron bombardment anneal out much more readily than changes caused by fission fragments. Fission-fragment damage to the graphite structure builds up much more rapidly than neutron damage and, according to present experimental evidence, reaches an equilibrium value.

RADIATION METALLURGY

CREEP UNDER IRRADIATION

W. W. Davis J. C. Wilson
J. C. Zukas

Several new tests have been completed in the LITR and the ORNL graphite reactor in which Inconel was subjected to stresses of 3000 and 4000 psi, at 1500°F, in air. The spread of the data and some variations in experimental conditions prevent quantitative estimates of the effect of neutron bombardment on creep, however, it can be stated safely that the effect is not large enough to cause material change in the design stress values for Inconel under these experimental conditions. The next work to be performed will be to assess the effect of the atmosphere in which the specimen is tested, since the atmosphere is known to be an important factor in the creep strength of Inconel.[1]

In Fig. 1, the data at 4000 psi show that there was less creep under irradiation than without irradiation. Both curves from the ORNL graphite reactor tests lie well below the bench test, the odd shape of curve *X*-1 is believed to have been caused by the loading weight resting against the microformer during the early part of the test. The difference between the two curves of the LITR-test may have been caused by the 24 hr of bombardment that the test shown by curve *L*-2 received before the furnace was turned on and the specimen was stressed.

The total strain in each of two, additional, 3000-psi, ORNL graphite reactor tests, and one LITR test, shown in Fig. 2, agrees within 15% (up to 400 hr) with the value in similar tests reported earlier.[2] On the basis of the single bench test with which all the in-pile curves are compared, it is not possible to state, until more data are available, whether more, or less, creep resulted from bombardment.

As the quarter ended, two tests were operating in the LITR in a helium atmosphere, and duplicate bench tests were about to start.

In order to determine the highest temperature at which neutron bombardment would cause an increase in hardness

(1) R B Oliver, D A Douglas, K W. Reber, J W Woods, and C W Weaver, *ANP Quar Prog Rep Dec 10, 1952*, ORNL-1439, Fig 12 1, p 160

(2) W W Davis, J C Wilson, and J C Zukas, *Solid State Quar Prog Rep Nov 10, 1952*, ORNL-1429, Fig 2, p 7

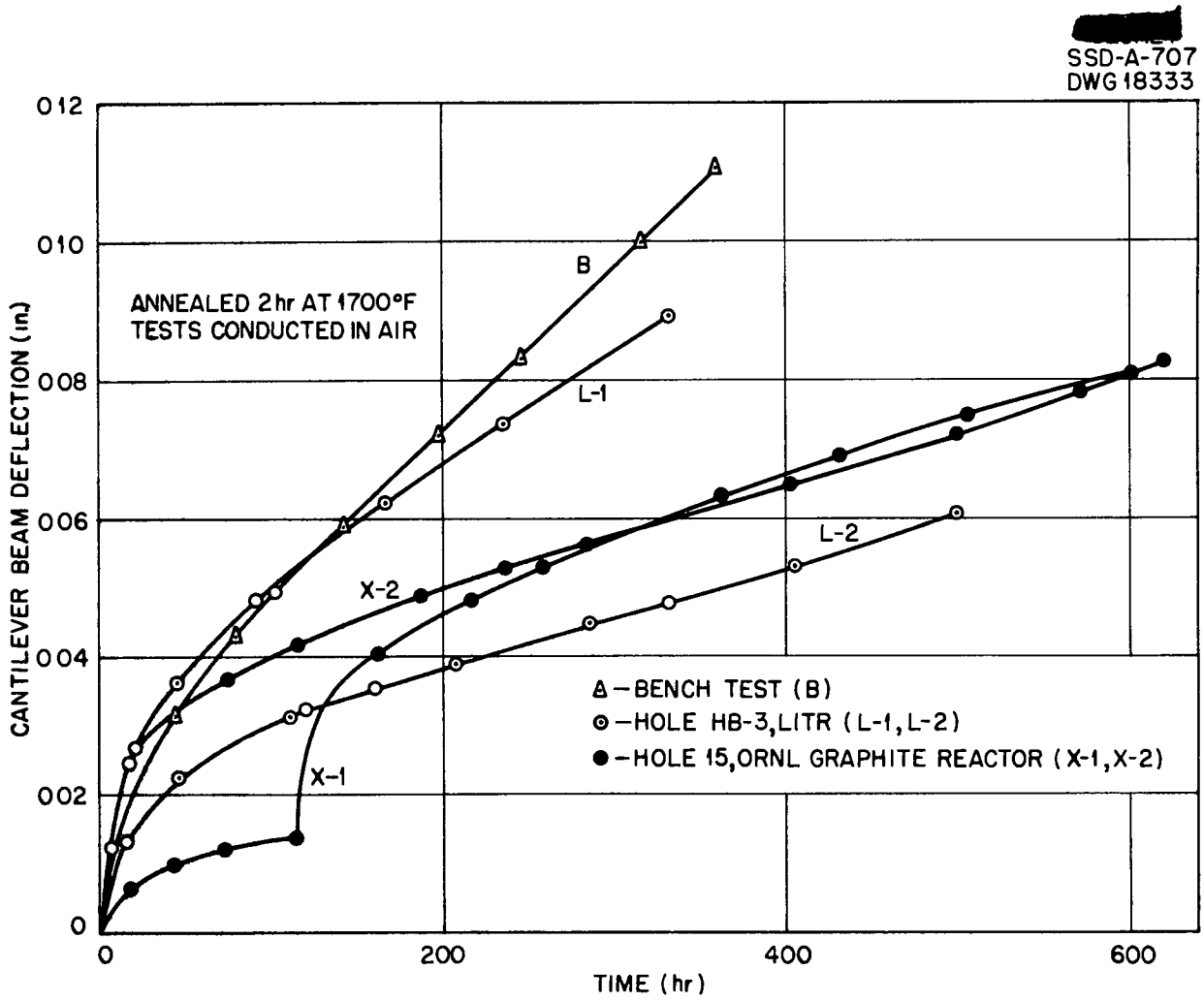

Fig. 1. Cantilever Creep Tests on Inconel at 1500°F and 4000 psi.

of the metals, annealed Inconel and type 347 stainless steel bars were exposed for one week in hole HB-3 of the LITR in a gradient furnace. The temperature gradient along the 4.5-in. specimens was from 1700 to 1150°F. Rockwell "B" hardness measurements were made after irradiation, and the results were compared with the initial hardness of the specimens and with the hardness of control bars that were subjected to the same time-temperature history. The Inconel was hardened slightly by bombardment at temperatures as high as 1550°F, and the stainless steel showed an increase in hardness only at temperatures below 1400°F. Earlier work on type 347 stainless steel[3] indicated that below 1400°F the creep rate of the material was reduced by neutron bombardment, whereas data at 1500°F[3] indicated that increased creep resulted during irradiation. A qualitative correspondence could be expected in the behavior of Inconel, and the hardness data may help to explain why no substantial effects of irradiation have yet been observed. Hardness

(3) J C Wilson, J C Zukas, and W W Davis, *Solid State Quar Prog Rep May 10, 1952*, ORNL-1301, Fig 2, p 6

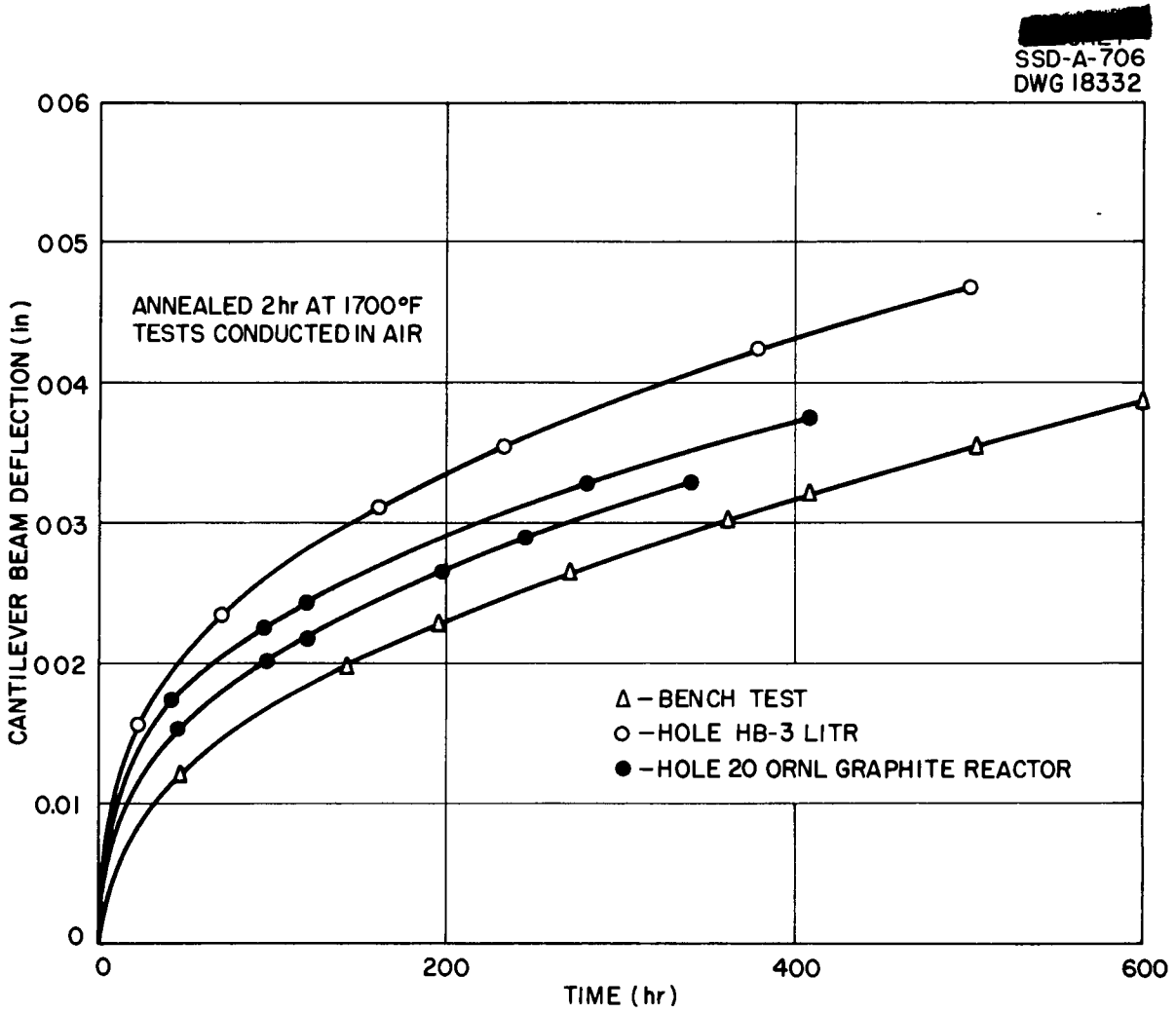

Fig. 2. Cantilever Creep Tests on Inconel at 1500°F and 3000 psi.

blocks placed alongside the creep specimens in future tests will enable more precise determination of irradiation hardening conditions at several temperatures, the steep gradients in the experiment reported here do not permit an accurate determination of temperature.

MTR TENSILE CREEP APPARATUS

N. E. Hinkle J. C. Wilson

After further study, the Phillips organization at Idaho Falls has found no objections to the present design of the MTR tensile creep apparatus, but has requested that strength tests be run on the pressurized experiment can and that temperature estimates be made on some of the structural parts. The safety circuit design has undergone several modifications, and the final approval for its construction is being awaited.

The bellows for loading the specimen has been tested to measure the effective area over the operating pressure range, and tests of the supporting means that were found necessary to prevent mechanical instability of the bellows at operating pressure have been made. Parts for

adapting the apparatus to the LITR have been designed and fabricated. All instrumentation has been received and installation has started.

Work on the specimen furnace (which is placed inside the tubular creep specimen) disclosed that mounting the thermocouples on the outer surface of the tube could cause a difference of nearly 100°F, at 1500°F, in the indicated temperature. A device that will check the true specimen surface temperature[4] has been constructed to aid in determining the best system of thermocouple mounting and to check the errors to be expected.

THERMOCOUPLES

W. W. Davis J. C. Wilson
J. C. Zukas

A piece of glass-insulated thermocouple wire was irradiated in a helium atmosphere at room temperature for one week in hole HB-3 of the LITR. The experiment was conducted to verify the suspicion[5] that neutron irradiation might cause sufficient carbonization of the organic binder in the insulation to lower the electrical leakage resistance between the wires and thus to cause the thermocouple to give erroneous readings. Postirradiation examination showed that the insulation was thoroughly impregnated with a black carbonaceous material. Measurements of the leakage resistance of the insulation and the thermal emf at 212°F will be made after the activity has decayed.

The sodium chloride-filled platinum capsule to be used for thermocouple calibration during in-pile experiments[5] is being checked daily to determine the reproducibility of the data to be expected from the apparatus. It has been found that an apparent change in the melting point may be caused by variations in the cooling rate. A motor-driven variac permits the cooling or heating rate of the furnace to be controlled. When the maximum temperature of heating and the rate of cooling were closely controlled, the reproducibility of the melting point during the first 200 hr of operation was ±2°F.

EXTENSOMETERS

R. A. Weeks J. C. Wilson

The microformers used in the latest creep experiments have had the lead-out wires from the coils insulated with Sauereisen cement. Glyptal had been used on a previous shipment, and a large number of failures occurred during in-pile experiments, however, no failures in the Sauereisen-insulated units have been experienced in nine in-pile tests. The insulation resistance between primary and secondary coils of the last group has been between 5 and 20 megohms during the experiments. In addition, the resistance of each microformer coil was measured to determine gross breakdown between turns of the Ceroc-insulated wire.

A plot of the insulation resistance between primary and secondary windings of two microformers vs. time of irradiation in a gamma source is shown in Fig. 3. Microformer No. 2303 has Sauereisen cement insulation on the lead-out wires from the coils, microformer No. 1960 is from the other group in which Glyptal is used instead of the cement. It should be noted that No. 2303 shows the greatest variation of resistance, and it has been suggested that the variation may result from improper (or lack of) curing of the cement. Additional support for this hypothesis may be found by comparing the insulation resistance at the start and end of the test, the two values were 35 and 480 megohms, respectively.

(4) N. Sasaki, *Rev Sci Instr* **21**, 1 (1950)

(5) W W Davis, R A. Weeks, J C Wilson, and J C. Zukas, *Solid State Quar Prog Rep Aug. 10, 1952*, ORNL-1359, p 7, 8

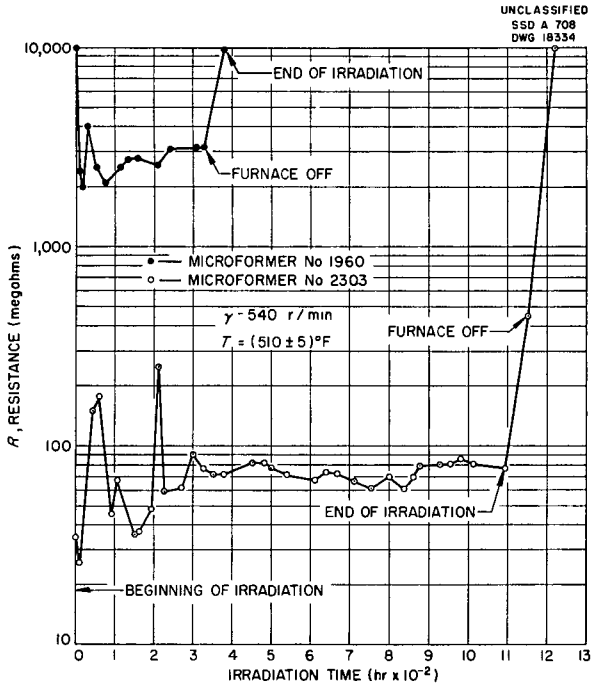

Fig. 3. Microformer Primary-to-Secondary Insulation Resistance vs. Time in Gamma Source.

Although the gamma-irradiation test indicates that microformers of the No. 1960 type have a higher insulation resistance than the No. 2303 type, in-pile experiments thus far show the No. 2303 type to be superior.

The geometry of the figure-8 Bourdon tube extensometer[6] was chosen in order to eliminate the zero shift with temperature, however, tests between 75 and 390°F showed that the zero moved 6.1×10^{-6} in./°F. It was suspected that the residual stress pattern, compressive on the inner fibers and tensile on the outer fibers of the tube, might be responsible. A 1-hr, stress-relieving anneal was found to reduce the zero shift to less than 0.7×10^{-6} in./°F. Two papers[7,8] were subsequently found that describe the effect of plastic deformation on the coefficient of thermal expansion. It is believed that unequal coefficients of expansion, caused by forming, on the tensile and compressive sides of the tube caused it to act as a bimetal and resulted in a zero-shift. A full-circle Bourdon tube has been calibrated for exposure in the LITR and subsequent postirradiation examination.

(6) J C Wilson and R A Weeks, *Solid State Quar Prog Rep Nov 10, 1952*, ORNL-1429, p 8

(7) J L Rosenholz and D T Smith, *Metal Progr* **61**, 85 (1952)

(8) J L Rosenholz and D T Smith, *J Appl Phys* **21**, 396 (1950)

IMPACT TESTS ON IRRADIATED METALS

R. G. Berggren N. E. Hinkle

Samples for impact tests of types 304 and 347 stainless steel, Ti 75A, and iodide titanium were exposed for three weeks in hole HB-4 (horizontal beam hole) of the LITR. The samples were exposed to an integrated neutron flux (greater than 0 5 Mev) equal to 1.3×10^{17} nvt at the low-flux part of the apparatus and up to 9.5×10^{17} nvt at the high-flux part of the apparatus. Impact tests of these samples will be made when modification of the impact testing machine is completed. The irradiation was conducted in a furnace at a temperature of 230°C, however, the heaters failed at 36 hr, and the irradiation was completed at a temperature of approximately 60°C. A new furnace has been designed and is being built to maintain a temperature of 250°C for use in hole HB-4 of the LITR. The design temperature was chosen because data obtained will be more readily applied to design problems in the HRP where temperatures will be in the region of 250°C. Impact samples of high-purity iron are being prepared for neutron irradiation in the furnace.

HIGH-TEMPERATURE STRAIN GAGES

R. G. Berggren J. C. Wilson

A continuing program to develop a high-temperature strain gage suitable for use under reactor irradiation is presently directed toward finding a

resistance wire that will have a small and/or predictable change of resistance under reactor irradiation.

Because of the large change in resistance of samples of Evanohm wire irradiated previously,[9] samples of seven resistance wires (0.001-in. dia) were exposed for 36 hr in hole HB-4 of the LITR to an integrated fast neutron flux (greater than 0.5 Mev). Although it was not possible to obtain values for the temperature coefficient of resistance under irradiation because of poor temperature control, there were indications, in most of the materials tested, that the coefficient was affected by irradiation. Sufficient data were obtained to indicate that the observation in the previous experiment[9] was not unique for the Evanohm wire. Table 1 lists the seven wire materials irradiated and the observed resistance change at 220°C. The initial resistance measurement at 220°C was made 3 hr after the start of irradiation.

[9] R. G. Berggren and J. C. Wilson, *Solid State Quar. Prog. Rep. Nov. 10, 1952*, ORNL-1429, p. 10.

TABLE 1. RESISTANCE INCREASE UNDER FAST-NEUTRON IRRADIATION

MATERIAL	CHANGE (%)
Evanohm No. 1	1.2
Evanohm No. 2	0.6
Karma, annealed	0.9
Karma, unannealed	1.4
Karma, special	2.5
Nichrome	1.2
Cupron	1.0

NUCLEAR MEASUREMENTS

NEUTRON-SPECTRA MEASUREMENTS IN THE BSF

J. B. Trice F. W. Smith[1]
F. J. Muckenthaler[2]

A series of measurements was made in the BSF in order to compare results from nuclear-threshold measurements with results from proton-recoil measurements. At present, it can be stated that both measurements, made adjacent to the reactor, show the general shape of a fission spectrum over the energy region where comparison is possible (>1.3 Mev). It is also possible to state that the absolute magnitudes found from the two methods are comparable. Spectral structure, which appears in the proton-recoil measurements, cannot be found with the threshold detector measurements because, at the present time, the threshold-detector method is not capable of very high resolution. More detailed comparison between the two methods may be possible in the future when data from the proton-recoil counter have been sufficiently examined.[3]

The reactor-fuel loading for the present series of measurements is shown in Fig. 4. An attempt was made to minimize local fluctuations in neutron flux at the site of measurement by holding the nearest control rod (>6 in. from the measurement) in a nearly constant position. All measurements were made for a reactor operating power of 100 kw.

The results are shown graphically in Figs. 5 and 6, which give spectral data for the energy regions above 0.5 Mev and below 0.01 Mev, respectively. The measurements shown

[1] Consolidated Vultee Aircraft Corp.
[2] Physics Division

[3] R. G. Cochran, *Proton Recoil Counter Data* (to be published).

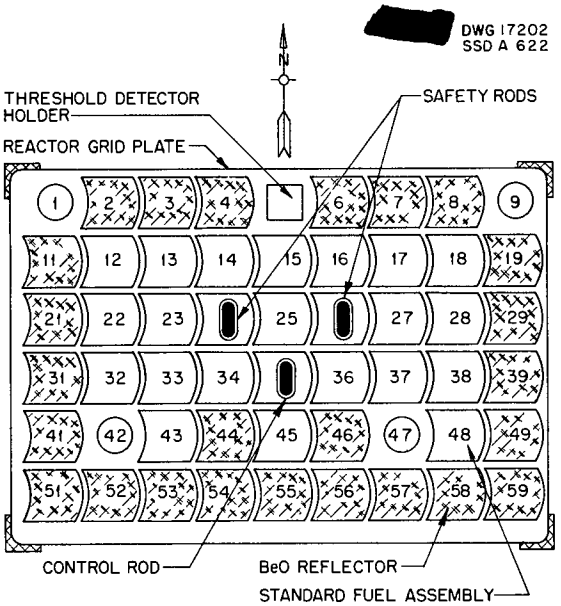

Fig. 4. Fuel Assembly Arrangement, Loading No. 17.

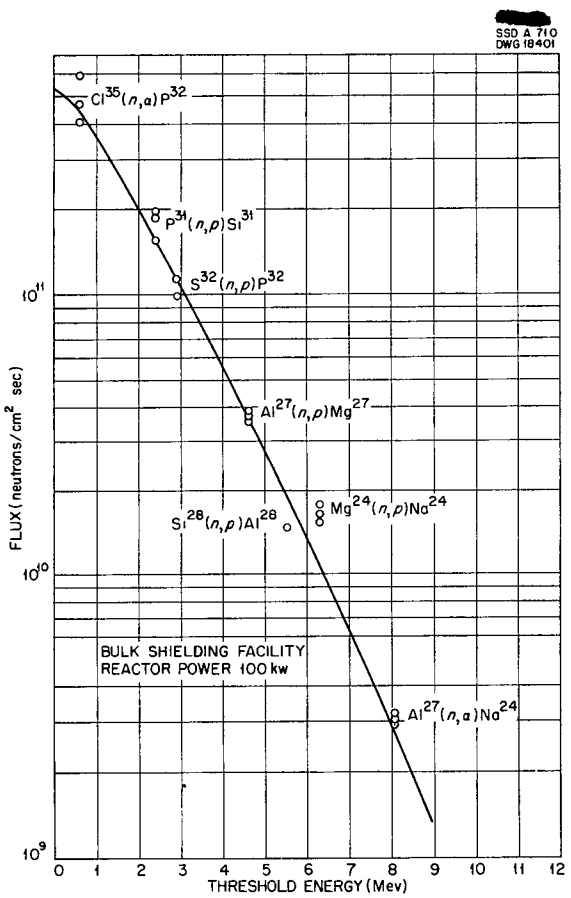

Fig. 5. Neutron Flux above Threshold Energy as a Function of Threshold Energy.

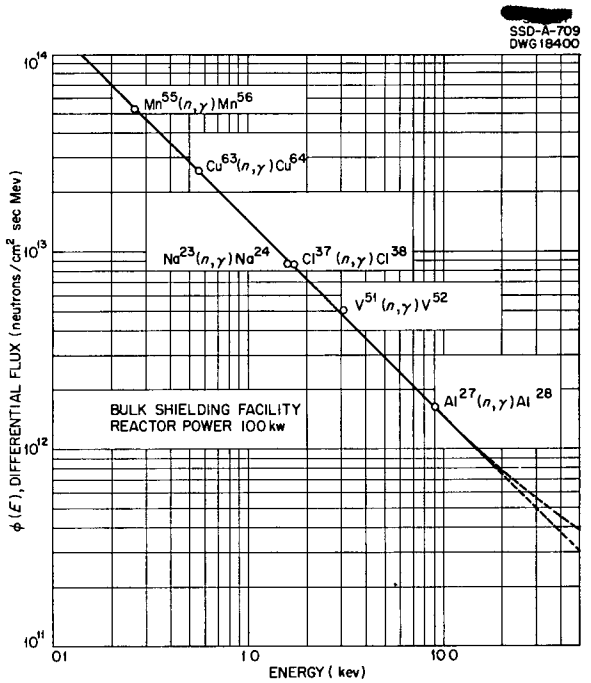

Fig. 6. Neutron Energy Spectrum for the Epithermal Energy Region (0.2 kev < E < 10 kev).

in Fig. 5 show the neutron flux above threshold energies as a function of threshold energies. The solid curve is taken from Watt's measurements[4] of the fission spectrum and is normalized to the present data at the threshold energy for the $Al^{27}(n,p)Mg^{27}$ reaction The data are also shown in Table 2, which gives an indication of the errors involved in the measurements.

Data for the low-energy region are shown in graphic and tabular form by Fig. 6 and Table 3. The data here, as in past measurements in moderating media, show a good agreement with $1/E$ spectral function.

IRRADIATION FACILITY FOR THE MTR

J. B. Trice F. W. Smith
F J. Muckenthaler

The design of a plug-type irradiation facility[5] that will permit

[4] B E Watt, *Energy Spectrum of Neutrons from Fissions Induced by Thermal Neutrons*, LA-718 (Dec 17, 1948)

[5] Design is being conducted under the direction of T L Trent of the Engineering Department

TABLE 2. NUCLEAR THRESHOLD DETECTORS USED IN A BSF TEST

NUCLEAR REACTION	THRESHOLD ENERGY (Mev)	NUMBER OF MEASUREMENTS	AVERAGE FLUX MEASURED (neutrons/cm^2·sec)	AVERAGE ERROR SPREAD* (%)
$S^{32}(n,p)P^{32}$	2.9	2	1.06×10^{11}	3
$P^{31}(n,p)Si^{31}$	2.4	3	1.79×10^{11}	9
$Cl^{35}(n,\alpha)P^{32}$	0.5**	3	4.9×10^{11}	13
$Al^{27}(n,p)Mg^{27}$	4.6	3	3.73×10^{10}	2
$Al^{27}(n,\alpha)Na^{24}$	8.1	3	3.10×10^{9}	2
$P^{31}(n,\alpha)Al^{28}$		3		6
$Si^{28}(n,p)Al^{28}$	5.5	1	1.48×10^{10}	

*Average error spread is defined by

$$\overline{\Delta\epsilon} = \frac{1}{n} \sum_{i=1}^{i=n} \left| \frac{\bar{x} - x_i}{\bar{x}} \right| ,$$

where $\bar{x}$ = average of all measurements, x_i = single measurement, n = number of measurements

**Value uncertain

TABLE 3. NUCLEAR RESONANCE DETECTORS USED IN A BSF TEST

NUCLEAR REACTION	APPROXIMATE RESONANCE ENERGY (ev)	CADMIUM RATIO*	ϕ_0, SPECTRAL FUNCTION (neutrons/cm^2·sec)	THERMAL FLUX** (neutrons/cm^2·sec)
$Mn^{55}(n,\gamma)Mn^{56}$	260	32 0	$1\ 39 \times 10^{10}$	$1\ 37 \times 10^{12}$
$Cu^{63}(n,\gamma)Cu^{64}$	562	36 0	$1\ 47 \times 10^{10}$	$4\ 09 \times 10^{11}$
$Na^{23}(n,\gamma)Na^{24}$	1710	54 7	$1\ 50 \times 10^{10}$	$1\ 68 \times 10^{12}$
$Cl^{37}(n,\gamma)Cl^{38}$	1800	56 0	$1\ 61 \times 10^{10}$	***
$V^{51}(n,\gamma)V^{52}$	3000	57 0	$1\ 57 \times 10^{10}$	$1\ 57 \times 10^{12}$
$Al^{27}(n,\gamma)Al^{28}$	9100	58 6	$1\ 49 \times 10^{10}$	$1\ 8 \times 10^{12}$

*Average for several tests

**Large differences in the measured values of thermal fluxes do not necessarily reflect errors into cadmium ratios, since such inaccuracies as those arising from cross-section data or decay schemes will not appear in a measurement of cadmium ratio

***In order to calculate the cadmium ratio for Cl^{38} it was necessary to use the thermal flux, as measured with Co^{60}, and to calculate the saturated activity of a sample of chlorine not enclosed in cadmium

rapid radiation measurements in some of the horizontal beam holes includes a pneumatic injection system for inserting and withdrawing 18 sample-carrying rabbits. A quick transfer of irradiated material from the rabbit to nonradioactive containers, suitable for immediate counting by high-pressure ionization chambers or scintillation counters, is effected by a remotely controlled mechanism in the shielded external (to the reactor shield) part of the plug facility.

A first model of the small, 3/4-in.-OD, probe-type, fission chamber[6] is complete and ready for initial testing. Natural uranium will be used at first. Later it is planned to use other fissionable materials such as Np^{237} and U^{238}, both of which are of interest because of their threshold energy characteristics. For MTR measurements with these chambers, it is planned to include as many fission-threshold detectors as possible.

[6] The special-purpose chambers have been designed and are being assembled by R E Zedler of the Instrument Department

ENGINEERING PROPERTIES

ORNL GRAPHITE REACTOR LIQUID-METALS LOOP

C. D. Baumann
F. M. Blacksher
W. E. Brundage
C. Ellis
M. T Morgan
A S Olson
O. Sisman

The sodium-Inconel loop for the ORNL graphite reactor[1] was completed and was bench tested for about a week. Near the end of the test, a leak was found at one of the points at which the inlet and outlet tubes were welded together. Previous runs had shown a pronounced bowing of the tubes that was caused by differential thermal expansion, the bowing apparently caused sufficient stress to tear the wall of one tube and cause the leak.

The internal section of the loop was cut off and replaced with a modified system. The in-pile end block, which had previously given trouble, was eliminated by forming a U bend of the tubing itself. At the section of the loop just inside the pile from the mounting flange, the tubes were spiraled around the heater tubes in order to provide for thermal expansion with a minimum of stress. The two tubes were held to the tubular heaters by a spiral winding of wire.

Two sets of corrosion specimens were inserted in the loop - one set in the in-pile end and one set in the out-of-pile portion of the loop. The specimens (Inconel, types 316, 310, and 347 stainless steel) were accurately weighed before they were inserted in the loop, and they will be cleaned and weighed again at the termination of the run.

The rebuilt loop was bench tested for 84 hours. After 80 hr, the circulation stopped in the filter. The filter circuit was then cut off and the loop was inserted in the reactor. The loop was operated for 218 hr at 820°C with a circulation rate of about 1 fps. One of the heaters on the in-pile section burned out after this period, and it was necessary to increase the power input to the second heater to the full rated wattage in order to maintain the temperature. After a few hours, the second heater burned out.

There was no apparent failure in the loop other than the heaters,

[1] C D Baumann *et al*, *Solid State Quar Prog Rep Nov 10, 1952*, ORNL-1429, p 12

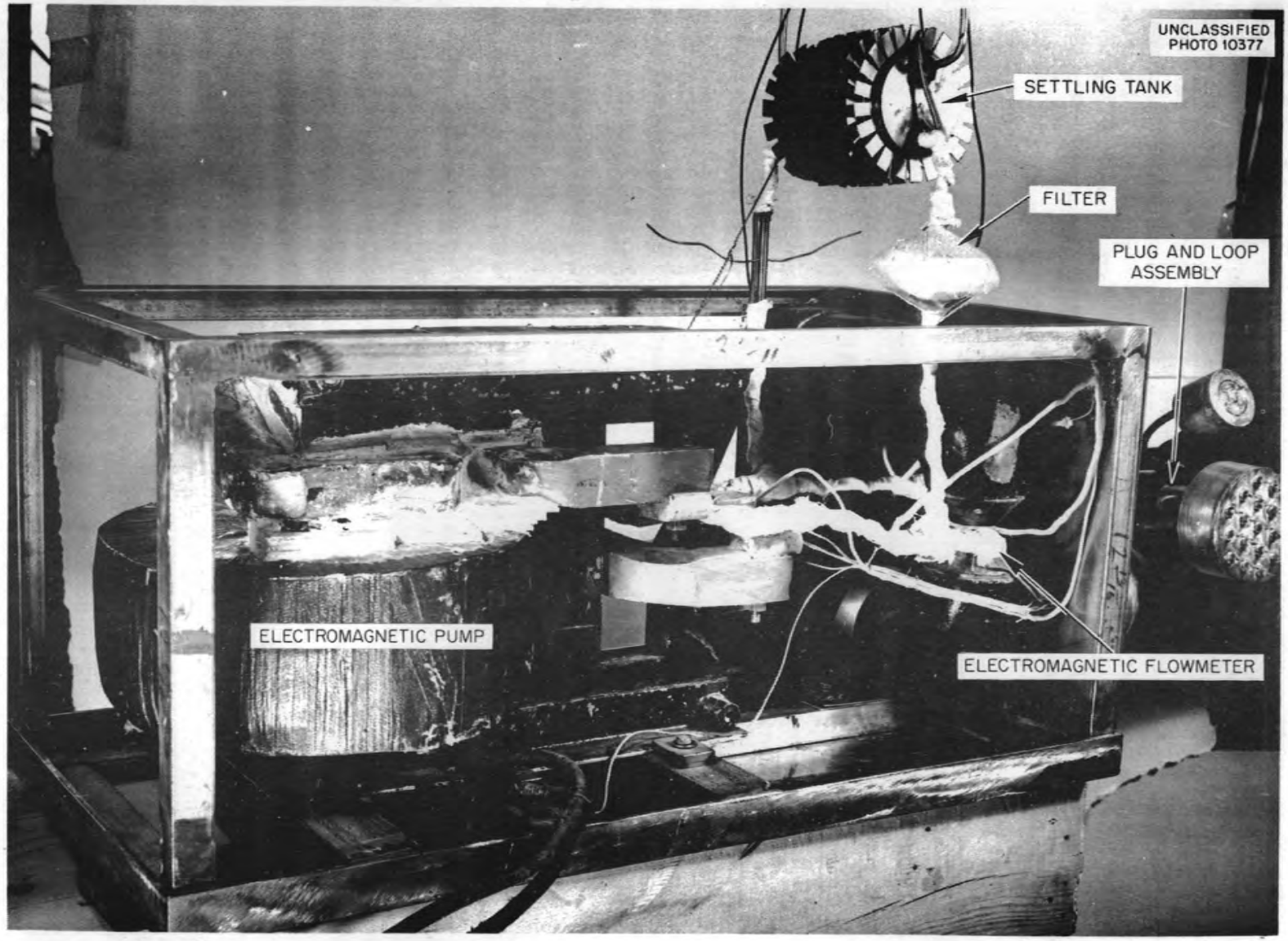

Fig. 7. External Portion of Inconel-Sodium Loop for LITR Tests.

therefore it is planned to remove the loop from the reactor, replace the heaters, and continue the run. The loop will be removed in a series of partial withdrawals to permit a decay of the short-time activity while it is in the concrete shield of the reactor. As it is pulled from the reactor, each portion will have the heaters and heat shielding removed so that the radiation level will be reduced. The first removal step has been performed and the loop was withdrawn about 8 feet.

LITR SODIUM STRESS-CORROSION LOOP

W. E. Brundage C. Ellis
F. M. Blacksher A. S. Olson
R. M. Carroll W. W. Parkinson
O. Sisman

The study of radiation effects in an Inconel-sodium loop has been extended to the higher fluxes of hole HB-2 of the LITR.[2] The external portion of the loop, along with the filter bypass loop, which was later removed, is shown inside the frame of the inert-gas housing in Fig. 7. During in-pile operation of the loop, the compartment was enclosed in a lead-brick shield. Figure 8 is a top view of the in-pile portion of the loop before it was enclosed in the vacuum jacket. In Fig. 9, the specimen section of the loop and the extensometer are shown in greater detail, with the heater removed.

The loop operated 110 hr at 1070°F; then the temperature was raised to 1270°F. After 49 hr of operation at 1270°F, circulation of sodium stopped and operation of the loop was terminated. During operation, a load was applied to the tension bar to maintain the specimen (see Fig. 9) under a stress of 1500 psi.

The activity of the sodium in the external parts of the loop was allowed to decay and, after removal of the lead shield, the external section of the loop was separated from the tubes that run through the plug, and was removed. Both the inner plug that carries the loop and the outer plug and water jacket were then withdrawn into a portable lead shield. After two months of storage in the lead shield, the inner plug was withdrawn from the outer plug, and the stainless steel jacket and specimen section (which were then the only radioactive portions) were removed from the rest of the plug and transported to the hot cells for further disassembly and examination.

In order to carry out the disassembly, a small, power hacksaw was adapted for remote operation. Several cuts were made through the plug jackets to remove the surge tanks and the specimen end of the loop. In

(2) W. E. Brundage *et al.*, *Solid State Quar. Prog. Rep. Nov. 10, 1952*, ORNL-1429, p. 12.

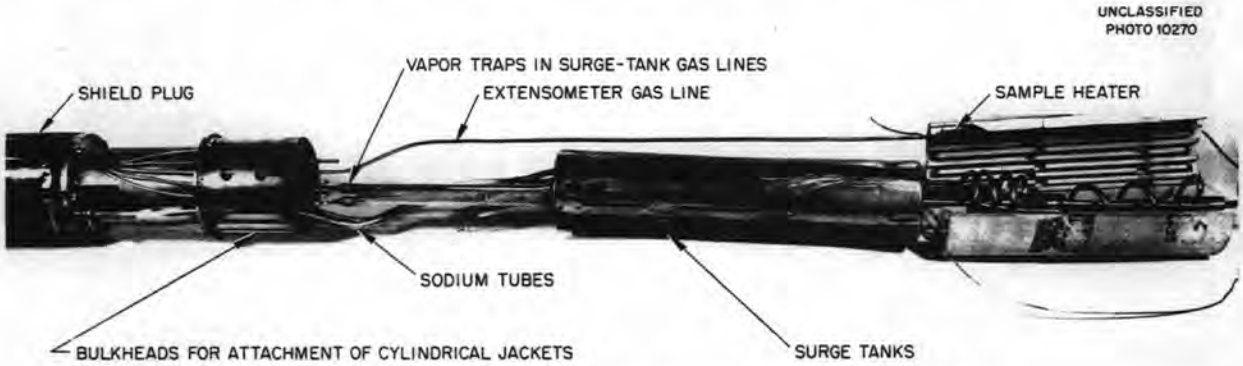

Fig. 8. In-Pile Portion of the Inconel-Sodium Loop.

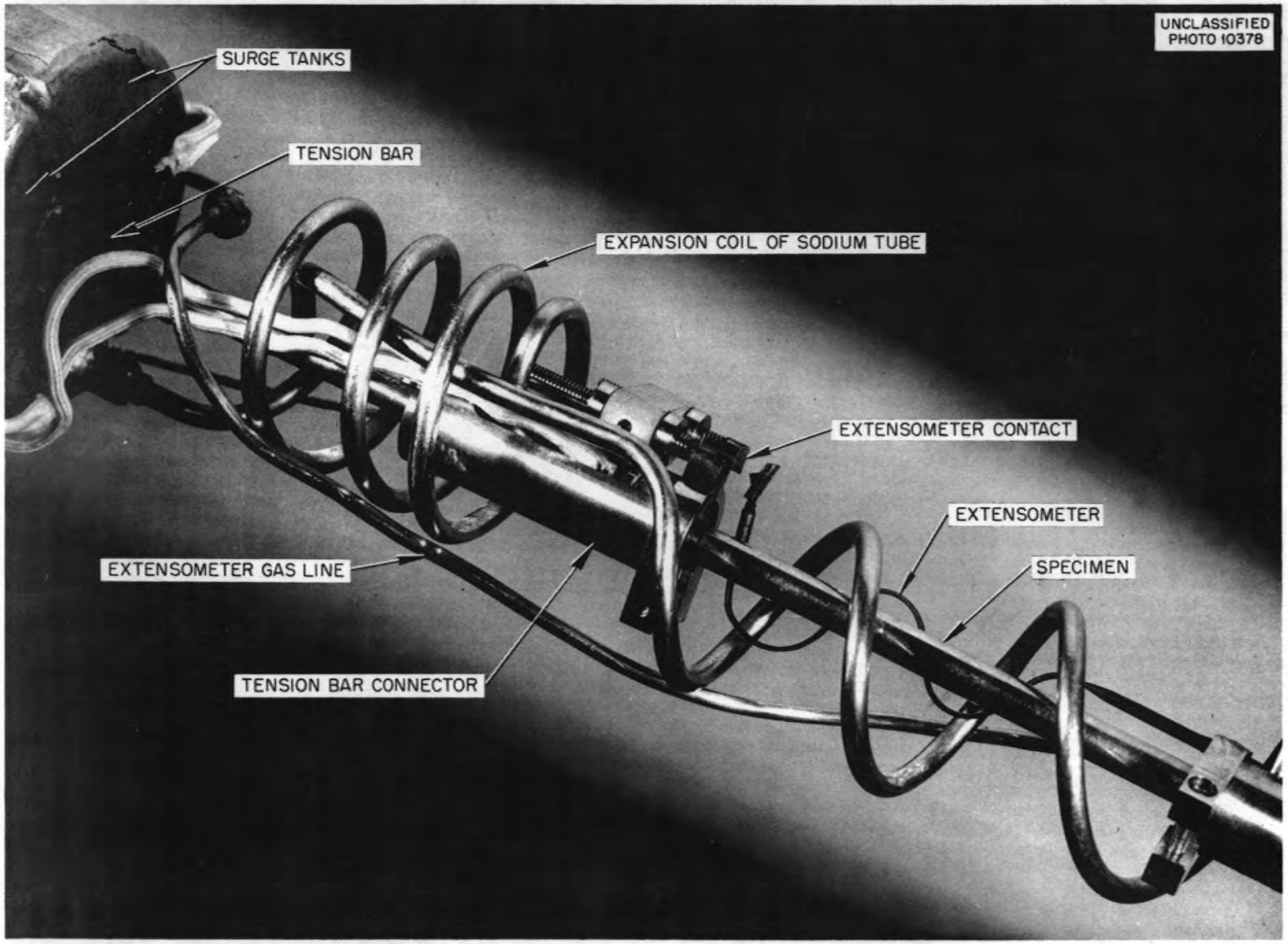

Fig. 9. Specimen Section and Extensometer of the Inconel-Sodium Loop.

addition, saw cuttings were obtained from regularly spaced intervals along the length of one of the jackets so that activity measurements could be made to determine relative flux values.

The portion of the loop that contained the creep-corrosion specimen and auxiliary tubing (see Fig. 9) was transferred from the large hot cell that was equipped with rectilinear manipulators to a smaller cell that was equipped with master-slave manipulators. The attached tubing and loading bars were removed from the specimen by means of the master-slave manipulators, and the specimen length will be measured to determine elongation during irradiation.

The appearance of the apparatus inside the plug jackets indicated that a sodium leak had occurred in the vicinity of the creep-corrosion specimen. The escaping sodium had disintegrated the ceramic heater form around the specimen and had reduced the liquid level in the surge tanks to such a point that gas entrainment and flow stoppage probably resulted.

The out-of-reactor portion of the loop was cut into sections, and the sodium was dissolved from several sections so that the long-lived activity of any possible corrosion products could be measured. A very small amount of activity that had half-lives of about 10 days and several months was found. To determine the extent to which radioactive corrosion products had been deposited on the walls of the tubing or had penetrated into them, successive 0.0003-in. cuts were taken from the inside of the tubing sections from which the sodium had been removed. The activity of the surface cuts appeared to be only slightly above background. Further measurements are being made on the deposits.

UNIVERSAL PLUG FOR HOLE HB-2 OF THE LITR

W. E. Brundage A. S. Olson
O. Sisman

Design has been completed on a sectional plug (Fig. 10) for use in the water-cooled outer jacket of the LITR stress-corrosion experiment. The plug is being made in sections 8 in. long and will be assembled on an axial rod. Each section has two grooves cut along a spiral on the surface. The plug design will permit easy modification and will be useful for many of the various experiments proposed for hole HB-2. Sections that become radioactive can be discarded and replaced with a minimum of expense, and the use of open-top grooves rather than the spiral tubing used in previous designs will facilitate the assembly of an experiment. To produce a seal for an inert atmosphere, a stainless steel jacket will be provided for the plug. Fabrication of the plug is now about 90% complete.

UNCLASSIFIED
DWG. 19299

ASSEMBLED SHIELD PLUG AND STAINLESS STEEL LINER

TOTAL LENGTH OF PLUG: 12 ft 8 in.
LENGTH OF LINER: 12 ft 11 3/8 in.
OUTSIDE DIAMETER OF LINER
LARGE SECTION: 5 3/4 in.
SMALL SECTION: 4 in.
INSIDE DIAMETER OF LINER
LARGE SECTION: 5 1/2 in.
SMALL SECTION: 3 7/8 in.

SECTIONS OF SHIELD PLUG

LARGE STEEL SECTION

LARGE GRAPHITE SECTIONS

5 3/8-in. DIA, 8 in. LONG

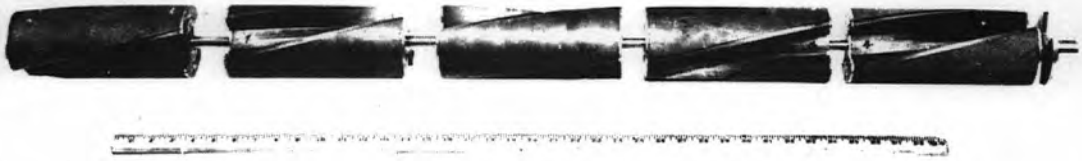

SMALL GRAPHITE SECTIONS
3 3/4-in. DIA, 8 3/4 in. LONG

Fig. 10. Universal Shield Plug for LITR Beam Hole.

FUSED SALTS

LIQUID FUELS IRRADIATION IN THE MTR

J. G. Morgan P. R. Klein
H. E. Robertson

Four, additional, thermal-flux measurements (Table 4) were made in facility A-38 of the MTR in which cobalt foil was used instead of the cobalt wire of the previous measurements. It appeared that the impurity content of the foil is considerably lower than that of the wire; in the foil, there was almost no short-lived activity such as that previously observed in the wire.

TABLE 4. THERMAL FLUX MEASUREMENTS IN THE MTR

FLUX TEST NO.	REACTOR POWER LEVEL	ϕ_{th} (× 10^{14})
3	0.5 N_f	1.34
4	0.834 N_f	2.33
5	N_f (beginning)	2.73
6	N_f (end)	2.89

There is an increase in the flux value of 5.86% near the end of a burnup cycle at N_f. The average control-rod travel is 30.8% in the same interval.

A fission analysis of a portion of the irradiated salt was conducted by the Analytical Chemistry Division to check the flux measurements. The cesium in a solution of the radioactive salt was precipitated with $HClO_4$ and C_2H_5OH; then the resulting precipitate of $CsClO_4$ was counted. The isotope, 33-y Cs^{137}, was counted in a counter that was calibrated in terms of uranium fissions. The experimental fission analysis for 0.39 g of No. 30 salt (4.0 mole % UF_4, 50.0 mole % NaF, 46.0 mole % ZrF_4), after 145 megawatt-days in the MTR, gave $4.61 \pm 0.18 \times 10^{18}$ fissions as compared with a calculated value of $4.86 \pm 0.49 \times 10^{18}$ fissions.

In order to secure a continuous record of the cooling air required during a run, an orifice, with a recorder, was installed in the cooling-air system on the north balcony of the MTR. A water baffle was installed around tube A-38 at the north water-inlet line to eliminate vibrations caused by the reactor-water flow.

The previously described capsule[1] had a corrected heat dissipation of 2700 watts/cm^2. Remote metallographic examination showed that there was, in general, a regular and dense intergranular corrosion, averaging about 2 mils, and subsurface voids 2 to 4 mils deep (see Fig. 11). Figure 12 shows the cross section of the bench-test capsule that had the same thermal history but was not exposed to radiation. Wall-thickness

[1] J. G. Morgan, A. E. Richt, H. E. Robertson, and P. R. Klein, *Solid State Quar. Prog. Rep. Nov. 10, 1952*, ORNL-1429, p. 15.

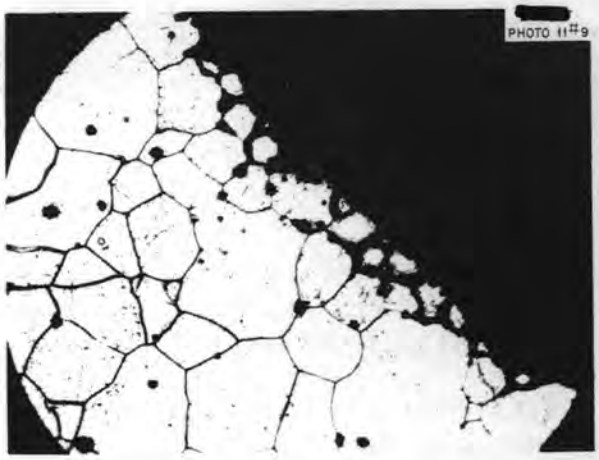

Fig. 11. Corrosion Interface of Capsule No. 201 after Bombardment in the MTR for 116 hr at 815°C.

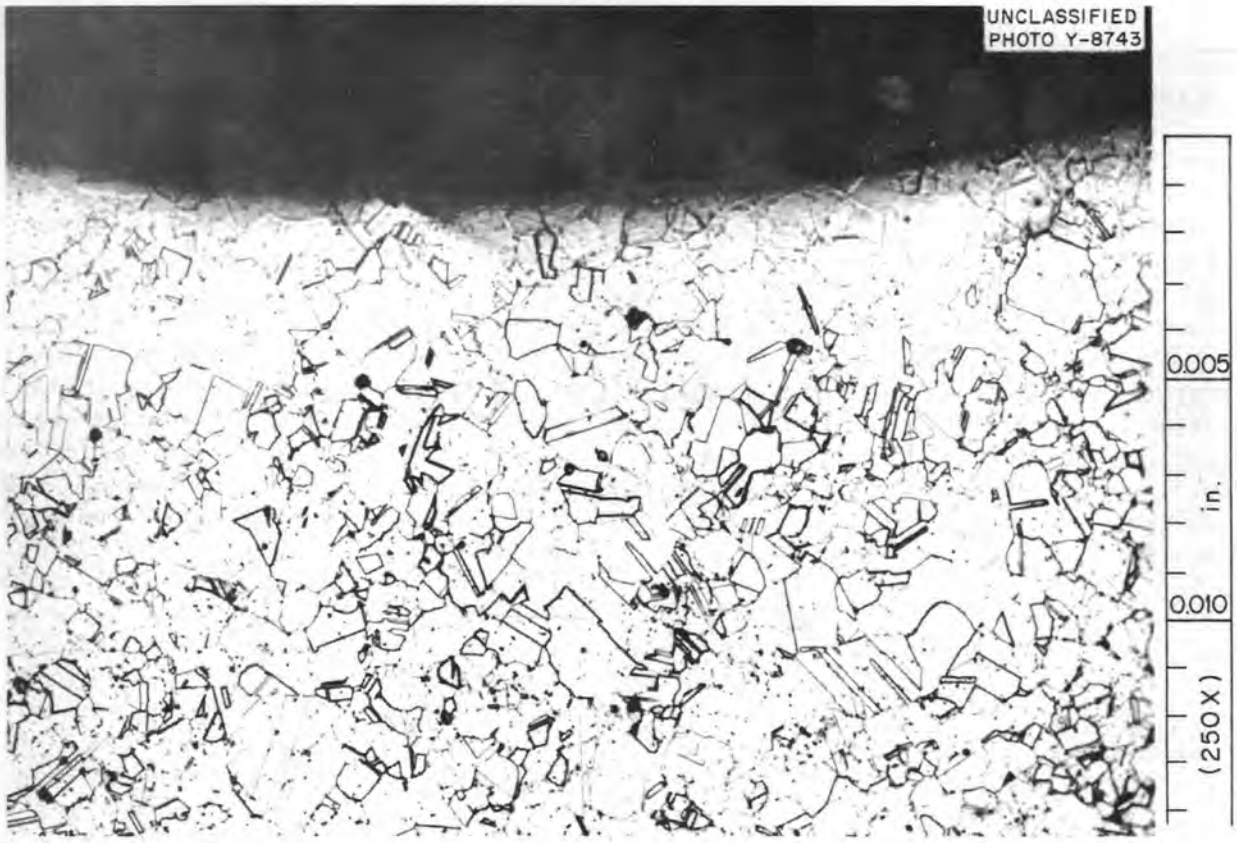

Fig. 12. Corrosion Interface of an Unirradiated Capsule after Undergoing the Same Thermal History as Capsule No. 201.

measurement showed no definite reduction in wall thickness; however, a corrosion penetration of 10 to 12 mils was observed at one section of the capsule. Because of the large grain size at this point, it is believed that excess temperature rather than radiation accounted for the corrosion. A grain-size study on Inconel, as a function of temperature, has been initiated in cooperation with the Metallurgy Division. The results will indicate whether grain size can be used as criterion for voiding data that show corrosion that is due to an excessively high-temperature region.

MTR capsule No. 204 that contained 0.39 g of No. 30 salt was charged in facility A-38 on November 17, 1952 and withdrawn on December 1, 1952 after 325 hr at 1500°F under full flux. Metallographic analysis showed an attack, which was similar to that of the previous capsule (No. 201), that consisted of intergranular penetration of 2 mils and subsurface voids to a depth of 3 mils; such attack is shown in Fig. 13. The activity of capsule No. 204 was measured 768 hr after it was removed from the active lattice of the MTR. By using a 60-r/hr probe, readings were obtained at distances of from 5 in. to 3 ft from the source. The $1/r^2$ law of activity vs. distance resulted from a plot of the measurements, and the experimental and theoretical results of capsule activity agreed within 14%. It was found that a delay time of

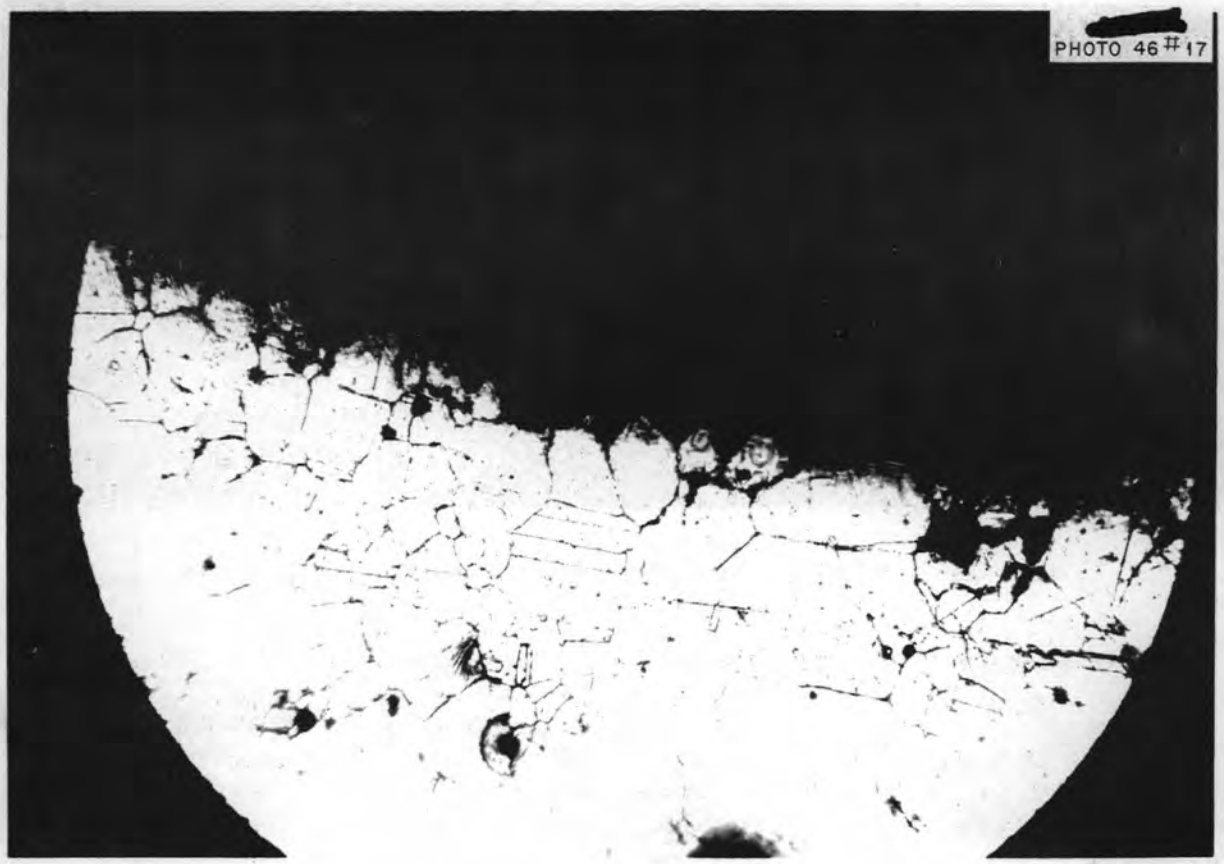

Fig. 13. Corrosion Interface of Capsule No. 204 after Bombardment in the MTR for 325 hr at 815°C.

23 hr reduced the capsule source from 106 curies to 43 curies and correspondingly reduced the shielding requirements for shipping.

Figure 14 shows the capsule assembly and breakdown used in the salt irradiations. Parts *C*, *D*, and *E* are heliarc-welded together to form a gas-tight capsule that contains the salt column. Thermocouples are spot welded on the outside surface to monitor and to control the salt temperature, and guide fins, *A*, position the capsule vertically in the cooling annulus. In order to irradiate a salt similar to No. 30 at a higher wattage dissipation, it is necessary to increase the uranium content. However, in the $NaUF_5$ - $NaZrF_5$ pseudobinary system, it was found that the compositions above 6.5 mole% UF_4 segregated to give uranium-rich regions. Investigation by chemical analysis, x-ray diffraction analysis, and petrographic examination showed segregation of UF_4 in the bottom portion of the salt-test capsules. The segregation at higher uranium concentrations would involve a cooling problem. Exploration of the NaF-rich region of the UF_4-ZrF_4-NaF system adjacent to the pseudobinary system has been initiated in order to establish composition limits such that the UF_4 would not separate, as the primary phase, upon cooling.

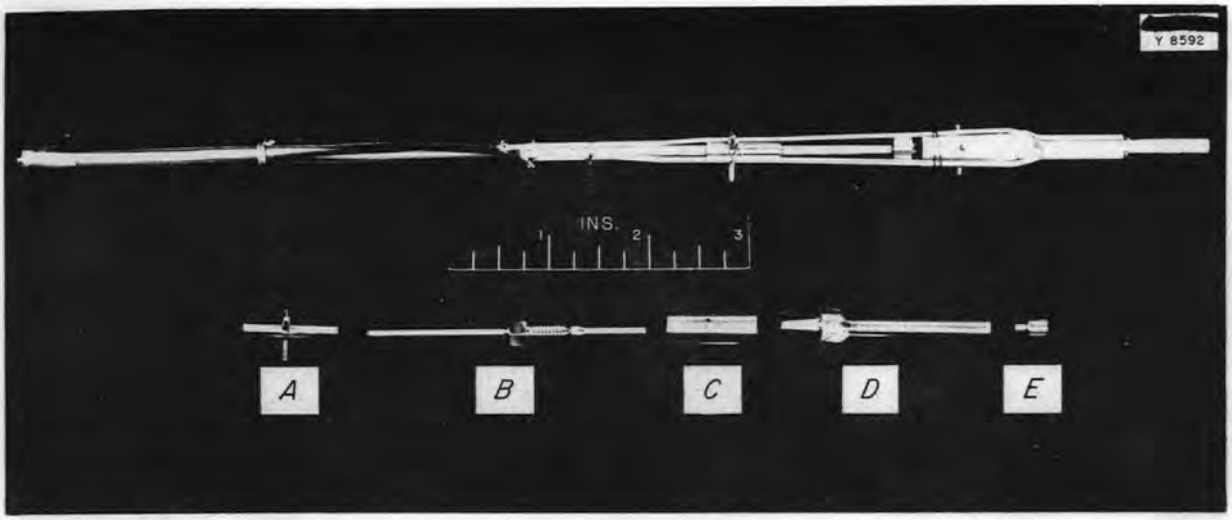

Fig. 14. Corrosion Capsule Assembly and Exploded Parts.

LIQUID FUEL TESTS IN THE LITR

D. D. Davies

A series of long-term irradiations in hole C-48 of the LITR has been completed. Each Inconel capsule, containing 0.7 g of No. 30 salt, was irradiated at a thermal flux of 2.3×10^{13} neutrons/cm^3·sec. The fission heat generated was approximately 140 watts/cm^2 of fuel. The capsules are to be opened immediately for studies of the container material and salt composition.

In order to study the effect of neutron flux on the salts and on Inconel containers, an additional irradiation that will parallel MTR irradiations is under way.

PHYSICAL PROPERTIES OF IRRADIATED SALTS

C. C. Webster W. R. Willis

It was necessary to change the thermocouple circuit to the Brown recorder from that shown in the previous report[2] in order to get reproducible results. The new thermocouple circuit is shown in Fig. 15.

The melting point was determined[3] for ANP salt samples that had been irradiated in the LITR and in the MTR. In the LITR irradiations, the control specimen was used as the standard; for the MTR irradiations, a specially filled capsule of the ANP salt, which had not been subjected to the same thermal history as that of the irradiated specimen, was used as the standard.

Some difficulty was encountered in the MTR capsule because it was necessary to attach the thermocouples to the outside of the capsule by remote means rather than to place them in wells in the capsule; this meant that the furnace core affected the results recorded by the thermocouple. It was impossible to make a positive melting point determination during the heating cycle; therefore all results are those determined during the cooling cycle. The melting points of the MTR capsules were:

No. 201 (irradiated)	488 ± 10°C
No. 206 (bench test)	475 ± 10°C

(2) C. C. Webster, *Solid State Quar. Prog. Rep. Nov. 10, 1952*, ORNL-1429, Fig. 9, p. 18.

(3) C. C. Webster, *op. cit.*, ORNL-1429, p. 16.

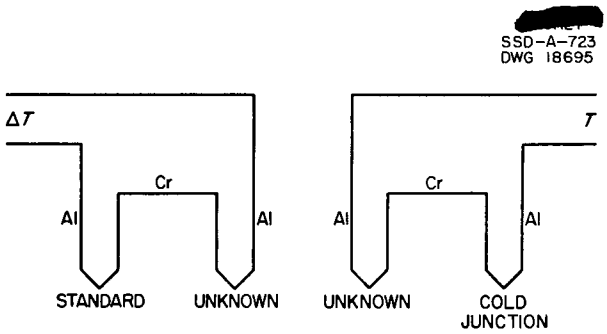

Fig. 15. Revised Thermocouple Arrangement for Determination of Melting Points for Irradiated Liquid Fuels.

The melting points for the LITR samples with thermocouples in wells in the sample were

10 Z-57 (irradiated)	500 ± 8°C (by two determinations)
13 Z-60 (bench test)	506 ± 8°C

The results from the LITR-irradiated samples indicate that, for the particular neutron flux exposure, there was no appreciable change in the melting point.

In measuring the melting point of MTR capsule No. 206, manual control of the cooling rate was used so as to obtain a very slow rate (less than 1°C/min). The slow cooling rate eliminated much of the furnace-core effect on the thermocouple that was attached to the outside of the capsule. A melting point of 505°C was observed, thus indicating that the discrepancy between MTR and LITR samples was not real.

The conditions of the experiment justify placing more emphasis on the LITR-irradiated fuels because of the larger sample size and the more ideal physical conditions. A program is under way for a more thorough investigation of the effects of irradiation upon the melting point of the ANP salt.

DEVELOPMENT OF LITR FACILITY C-46

J. G Morgan A. E. Richt

So that a greater number of capsules could be irradiated and so that two, separate, irradiation projects could be run concurrently, an additional testing facility was completed. The new location, C-46, is directly north of C-48 and extends through the top plug of the reactor Furnace controls and recording instruments are located in Building 3006. The first irradiations will be of fused salts that have anions of low cross section.

DYNAMIC CORROSION TESTS

J. G Morgan A. E. Richt

A capsule containing 3 g of normal Na-Zr-U-fluoride salt was tested in the rocking mechanism[4] on the bench The hot end was maintained at an average temperature of 1500°F and the cold end at 1150°F. The Inconel capsule, 0.375-in. ID by 3-in. long, was tilted through a 60-deg angle. After 15,400 complete cycles, the test was terminated because of bellows failure on the tilting mechanism. To eliminate the bellows, an angular-displacement mechanism that uses a piston in opposition to a spring was constructed. The plug containing the capsule and lead-out tubes for the new apparatus has been fabricated.

THERMODYNAMIC STUDIES OF SULFATE SYSTEMS

M T. Robinson

In addition to the fluoride tests, studies are being made of other salt systems that are of interest as reactor fuels or coolants. Among the possibilities are sulfates, phosphates, fluorophosphates, silicates, and borates. Thermodynamic data are very

[4] D F Weekes, P R Klein, J G Morgan, H E Robertson, and A E Richt, *Solid State Quar Prog Rep Aug 10, 1952*, ORNL-1359, Fig 20, p 23

limited except for the sulfates. Free-energy changes have been computed for various reactions, and one example was examined experimentally.

The reactions studied thermodynamically were

$$MSO_4(c) = MO(c) + SO_3(g) \quad (1)$$

$$2MSO_4(c) + UF_4(c) = 2MF_2(c) + U(SO_4)_2(c) \quad (2)$$

$$MSO_4(c) + UF_4(c) = UO_2F_2(c) + MF_2(c) + SO_2(g) \quad (3)$$

$$2MSO_4(c) + UF_4(c) = UO_2SO_4(c) + 2MF_2(c) + SO_2(g) \quad (4)$$

The necessary standard heats of formation[5] ($\Delta H_f{}^\circ$) and standard entropies[5] (S°) were used to compute free energies of reaction (ΔF). The results were then combined with the appropriate high-temperature heat-content equations[6] to yield free energies of reaction at 1000°K (727°C). Some results of the computations are given in Tables 5, 6, and 7 for the first three reactions.

Some of the data employed require explanation. The entropy of $U(SO_4)_2$ was estimated from the entropy change (ΔS_{298}) for reaction 1 of 45.2 ± 1 9 cal mole^{-1} deg^{-1} per sulfate ion for 14 compounds for which experimental data were available. The result was S°_{298} = 51 cal mole^{-1} deg^{-1}. The heat capacity of $U(SO_4)_2$ was estimated by a method similar to that of Kelley.[6] The result was C_p = 31 + 0.039 T cal mole^{-1} deg^{-1}. The heat of formation of UO_2F_2 was taken to be $\Delta H^\circ_{f,298}$ = −391 kcal mole^{-1}.[7] The heat capacity

TABLE 5. CALCULATED THERMODYNAMIC DATA FOR THE REACTION $MSO_4(c) = MO(c) + SO_3(g)$

COMPOUND	ΔF AT 298°K (kcal)	ΔF AT 1000°K (kcal)	P_{SO_3} AT 1000°K (atm)
Na_2SO_4	124 2		
$CaSO_4$	82 5	105	1×10^{-24}
$Al_2(SO_4)_3$	97 1	17 1	0 057
$PbSO_4$	59 7	54 3	1×10^{-12}
$U(SO_4)_2$	77	12	0 049

TABLE 6. CALCULATED ΔF FOR THE REACTION $2MSO_4(c) + UF_4(c) = 2MF_2(c) + U(SO_4)_2(c)$

COMPOUND	ΔF AT 298°K (kcal)
Na_2SO_4	1
$CaSO_4$	−15
$Al_2(SO_4)_3$	+32
$PbSO_4$	+1

TABLE 7. CALCULATED THERMODYNAMIC DATA FOR THE REACTION $MSO_4(c) + UF_4(c) = UO_2F_2(c) + MF_2(c) + SO_2(g)$

COMPOUND	ΔF AT 298°K (kcal)	ΔF AT 1000°K (kcal)	P_{SO_2} AT 1000°K (atm)
Na_2SO_4	30		
$CaSO_4$	10	−6	20
$Al_2(SO_4)_3$	95		
$PbSO_4$	28		

(5) F D Rossini, *et al*, *Selected Values of Chemical Thermodynamic Properties*, NBS Circular No 500 (Feb 1, 1952)

(6) K K Kelley, *U S Bur Mines, Bull* **476** (1949)

(7) R P Metcalf, personal communication

data for UO_2F_2 given by Katz and Rabinowitz[8] were extrapolated to high temperatures by using the equation

$$C_p = 31.98 + 1.4789 \times 10^{-3}\ T - \frac{2313}{T}\ .$$

Reaction 4 was examined only in the case of $CaSO_4$ at 298°K. The result obtained was $\Delta F_{298} = -49$ kcal. The entropy of UO_2SO_4 was estimated to be $S^\circ = 40$ cal mole^{-1} deg^{-1} by the same method used for $U(SO_4)_2$. The heat of formation of UO_2SO_4 was estimated to be -511 kcal mole^{-1}.

The reaction of $CaSO_4$ and UF_4 was studied experimentally. A mixture of 1.911 moles of $CaSO_4$ per mole of UF_4 was heated to 1000°K in a graphite crucible. The gases evolved were condensed in a liquid-nitrogen-cooled trap. In one experiment, the reaction was carried out under a 1-atm pressure of helium, while in another, a vacuum of 3×10^{-5} mm Hg was maintained. At 627°C, the reaction proceeded very slowly - it was still incomplete in 18 hr - but at 727°C, the reaction went to completion in an hour or less. The solid residue was black, with flecks of yellow, compared with the light-green starting mixture. X-ray diffraction studies showed the principal components to be CaF_2 and U_3O_8, with small amounts of $Ca(UO_4)$ and possible traces of UO_2F_2. The gaseous products were analyzed by absorption in standard NaOH, titration with standard HCl to determine total gases absorbed, and titration with standard I_2 to determine SO_2. The gases contained 52 mole % SO_2 in one case and 75 mole % SO_2 in the other. From these results and the actual weight losses, it appears that the reaction may be best represented by the following steps

$$2CaSO_4 + UF_4 = 2CaF_2 + UO_3 + SO_2 + SO_3 \quad (5)$$

$$UO_3 = 1/3\ U_3O_8 + 1/6\ O_2 \quad (6)$$

$$CaSO_4 + UO_3 = CaUO_4 + SO_3 \quad (7)$$

The first stage is essentially reaction 4, followed by decomposition of UO_2SO_4, according to reaction 1. Reaction 6 is a well-known high-temperature reaction of UO_3. Reaction 7 is included to explain the formation of $CaUO_4$. The process

$$6CaSO_4 + 3UF_4 = 6CaF_2 + U_3O_8 + 2SO_2 + 4SO_3 \quad (8)$$

must play only a minor role in the reaction, since it requires only 33 mole % SO_2 in the gaseous products.

Insufficient thermodynamic data exist for phosphates, phosphorus oxides, and other compounds of interest, therefore parallel computations cannot be made.

On the basis of the above calculations and experiments, it appears certain that UF_4 cannot be used in sulfate systems.

[8] J J Katz and E Rabinowitz, *The Chemistry of Uranium*, Vol 2, McGraw-Hill, New York, 1951

CRYSTAL PHYSICS

ORNL 86-In. CYCLOTRON STUDIES

W J Sturm R. T Jones[1]

The final cyclotron bombardments and analyses that have made up a program devoted to the examination of radiation effects on uranium eutectics in Inconel have been completed A total of 65 fuel pins was studied in the course of the experiments, this represents 1- to 92-hr proton bombardments of individual targets and a series of bombardments on each of four uranium-eutectic mixtures A report[2] summarizing the findings of these experiments is being prepared and should be available soon The report will present conclusions with regard to the effect of 20- to 22-Mev proton bombardment on the relative and absolute Inconel corrosion rates and on the fuel stability of the four eutectic mixtures of the series

One of the considerations of major importance in the eutectic-fuel bombardments was the maximum quantity of energetic protons that could be introduced into the target per unit time, while the target was maintained at a fixed temperature Beam heating alone provided the heat, and the problem was one of maximizing the rate of heat removal Although water cooling was used during most of the bombardments, approximate calculations indicated that if proper flow rates were attained, a somewhat greater amount of heat could be removed by a refrigerated stream of helium gas

A target was designed that would accommodate a modified version of the cylindrical liquid-fuel target in a header that allowed gas passage on all surfaces of the target The first version of the target, somewhat larger than the water-cooled equivalent, drew sparks from the dees, and prevented a proton beam from being produced. Two examples of a modified target could be bombarded only after the entire proton spiral path inside the dees had been displaced magnetically, and a small spot in the thin (0.010-in.) outer wall of each was melted by a very small ($\sim 2\mu a$) beam of protons. It could not be determined whether the cause was a beam that was rendered inhomogeneous by magnetic perturbation or whether the rate of helium flow was too small for adequate cooling.

Therefore it was not possible to evaluate the relative cooling effectiveness of the method with the targets that have been bombarded thus far For routine irradiation of fuel targets, however, it is probable that, with the recent successful irradiations in the MTR, the current situation does not justify the additional expense and effort required to introduce cooling by refrigerated helium as part of the internal-beam cyclotron

PROTON IRRADIATION OF TITANIUM IMPACT SPECIMENS

W J Sturm R. J. Jones[1]

A series of five titanium impact specimens of the substandard Izod type previously discussed[3] has been bombarded with 20-Mev protons for 200 to 1000 μa-hr It is intended to compare the impact results from these specimens with the results from unirradiated and reactor-irradiated specimens. Because it is difficult to produce very many of the cyclotron specimens in the limited time available for the bombardments, the impact measurements will be made after a

(1) Electromagnetic Research Division

(2) W J Sturm *et al*, *The Stability of Several Inconel-UF_4 Fused Salt Fuel Systems under Proton Bombardment*, ORNL-1530 (to be published)

(3) R G Berggren and N E Hinkle, *Solid State Quar Prog Rep Nov 10, 1952*, ORNL-1429 p 9

curve for reactor-irradiated titanium has been obtained so that the neutron data can be used as a guide for the parameters of the proton test. An additional variable, introduced in this case because of the line-deposition of hydrogen introduced by proton bombardment, will be the relative angle between the incident proton direction and the impact. After fracture, the samples will be subjected to vacuum-fusion analysis to determine residual hydrogen content.

PROTON IRRADIATION OF ALUMINUM

D. Binder W. J. Sturm
T. K. Roche[4]

The solubility and the fusion of hydrogen in aluminum at temperatures below 450°C are believed to be negligible, therefore it is possible that proton bombardment offers a unique method of introducing and retaining hydrogen in this metal. In the last report,[5] some indication was presented that the monoenergetic protons, in passing through the aluminum, do affect the hardness of the metal in a small region at the end of the proton range. Since the hydrogen (if it is retained without fusion) would be retained in a small band displaced from the face of incidence by a distance equal to the range of the monoenergetic protons in the metal, the increase in hardness actually observed at this distance is possibly of ambiguous origin. When near the end of its path in aluminum, the proton causes many knock-on atoms that might, in themselves, account for the hardening, or the protons that terminate at this band and remain there as trapped atoms could cause this effect by a mechanism similar to the mechanisms that account for hydrogen embrittlement in other metals.

The metallographic status of aluminum bombarded with 500 μa-hr of 20-Mev protons is shown in Fig. 16. The polished specimen is shown in a macrophotograph (Fig. 16*a*), in which 1/8- by 5/8-in. section has been obliquely illuminated to show the 0.010-in. hardened band (the effect of grain-boundary separation) that cannot be removed by polishing. The semiphotomicrographs (Fig. 16*b*) and photomicrographs (Fig. 16*c*) of the same sample show what appears to be a striated precipitate or locally melted spots formed in the region of the intense knock-ons, together with separation of the crystals in this band. It may be noted that the precipitate forms in a direction parallel to that in which the sheet was rolled. A hardness traverse repeated on this specimen again showed an increase of 12 Tukon DPH numbers in the affected band.

Vacuum-fusion analyses were made to determine whether the hydrogen was retained, and the results of several such analyses show that, in each case, a large fraction (>50%) of the bombarding hydrogen was retained in the aluminum block. In order to distinguish between hydrogen embrittlement and work hardening, it is proposed to heat a sample to 325°C in an effort to anneal the effects of the knocked-on atoms and yet retain the hydrogen with little diffusion. X-ray diffraction pictures of the affected region will be made in an effort to determine the nature of the apparent precipitate formed.

IRRADIATION OF TEFLON CABLE

D. Binder W. J. Sturm
R. A. Weeks

As described in the last quarterly report,[6] a change in the dielectric constant of the coaxial cable insulation

[4] Metallurgy Division

[5] D Binder, *Solid State Quar Prog. Rep Nov 10, 1952*, ORNL-1429, p 20.

[6] D Binder and R. A. Weeks, *Solid State Quar. Prog Rep. Nov. 10, 1952*, ORNL-1429, p. 21.

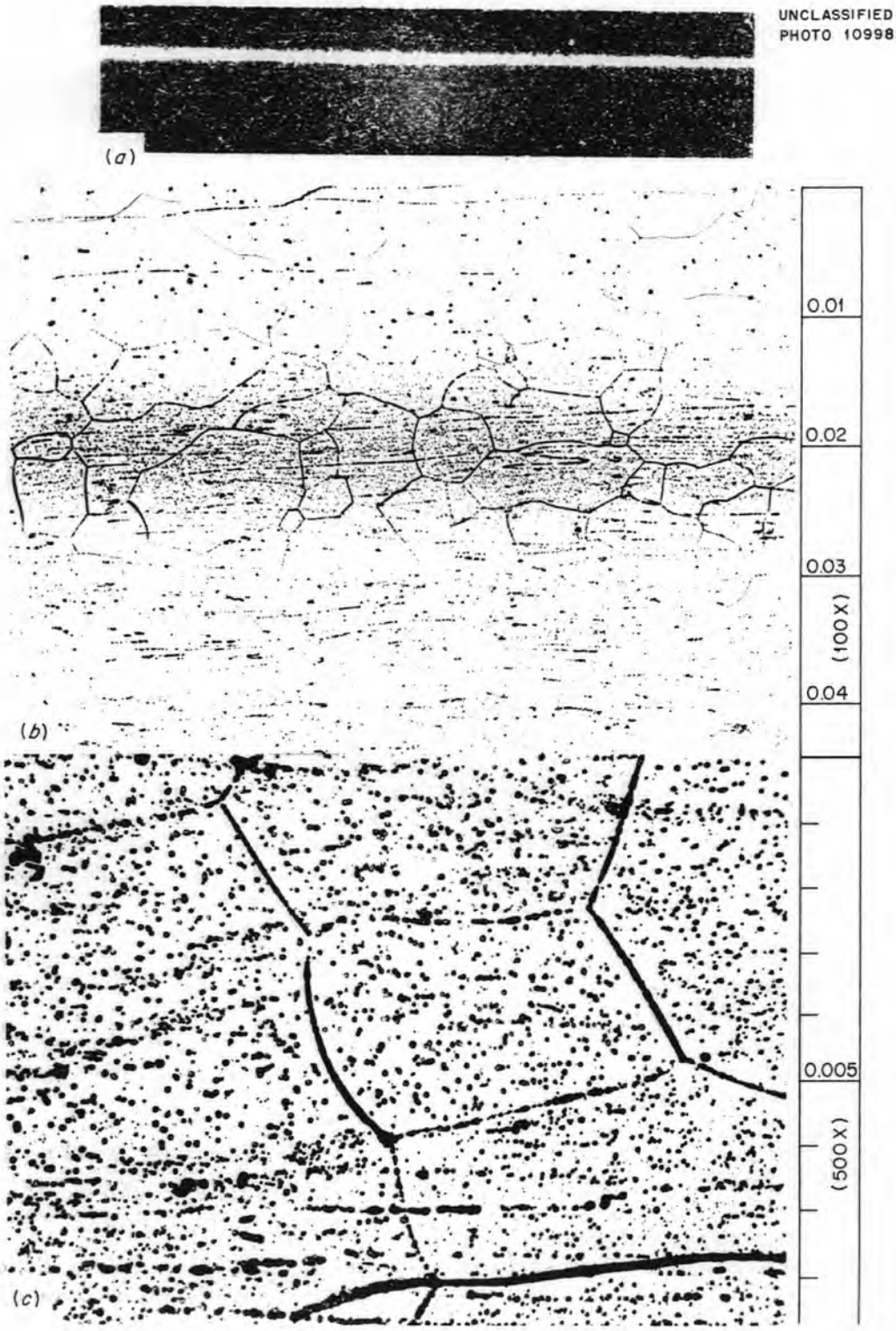

Fig. 16. Aluminum after Bombardment with 500 μa-hr of 20-Mev Protons.

may be detected by a change in quarter-wave frequency of a quarter-wave line constructed from that cable. The quarter-wave frequency equation is

$$f_{\frac{1}{4}} = \frac{4c}{\lambda\sqrt{K}},$$

where c is the velocity of light, λ is the wavelength, and K is the dielectric constant. When the frequency was varied around $f_{\frac{1}{4}}$, and the line was terminated by a small load, the input susceptance was shown to vary linearly from positive to negative values. A sensitive test of changes in $f_{\frac{1}{4}}$, and therefore in K, was thus assured.

The input impedance of the line was measured by a General Radio Twin-T bridge, and the signal input was from a General Radio signal generator. A National HRO-60 receiver was used as a null indicator (or bridge detector). The frequency was checked by a Signal Corps BC-221 frequency meter, and the most satisfactory technique was to zero beat the signal generator against the frequency meter.

Three tests were made of Teflon, high-voltage, coaxial cable under irradiation. In the first test, a coiled quarter-wave line was lowered into the gamma-ray source in the water canal of the Physics of Solids Building. The signal was brought to the surface by an additional half-wave line, and the operating frequency was 16.8 megacycles per second. After an irradiation of 10^6 r, an apparent shift toward a higher dielectric constant was noted, but this was within the experimental error of 2×10^{-3}.

The next two tests were in the ORNL graphite reactor. Improvements in technique decreased the experimental error and demonstrated a small shift in K. Among the improvements were the more careful balancing of the bridge and the beating of the signal generator against the frequency meter instead of putting both signals into the receiver at a fixed position of the tuning condenser. The first test in the reactor employed a three-quarter line as before, with one quarter of the line under irradiation in hole 1867. At a frequency of 9.5 megacycles, a relative decrease of $1.9 \pm 0.3 \times 10^{-3}$ in $f_{\frac{1}{4}}$ or an increase of $3.8 \pm 0.6 \times 10^{-3}$ in K was observed after six days (total integrated power of 320,000 kw-hr), this is some sort of average for the whole line, about two-thirds of which is unirradiated. In order to remove this ambiguity to a large extent, a second reactor test was made in hole 1867 with a quarter-wave line only, a short length of which led to the bridge equipment. This showed a decrease at 6.1 megacycles of $3.1 \pm 0.7 \times 10^{-3}$ in $f_{\frac{1}{4}}$ or an increase of $6.2 \pm 1.4 \times 10^{-3}$ in K for a similar irradiation. The variation in $f_{\frac{1}{4}}$ with integrated reactor power is shown in Fig. 17, the decrease is gradual and saturates.

The remaining question is whether the apparent increase of less than 1% in the dielectric constant of Teflon is due to temperature, which may be high enough to induce the reaction. It is planned to measure the temperature in a separate run by sinking a thermocouple into the line and following this by an oven experiment.

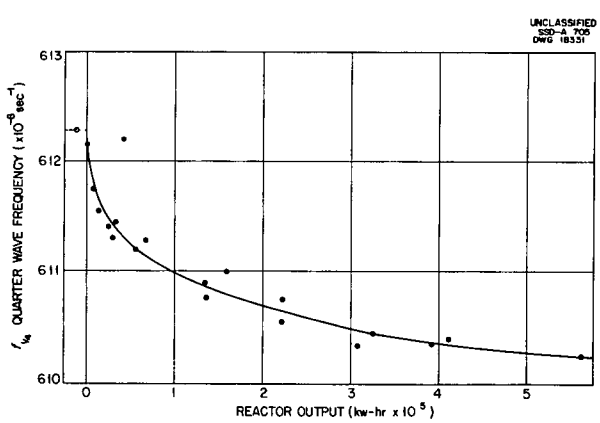

Fig. 17. Change in Quarter-Wave Frequency for Teflon Cable Exposed in the ORNL Graphite Reactor.

NEUTRON IRRADIATION OF LiF CRYSTAL

W. J. Sturm D. Binder
G E. Klein

The existence of a large cross section for the (n,α) reaction in Li^6 suggests that neutron irradiation may produce defects in LiF crystals at a rate more rapid than that in the other alkali halides. In this crystal, damage effects may be produced by the instantaneous alpha particles of the (n,α) reaction, in addition to the effects produced by the neutron flux. The use of lithium with its larger cross section might be compared with the use of a reactor with a larger flux than is ordinarily available. In order to test the idea, a LiF crystal was cleaved to form two smaller crystals, one was irradiated but the other was not. The crystal was irradiated for 5 days in hole 12 of the ORNL graphite reactor and became too opaque for optical-absorption measurements. Both samples were large enough for density measurements, however, and the irradiated crystal showed a decrease of 0.45 ± 0.02% over the unirradiated specimen. X-ray, lattice-parameter measurements indicated an increase of 0.22 ± 0.02% produced by radiation. In the unlikely case of pure expansion, the latter value would be equivalent to a density decrease of 0.66 ± 0.06% and would be in approximate agreement with the density measurement.

The simultaneous irradiation of KCl and LiF crystals for 5 hr in the rabbit of the graphite reactor indicated that the coloring is much deeper for LiF. In order to make a more rigorous test of the cause of the damage, it is planned to irradiate two LiF crystals, in the same hole, one crystal will be enclosed in a cadmium or boron shield that will eliminate slow neutrons. If the shielded crystal is relatively unaffected, then the damage must be caused by the slow neutrons Order-of-magnitude calculations indicate that the observed effects may be explained by displacements produced by the alphas and tritons in the $Li^6(n,\alpha)H^3$ reaction

SPECIAL PROJECTS

IRRADIATION OF MISCELLANEOUS MATERIALS

M. C. Wittels

The expansion[1] of diamond that results from fast-neutron bombardment is being investigated as a possible fast-neutron monitor that would be capable of rapid, qualitative measurements. Samples of diamantine powder were placed in selected positions between the fuel plates of facility C-19 of the LITR and were all irradiated during the same time interval. The relation between the resulting density changes and the irradiation positions (Fig. 18) is clearly defined and indicates that this property might be a useful tool for fast-neutron measurements.

Density measurements on diamonds irradiated in the LITR are being continued. The rate of change of density diminished rapidly when the integrated neutron flux reached a level of approximately 7×10^{19} nvt. Data by Primak and Day[2] are replotted in Fig. 19, together with data taken from LITR irradiations. The difference in the two curves indicates the possible importance of rate of flux, as well as the concentration of fast flux, to the expansion properties of diamond, it is also possible that the

(1) W H. Zachariasen and H A Plettinger, *Argonne National Laboratory Quarterly Report for September, October and November 1949*, ANL-4400, p 12

(2) W Primak and P Day, *Argonne National Laboratory Quarterly Report for January, February, and March, 1952*, ANL-4833, p 20

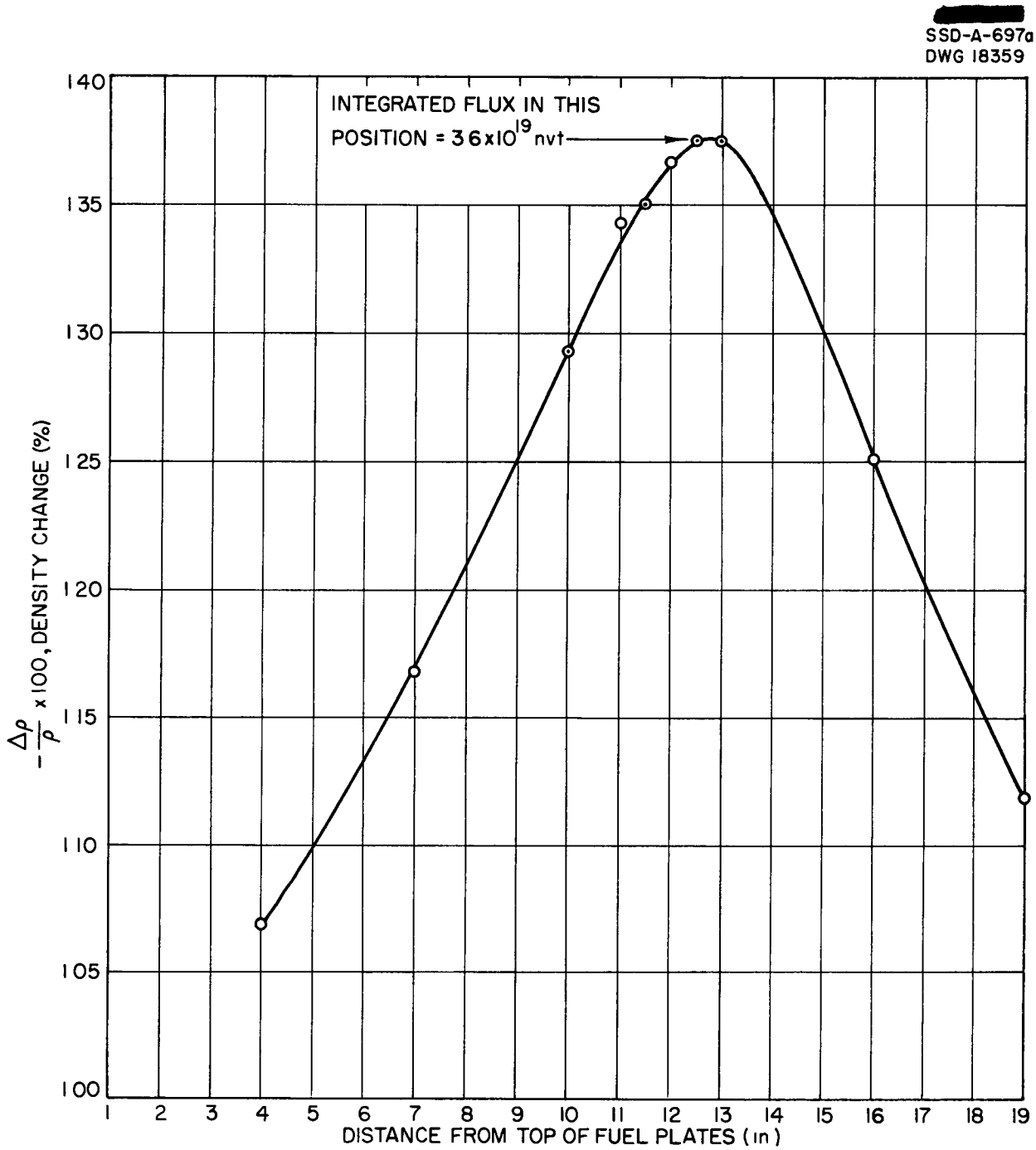

Fig. 18. Density Change of Diamonds as a Function of Position in Hole C-19 of the LITR.

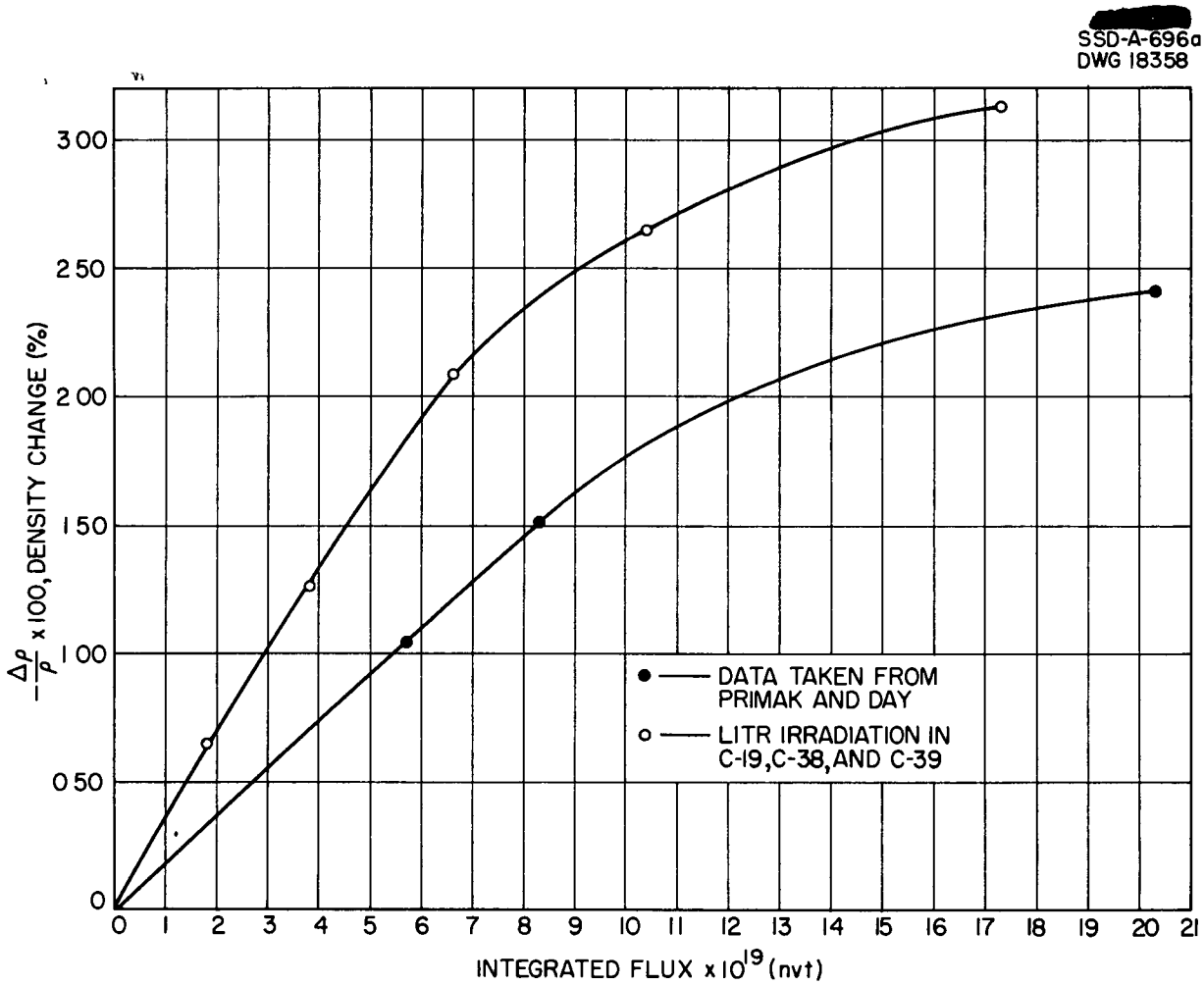

Fig. 19. Density Change of Diamond as a Function of Neutron Flux.

irradiation temperatures were considerably different.

X-ray and thermal studies of irradiated quartz[3,4] revealed the deep-seated effects resulting from fast-neutron bombardment. The x-ray diffraction patterns of disordered material annealed at 900°C show a reordering of the structure insofar as normal lattice parameters are concerned. However, the intensities of several reflections are weaker than normal and indicate that a residual disorder or strain exists in the crystal structure despite the high-temperature treatment. Differential thermal curves of the irradiated material failed to show the characteristic break in specific heat at 573°C that accompanies the inversion of low-high quartz. This phenomenon was observed in material that was carried through the thermal cycle, 20 to 900 to 20°C, several times.

Quartz that was irradiated by a total integrated neutron flux of 1.35×10^{20} nvt was found to undergo a high degree of disorder. The x-ray diffraction patterns of the irradiated

(3) M. C. Wittels and J. B. Trice, *Solid State Quar. Prog. Rep. Nov. 10, 1952*, ORNL-1429, p. 38.

(4) M. Wittels, *Phys. Rev.* **89**, 656 (1953).

crystal are similar to those of vitreous silica, and the density change as measured by the hydrostatic method was $\Delta\rho/\rho = -12.4\%$. Single-crystal quartz breaks down into a polycrystalline material under this irradiation. X-ray and thermal studies of this material are in progress.

The irradiation of diamond, silicon carbide, titanium carbide, and other high-temperature materials is in progress.

ANNEALING OF IRRADIATED GRAPHITE-UO_2 MATERIALS

R. H. Kernohan

In previous reports,[5] test results were given for graphite that contained 5 wt % uranium in the form of UO_2. These bars contained UO_2 nodules of varying sizes and had been irradiated for one month in the ORNL graphite reactor, and measurements, before and after irradiation, of weight, dynamic modulus of elasticity, electrical resistivity, and relative thermal conductivity were made.

The highest temperature reached by a thermocouple in surface contact with the specimens during the reactor irradiation was 88°C. However, the measurement of relative thermal conductivity necessitated the immersion of one end of the 3-in.-long specimens in a molten-metal bath at 160°C. The other end of the specimen then reached a temperature of about 90°C (depending on its conductivity) after a period of about 20 minutes. There was a slight drop in the electrical resistivity values of specimens measured after this thermal conductivity measurement, and this was particularly true of the control specimens containing no UO_2. Such a result would indicate that resistivity changes induced by neutron bombardment anneal out much more readily than changes caused by fission fragments.

(5) R. H. Kernohan, *Solid State Quar. Prog. Rep. May 10, 1952*, ORNL-1301, p. 30; *Solid State Quar. Prog. Rep. Jan. 31, 1952*, ORNL-1261, p. 41.

To permit a study of the effects of annealing, a jig was constructed of lavite, and metallic parts were used to hold the specimen and to apply electrical contacts. The jig was fastened to a sliding mechanism that permitted it to be easily inserted into or removed from a remotely controlled furnace in the hot cell. A process of step annealing was used. Each specimen was heated for 1 hr at each temperature, beginning with 150°C and going up by 25°C steps. A stream of dry nitrogen was kept flowing over the specimen while it was in the furnace. After each hour (or every 2 hr after 225°C), the specimen was removed from the furnace and cooled to less than 30°C, then resistivity measurements were taken. Measurements were also taken on the specimens while they were in the furnace and measurements on the cooled specimens were all corrected to 20°C. Table 8 gives the initial and final results, and Fig. 20 shows the values of resistivities adjusted so

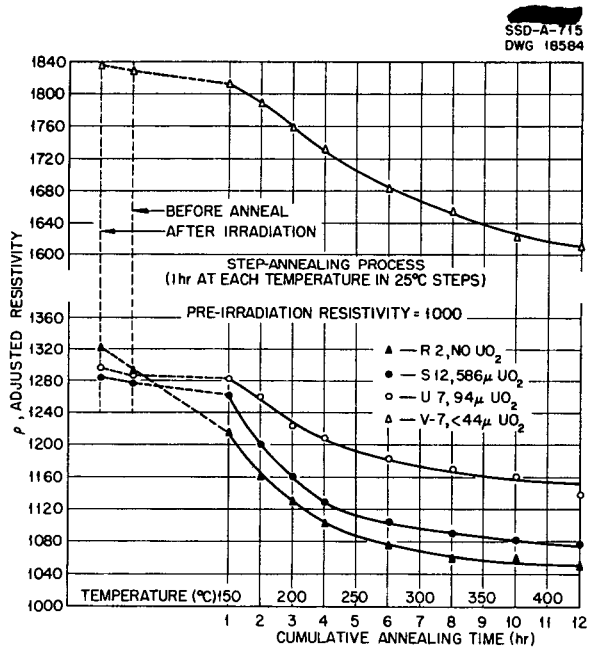

Fig. 20. Adjusted Electrical Resistivity of Graphite-UO_2 Bars at 20°C.

TABLE 8. RESISTIVITIES OF GRAPHITE-UO_2 BARS

SPECIMEN	CONTENT	RESISTIVITY, ρ*				
		Before Irradiation	After Irradiation	After Thermal Conductivity Measurements	After Eight Months	After Step-Anneal for 12 hr Between 150 and 425°C
R-2	No UO_2	1432	1892	1856	1852	1502
S-12	UO_2-586μ nodules	1437	1843	1840	1834	1547
U-7	UO_2-94μ nodules	1404	1819	1811	1806	1598
U-7	UO_2-<44μ nodules	1509	2771	2773	2755	2429

*ρ in ohm-cm corrected to 20°C

that the preirradiation resistivity for all specimens may be considered as having the arbitrary value of 1000. The first set of points on the left in Fig. 20 shows values of resistivity taken after irradiation. The next set of points was taken in the furnace resistivity measuring device after the thermal conductivity was measured and a time lapse of about eight months. If 1000 is subtracted from the ordinate values of the graph and the result is divided by 10, the percentage increase over the preirradiation resistivity is obtained. Figure 21 gives the per cent resistivity damage remaining in each specimen. Again, for this curve, adjusted resistivities corrected to 20°C were used. On the ordinate, 100% represents the postirradiation resistivity, and 0% would represent preirradiation resistivity.

Also, during the past quarter a short-time irradiation, 7.5 hr in hole 19 of the ORNL graphite reactor, was made on three graphite-UO_2 test bars. From cobalt-foil measurements, the integrated flux was 2.1×10^{16} nvt or about 1% of the neutron bombardment given to previous test bars.[5] Pre- and postirradiation results are shown in Table 9. Comparison with

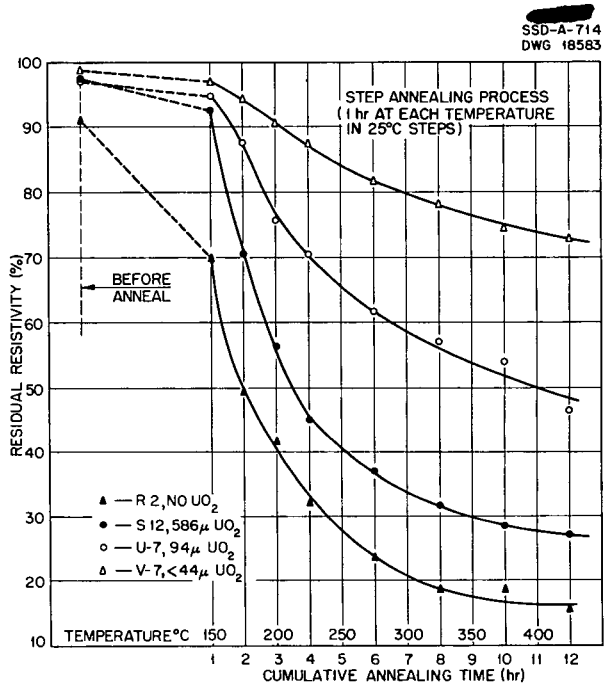

Fig. 21. Residual Resistivity Damage of Graphite-UO_2 Bars.

previous results[6] indicates that fission fragment-damage to the graphite structure builds up much more rapidly than neutron damage and probably reaches an equilibrium value.

(6) R. H. Kernohan, *Solid State Quar. Prog. Rep Nov. 10, 1952*, ORNL-1429, p. 38

TABLE 9. BEFORE AND AFTER IRRADIATION MEASUREMENTS ON GRAPHITE-URANIUM OXIDE BARS

MEASUREMENT	SPECIMEN		
	R-16	U-9	V-6
UO_2 content (wt %)	0	5	5
Nodule size (μ)		94	<44
Weight before irradiation (g)	5.8214	5.6743	5.4953
Weight after irradiation (g)	5.8215	5.6622	5.4834
Weight change (mg)	+0.1	-12.1	-11.9
Weight change (%)	0	-0.21	-0.22
Modulus of elasticity			
Before irradiation (10^6 psi)	3.11	2.98	2.93
After irradiation (10^6 psi)	3.11	3 13	3.64
Change (%)	0	+5	+24
Electrical resistivity			
Before irradiation (μohm-cm)	1434	1445	1495
After irradiation (μohm-cm)	1441	1514	1829
Change (%)	+0.5	+4.8	+22.4

Part II

UNCLASSIFIED PROJECTS

CONTENTS

PART II UNCLASSIFIED PROJECTS

PAGE

SUMMARY 41

SOLID STATE REACTIONS . 43
Estimation of Effective Fast Flux in Hole 52N . . 43
Mobility and Hole Concentration in Bombarded *P*-type Germanium . . 43
Low-Temperature Irradiation of Copper-Beryllium Alloy 46
Transistor Bombardment 46
Rectifier Measurements 47
Field Control for the ADL Magnet 49
Magnetic Susceptibility of Germanium 52
Radiation Effects in Ionic Crystals 54

ENGINEERING PROPERTIES 56
Radiation Stability of Plastics and Elastomers 56

CRYSTALS PHYSICS 57
Deformation of Copper Single Crystals at 300 and 78°K 57

SPECIAL PROJECTS 67
Hall and Magnetoresistance Effects in Metals 67

SUMMARY

SOLID STATE REACTIONS

Estimation of Effective Fast Flux in Hole 52N. Three *N*-type germanium samples were irradiated at ambient temperature (~30°C) in the horizontal cryostat of hole 52N in the ORNL graphite reactor The rate of electron removal was determined and compared with values of electron removal previously obtained at the center of the reactor where the fast flux is assumed to be 4×10^8 kw. The resulting effective fast-neutron flux in the cryostat is 1×10^8 nv/kw ± 20%.

Mobility and Hole Concentration in Bombarded *P*-Type Germanium. Continuous conductivity measurements made on *P*-type germanium during bombardment and during decay indicated that room-temperature annealing was negligible. At intervals during the exposure, the sample was removed and the Hall coefficient and resistivity measurements were made as a function of temperature. From this data, hole concentrations were calculated as a function of temperature. The hole concentration before irradiation was practically independent of temperature. The hole concentration after irradiation showed a linear increase with increase in temperature except for an inflection at about 140°K. A broad energy distribution with continuous or numerous discrete levels of acceptors is indicated.

A study was made of the variation of hole concentration with Fermi level. A broad distribution of acceptors is present and there is evidence for structure in the distribution. An attempt to fit these data with theory would be of doubtful value. A better approach would be to use *N*-type specimens, converted to *P*-type by irradiation, and to study a much wider range of bombardment-induced carrier concentrations.

The Hall coefficient and resistivity data also yield information concerning the mobility of holes. After short periods of bombardment, there was a marked initial increase of mobility at low temperature, the past history of the sample may have been responsible for the increase. After the initial low-temperature increase, the hole mobility exhibited an apparently normal decrease in value as the temperature was raised.

Low-Temperature Irradiation of Copper-Beryllium Alloy. A solution-quenched sample and a cold-worked sample were irradiated in the hole-52N cryostat at approximately −150°C. During the warmup period, the increase in resistivity was such that the total resistance change was approximately that which would have been expected had the irradiation been carried out at room temperature. This behavior definitely indicates that disorder stored at low temperature rearranges by a thermally activated process.

Transistor Bombardment. Two RCA NPN-junction transistors were irradiated in a water-cooled hole in the ORNL graphite reactor to test the feasibility of using transistors as circuit elements, or as tools for investigating the nature of radiation on solids. An integrated fast-neutron flux of about 10^{12} nvt very nearly destroyed the amplification features, and the amplification further decreased, in the absence of further radiation, until it was too small to be detected.

Rectifier Measurements. The current-voltage characteristics of rectifiers are now plotted directly with a function plotter. This enables a study to be made of the entire characteristic curves of rectifiers under bombardment. A specialized circuit has been designed for obtaining

reproducible data, and the circuitry is described in detail.

Field Control for the ADL Magnet. Measurement of magnetic susceptibility, to a precision of 0.1%, requires control of the magnetic field to ±0 05% The control is accomplished by a negative feedback through the passive network to the amplidyne used to energize the field of the generator that supplies power to the magnet and by an active compensating circuit that supplies compensating current in the control coils of the magnet.

Magnetic Susceptibility of Germanium. The program for developing and calibrating the equipment for determining the magnetic susceptibility of germanium is nearly complete. One test run was made on an *N*-type germanium cube in the range from room temperature to liquid nitrogen temperature. Data were self-consistent within 0.1%. Since measurements are made of the forces acting on the sample suspended in oxygen and vacuum, it is possible to determine the susceptibility of materials to an absolute accuracy that is equal to the accuracy to which the susceptibility of oxygen is known.

Radiation Effects in Ionic Crystals. Ionic-conductivity and annealing studies were made of radiation-colored potassium chloride crystals at temperatures ranging from 25 to 280°C. It was found that gamma irradiation reduces the conductivity σ and that long neutron irradiation enhances σ. The annealing process is complicated by the several processes that appear to take place in this temperature range. Unirradiated potassium chloride crystals also undergo some annealing in vacuum at these temperatures, interpretation of this unexpected phenomenon is not yet complete.

ENGINEERING PROPERTIES

Radiation Stability of Plastics and Elastomers. Effects of exposure to Co^{60} and Au^{198} sources on the elongation properties of elastomers were investigated. In the range of exposure studied, there appears to be no dependence of damage or dose rate or energy within a factor of 3.

Ozone is formed in air in a radiation field Stressed and unstressed rubber was therefore subjected to irradiation in air and under a helium atmosphere. Cracks appeared in the sample irradiated in air under stress, rubber irradiated in the unstressed condition showed no damage. No damage was evident on rubber that was irradiated under stress in helium.

CRYSTAL PHYSICS

Deformation of Copper Single Crystals at 300 and 78°K. Single crystals of copper were deformed at 78 and 300°K. There was slight temperature dependence of the critical shear stress in this range of temperature and, for shear strains less than about 0.25, the stress-strain relationship was linear and independent of temperature. At 78°K, the linear relationship of the stress-strain curve persisted for higher strains At 300°K, the annealing of crystals deformed at 78°K showed a decrease in electrical resistance that was accompanied by a phenomenon suggestive of strain aging The magnitude of the recoverable resistance was dependent on the strain and varied at a faster rate than shown by a linear relationship. A measurable decrease in electrical resistance was not observed for strains less than about 0.30. These results are interpreted according to the theory of dislocations and indicate some limitations to the theory of work hardening that was suggested by N F. Mott.

SPECIAL PROJECTS

Hall and Magnetoresistance Effects in Metals. In order to prevent variations in the temperature of metals while they are being measured for magnetoresistance, an oil bath

has been constructed to fit between the poles of the ADL magnet. Some temperature variation remains, and an attempt will be made, by revision of the oil circulation system, to decrease the variation to less than 0.04°C.

In trial runs, two determinations were made of the Hall constant for copper, agreement was within 3% and the values compare favorably with published values. The Hall constant for beryllium-copper was determined to be -4.1×10^{-5} cm^3/coulomb.

SOLID STATE REACTIONS

ESTIMATION OF THE EFFECTIVE FAST FLUX IN HOLE 52N

J. W. Cleland J. H. Crawford
J. C. Pigg

The effective fast-neutron flux in hole 52N of the ORNL graphite reactor, which contains the horizontal cryostat, has been estimated relative to the center of the reactor by using the initial rate of removal of electrons from *N*-type germanium as a means of comparison. Three *N*-type germanium samples were irradiated in the cryostat at ambient temperatures (~30°C). The conductivity was measured during the exposure, and the initial rate of conductivity decrease at constant power was determined. The rate of electron removal was determined from these data by using the values of the initial electron concentration, n_e^0, determined from the Hall-coefficient measurements based on the assumption that the mobility was not affected during the initial part of the irradiation. The results are given in Table 10.

The fast flux at the center of the reactor has been assumed to be about 1.1×10^8 per kw, this yields a value for the rate of electron removal in this position of about 3 per incident neutron.[1] Since the average value of (dn_e/dt)/kw is approximately 3×10^8 in the cryostat, the effective fast-neutron flux in the cryostat is 1×10^8 nv/kw to a precision of about 20%.

MOBILITY AND HOLE CONCENTRATION IN BOMBARDED *P*-TYPE GERMANIUM

J. W. Cleland J. H. Crawford
J. C. Pigg

In connection with a program of investigation of the energy distribution of bombardment-produced acceptors in *P*-type germanium, Hall coefficient and resistivity measurements,

[1] J. H. Crawford, Jr. and K. Lark-Horovitz, *Phys. Rev.* **78**, 815 (1950).

TABLE 10. INITIAL EFFECT OF BOMBARDMENT ON *N*-TYPE GERMANIUM

SAMPLE	POWER LEVEL (kw)	σ^0 (ohm^{-1} cm^{-1})	$\frac{d\sigma}{dt}$ (ohm^{-1} cm^{-1} sec^{-1})	n_e^0 (cm^{-3})	$\frac{dn_e}{dt}$ (cm^{-3} sec^{-1})	$\frac{dn_e/dt}{kw}$* (cm^{-3} sec^{-1} kw^{-1})
1	3900	3.22	2.86×10^{-4}	1.21×10^{16}	1.07×10^{12}	2.74×10^8
2	4000	0.758	2.53×10^{-4}	3.75×10^{15}	1.15×10^{12}	2.88×10^8
3	3900	0.658	3.26×10^{-4}	2.51×10^{15}	1.24×10^{12}	3.18×10^8

*Average value of $(dn_e/dt)/kw = 2.93 \times 10^8 \pm 20\%$

as a function of temperature, have been made periodically during an extensive bombardment run of a P-type germanium sample. The conductivity of the sample was followed during the irradiation period and during the short period required for radioactive decay, this permitted observation of the progress of the irradiation and any room-temperature annealing (this was found to be negligible). After the prescribed exposure, the Hall coefficient and resistivity were measured as a function of temperature, and the sample was returned to the reactor for additional irradiation.

A representative selection of log R vs. $1/T$ and log ρ vs. $1/T$ curves is shown in Fig. 22, some preliminary data were given in a previous quarterly report.[2] The total exposure given the sample was 335 hr and corresponded to an integrated fast flux of approximately 1×10^{18} nvt. Hole concentrations were calculated as a function of temperatures from the data. The hole concentration, n_h, vs. temperature curves for 91.3- and 334.8-hr exposure are shown in Fig. 23. The value of $M_h \longrightarrow n_h$ before irradiation, also shown, was $1.88 \times 10^{15}/cm^3$ and was essentially temperature independent. The temperature dependence of n_h after bombardment is almost linear both above and below a small step in the curve, the inflection point of which occurs in the region of about 140°K. This type of temperature dependence definitely indicates a broad energy distribution with continuous or numerous discrete levels of acceptors.

An instructive method of examining the nature of the energy-level distribution is afforded by the variation of the hole concentration with Fermi level. The Fermi level of a given specimen can be varied by varying

(2) J. W. Cleland and J. H. Crawford, Jr., *Solid State Quar. Prog. Rep. Nov. 10, 1952*, ORNL-1429, p. 44

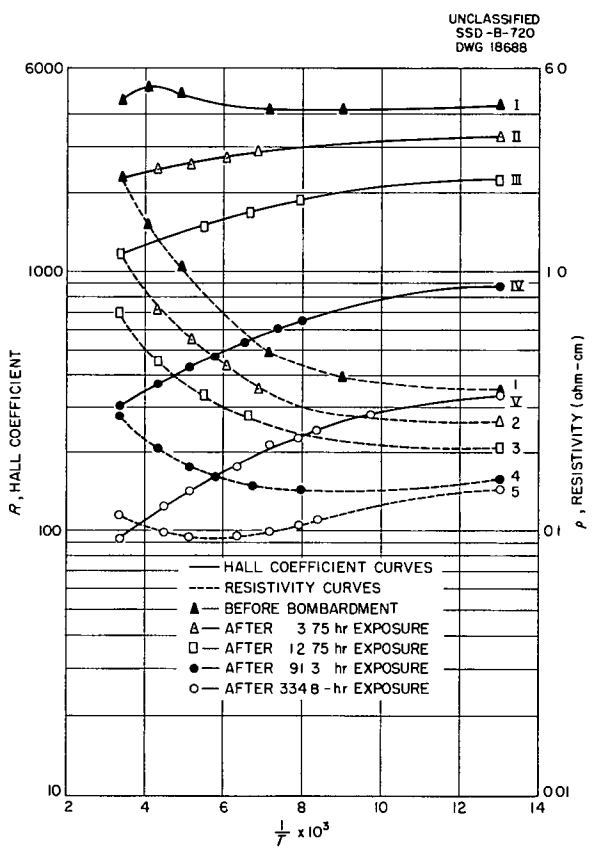

Fig. 22. Hall Coefficient and Resistivity vs. $1/T$ for P-Type Germanium for Various Periods of Exposure.

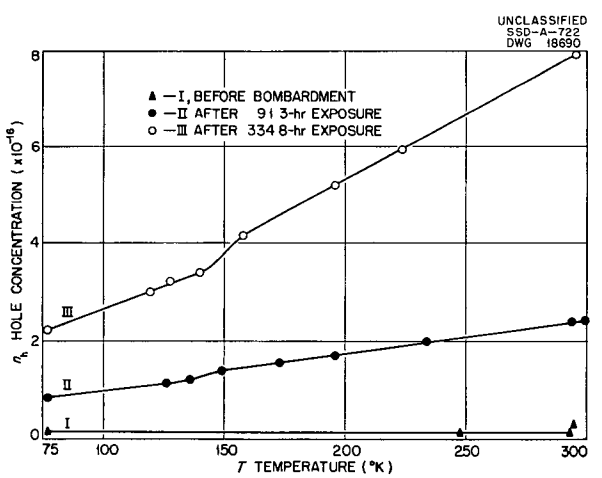

Fig. 23. Hole Concentration vs. Temperature of Bombarded P-Type Germanium.

the temperature. Since ζ is that energy at which the value of the Fermi distribution function is 1/2, it may be assumed, to a fair approximation, that all acceptors above that energy are not ionized and that all acceptors below that energy are ionized. Thus, in the case of a single discrete acceptor level with an ionization energy ΔE and an acceptor concentration N_a, n_h is very small for $\zeta < \Delta E$, but n_h rapidly approaches N_a for $\zeta > \Delta E$. Curve III in Fig. 24 is a calculated n_h vs. ζ curve for the case $\Delta E = 0.1$ ev and $N_a = 10^{17}$ cm^{-3}, from which the "resolution" of this approach can be readily seen. The range of transition from $n_h << N_a$ to $n_h \approx N_a$ occurs rapidly at low ζ values (low temperatures) and more gradually at higher ζ values (high temperatures). The reason for this is that the transition of n_h from small to large values occurs over a range of $\Delta\zeta \sim 4kT$.

Curves I and II of Fig. 24 are the n_h vs. ζ curves for the exposures of 91.3 and 335 hr, respectively. It is obvious from the shape of the curves that some sort of broad distribution of acceptors is present. Closer examination of the curves indicates that there is evidence for structure in the distribution. Both curves exhibit a sigmoid involution in the region $\zeta \sim 0.07$ ev, and this feature is also present in the n_h vs. T curve (Fig. 23). Attempts have been made to fit the data by using both a square-wave distribution of acceptors and a square-wave distribution with a discrete level superimposed to account for the sigmoid character, and the latter approach met with some success. However, because it is necessary to use four adjustable parameters for the latter distribution, it is questionable that these parameters (width and position of the continuous distribution, position of the discrete level, and relative concentration of acceptors) have any real value. It appears that a better approach would

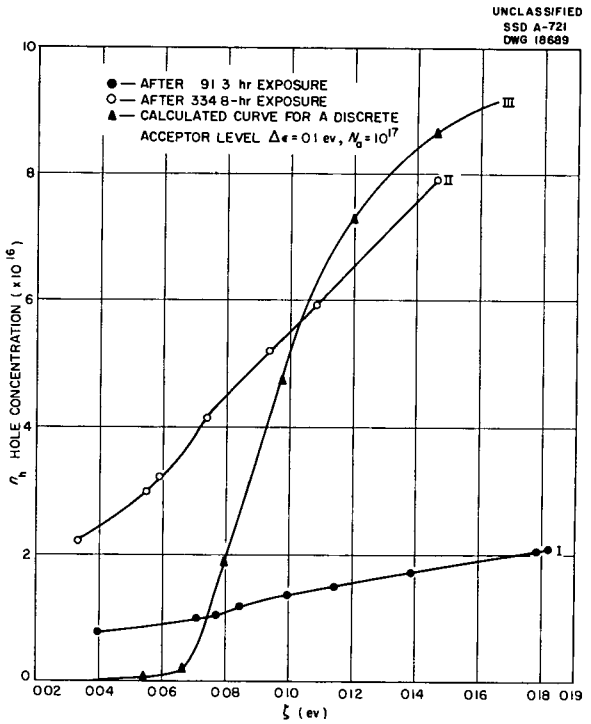

Fig. 24. n_h vs. ξ for P-Type Germanium.

be to use N-type specimens, converted to P-type by irradiation, and to study a much wider range of bombardment-induced carrier concentrations.

The Hall-coefficient and resistivity data also yield information concerning the mobility of holes. Mobility vs. temperature curves for a number of exposures are shown in Fig. 25. The general effect of bombardment is to cause a decrease in hole mobility, and the relative decrease at 77°K is greater by about a factor of 2 than that at 300°K. At 77°K, μ_h is decreased by about a factor of 5 for an exposure of 334.8 hr as compared with a decrease of about a factor of 3 at 300°K for the same exposure. An unexpected feature of the data is the marked initial increase of μ_h at low temperature by short periods of bombardment. The sample used had been bombarded previous to this experiment but had been heat treated to remove

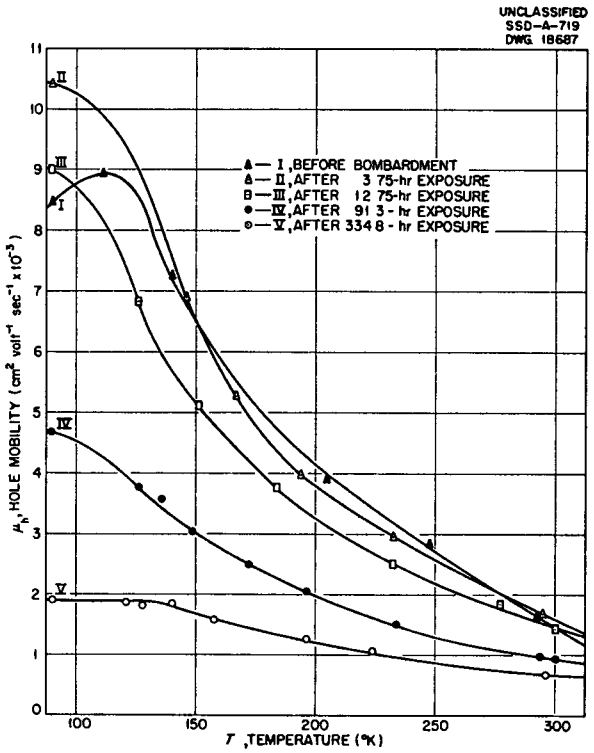

Fig. 25. Hole Mobility vs. Temperature for Various Periods of Exposure.

the effects. It is possible that sufficient disorder remained to modify the electronic scattering at low temperature, and that the initial effect of bombardment was to transform this type of scattering mechanism. The need for additional information is obvious and plans have been made to extend the investigations.

LOW-TEMPERATURE IRRADIATION OF COPPER-BERYLLIUM ALLOY

J. W. Cleland J. H. Crawford
E. S. Schwartz

Investigations of the effect of reactor irradiation on the resistivity of solution-quenched and cold-worked Cu-2% Be alloy has been continued. Two additional specimens, one solution-quenched and one cold-worked by 50% reduction, were irradiated in the ORNL graphite reactor cryostat at approximately -150°C. The results at low temperature and the behavior on warmup confirmed the previous experiment. During the first warmup, the samples were warmed to about 50°C for about 3 hours. During this period, the resistivity increased such that the total resistance change was approximately that which would have been expected had the irradiation been carried out at room temperature. This behavior definitely indicates that disorder stored at low temperature rearranges by a thermally activated process. The most probable process of rearrangement is the formation of precipitate nuclei by the enhanced microdiffusion associated with crystal disorder, as postulated by Taylor and Murray[3] and as demonstrated by Blewitt and Coltman[4] for the case of radiation ordering of Cu_3Au.

A detailed analysis of the data is being made and will be presented in a later report.

TRANSISTOR BOMBARDMENT

J. C. Pigg J. W. Cleland

In order to test the feasibility of using transistors as circuit elements in regions where a neutron field is present and to investigate the possibility of using such units as tools to investigate the nature of radiation effects on solids, two RCA NPN-junction transistors were irradiated in a water-cooled hole in the ORNL graphite reactor. Figure 26 shows the circuit used. The emitter current was held constant at 1 ma throughout the tests, and the temperature was held constant to within ±1°C. The amplification factor, α, was computed from $\alpha = 500\ E_o/E_s$, where E_o is the output voltage across the collector resistor and E_s is the signal voltage from the oscillator.

[3] G. T. Murray and W. E. Taylor, *Effect of Neutron Irradiation on Supersaturated Solid Solution of Beryllium in Copper*, ORNL-1323 (Jan. 29, 1953).

[4] T. H. Blewitt and R. R. Coltman, *Phys. Rev.* 85, 384 (1952).

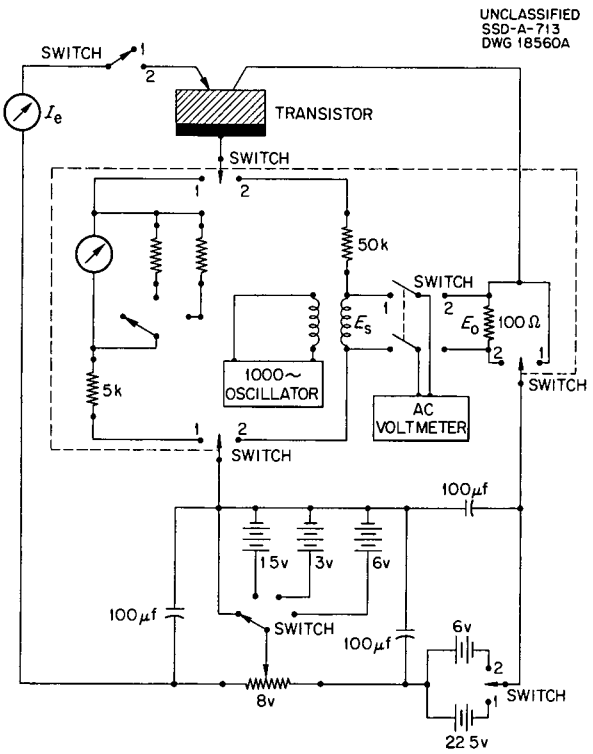

Fig. 26. Transistor Test Circuit.

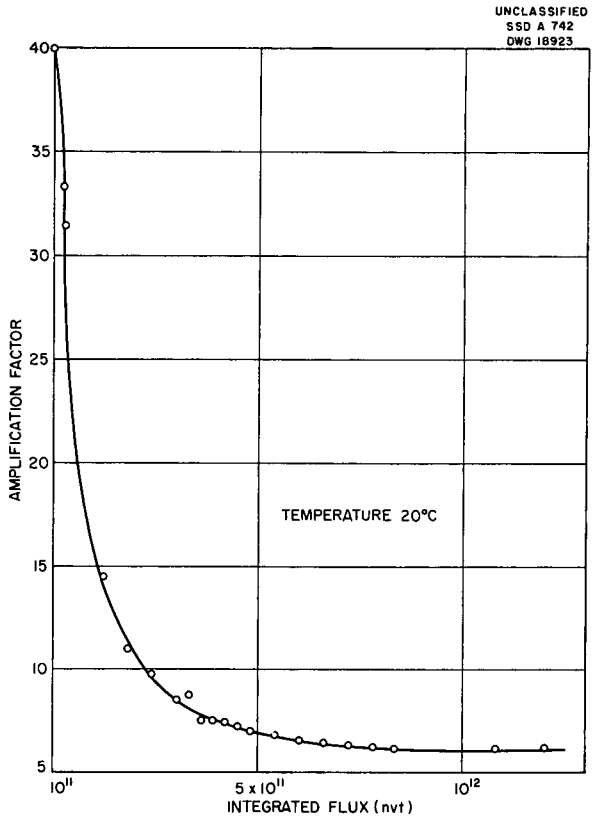

Fig. 27. RCA Transistor No. 1241 Irradiated in Hole 51N at 950 kw.

Figure 27 shows α vs. nvt for one transistor. At the end of the exposure, the transistor was removed from the reactor and stored during radioactive decay. After one week, further tests showed α to be zero within the limits of the measurement.

Figure 28 shows α vs. nvt for a second transistor that was exposed during a low-power run to permit investigation of the detail of the first portion of the curve. The healing observed in sample No. 1266 during reactor shutdown is similar to that previously observed in germanium rectifiers. Although no attempt will be made to analyze these curves until more complete data are available, some conclusions can be drawn and comparison with previous work on bulk materials and point-contact rectifiers can be made.

An integrated fast-neutron flux of the order of 10^{12} nvt destroyed the amplification features of the NPN-junction transistors. Although destruction was not complete after 10^{12} nvt, the amplification further decreased, in the absence of further radiation, until it was too small to be detected by the instruments used.

RECTIFIER MEASUREMENTS

J. C. Pigg

A function plotter is now available for directly plotting the current-voltage characteristics of rectifiers. With this device, it is possible to study the complete characteristic curves of rectifiers during bombardment. However, with manual change of the voltage or current applied to the

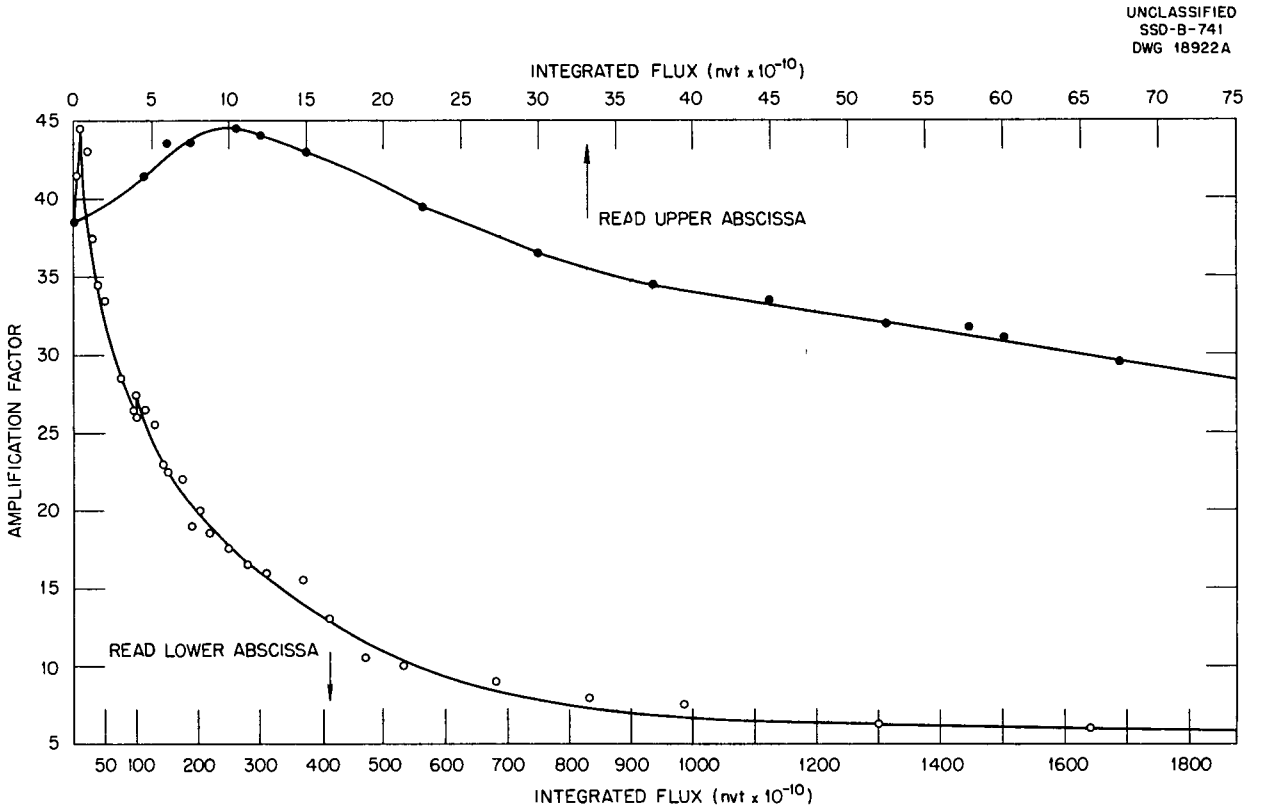

Fig. 28. Effect of Reactor Bombardment on Amplification Factor of RCA Transistor No. 1266.

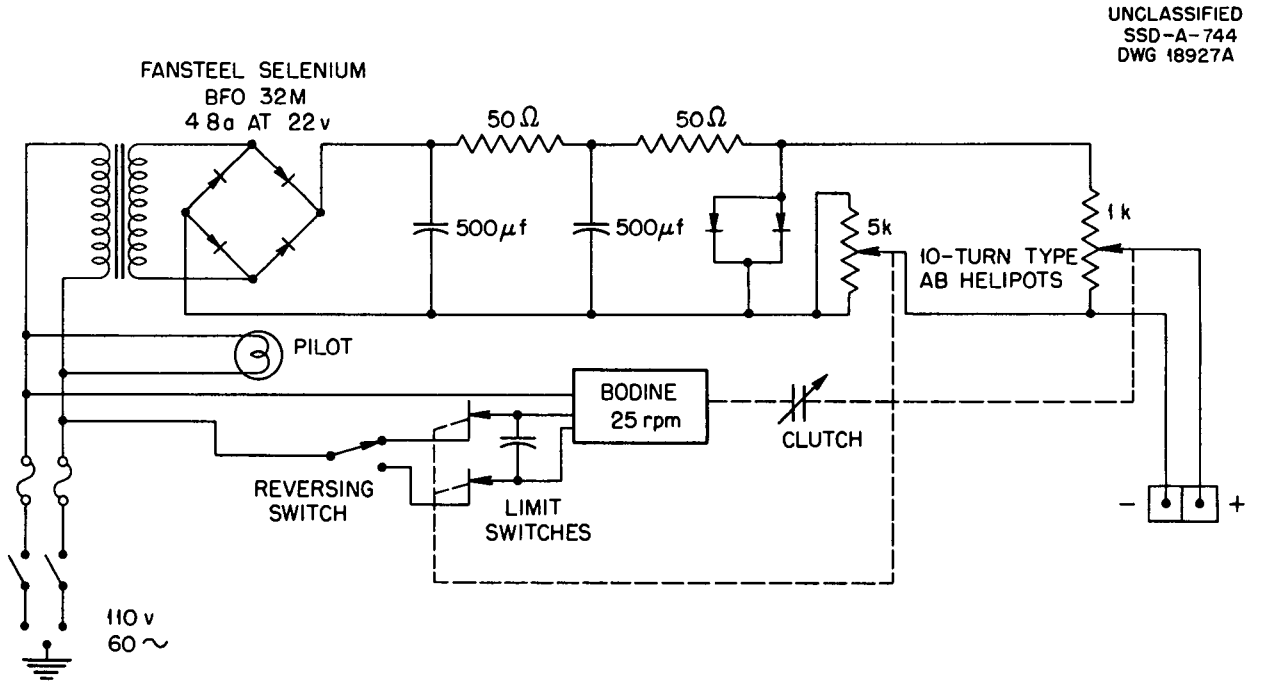

Fig. 29. Power Supply for Rectifier Experiment.

rectifier, it is difficult to achieve sufficient smoothness to prevent irregularities in the trace of the function plotter.

The changes in the rectifier characteristic are fairly linear above 0.5 volt for plotting purposes, but below 0.5 volt they are more complicated. Thus, to ensure reproducibility in the plot, the rate of changes in voltage applied to the rectifier should be smaller in the lower voltage range than it need be in the higher voltage range.

A smooth output voltage change is provided by driving the voltage control helipots with a 25-rpm Bodine motor (Fig. 29). A concave upward curve in the output voltage vs. time is achieved by the manner in which the control helipots are connected.

Since the d-c resistance of the sample will vary from the order of 10^2 to 10^6 ohms during the plotting of a single characteristic, the output voltage across the helipots should be essentially load independent. Since VR tubes are not operative at such low voltages, two selenium rectifiers, biased in the forward direction, are used in lieu of VR tubes.

As an illustration, Fig. 30 shows a typical semiconductor-rectifier characteristic curve. Biased in the forward direction at some voltage, v_c, a large change in current through the rectifier is required to produce a small change in voltage across the unit. In this manner, these rectifiers may be used as voltage-control units. Biased in the negative direction by a voltage, v_c^1, there will be a current I_c through the rectifier. This current will show little change from I_c for large changes in voltage across the rectifier.

FIELD CONTROL FOR THE ADL MAGNET

J. C. Pigg

The magnetic-susceptibility measurements that are to be made by using the ADL magnet are desired to a precision of 0.1%. This requires a magnetic-field control of ±0.05%. The magnet field is controlled in two ways negative feedback through a passive network to the amplidyne used to energize the generator field controls the output of the 25-kw, d-c generator that supplies power to the magnet, and an active compensating circuit supplies compensating current in the control coils of the magnet.

Fast fluctuations in the output of the amplidyne are fed back through a capacitor, C_1, into one of the amplidyne control coils in a manner that provides negative feedback (Fig. 31). The capacitor, C_1, with the largest convenient capacity, consistent with available capacitors, that could be used without producing oscillations was chosen. The measured voltage gain of the amplidyne is 200.

Changes in the output current of the generator are controlled by a portion of the emf that is developed across one of the magnet coils being applied in opposition to the output of the 6-volt storage battery used to energize the amplidyne field. The amount of voltage thus fed back determines the total current in the magnet coils and compensates for changes in the current. Because of the capacitor network, essentially all the rapid fluctuations in generator output are applied back to the amplidyne control coil. Also, since there is considerable inductance in the magnet coils, the feedback tends to lead the change in current in the coils and to diminish the change in magnetic field. The over-all current gain of the amplidyne generator combination was measured to be 4×10^4.

Since the time constant of the system is large, there are changes in the field that the passive network cannot correct. These changes, however, can be corrected by the addition

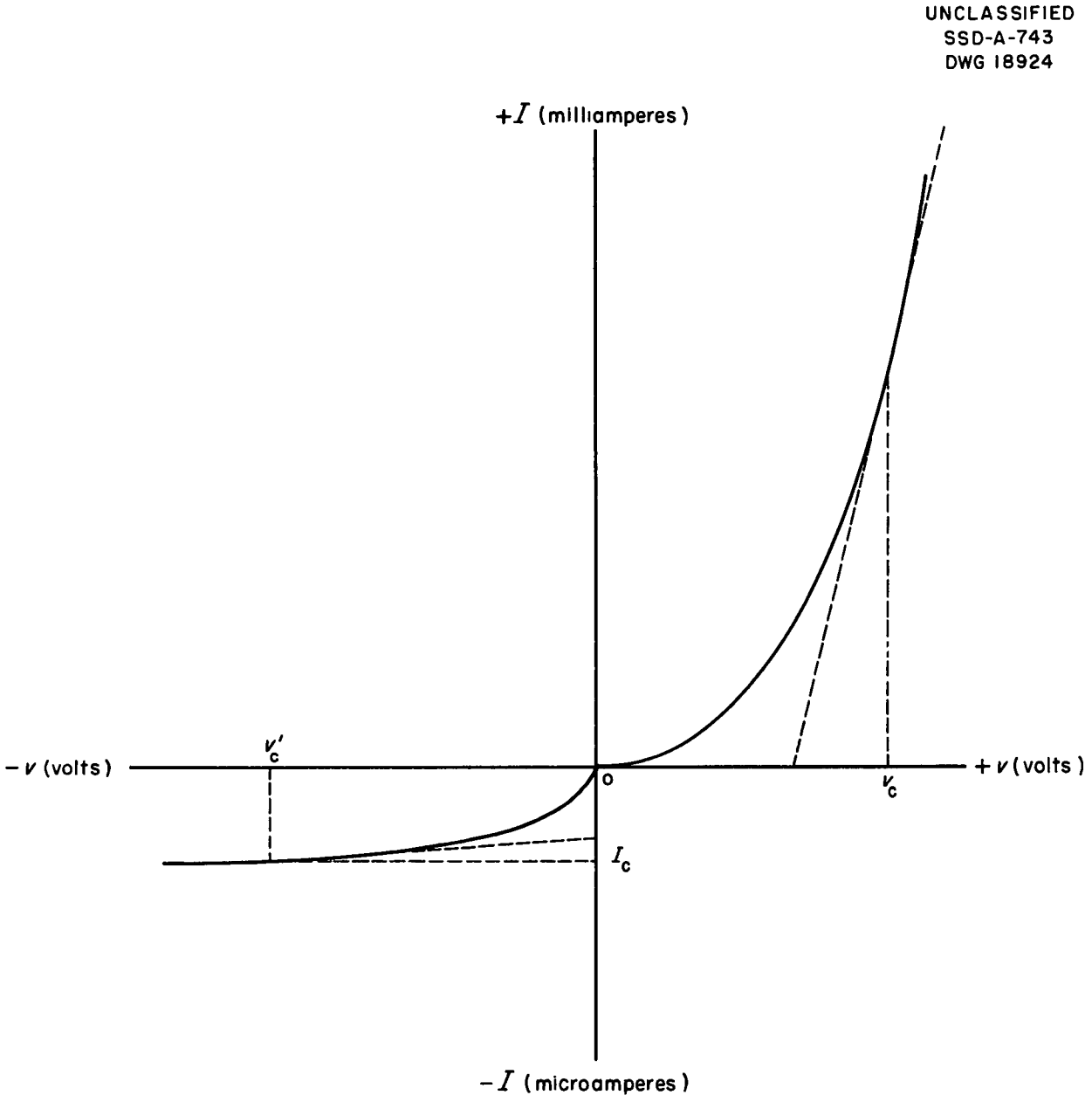

Fig. 30. Typical Semiconductor Rectifier Volt-Ampere Curve.

UNCLASSIFIED
SSD-A-702
DWG 18242A

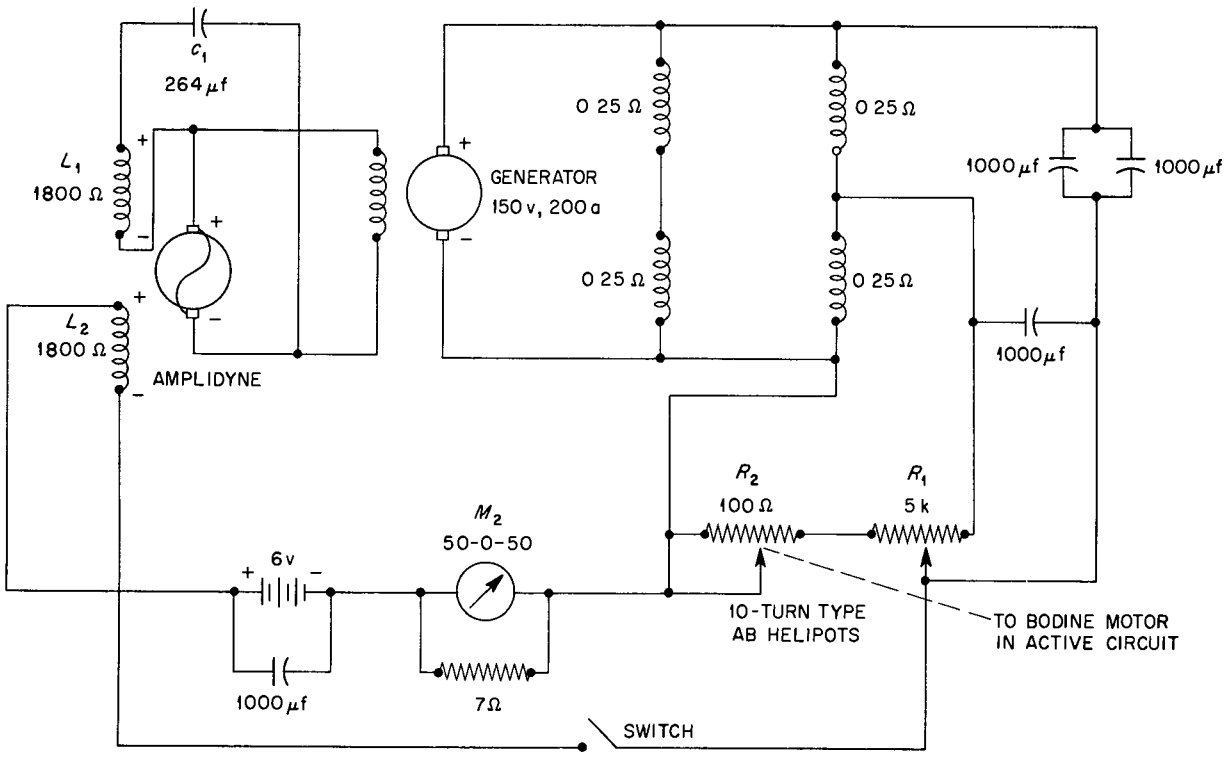

Fig. 31. ADL Magnet-Field Control, Passive Circuit.

of a compensating current in the control coils provided in the magnet.

A germanium plate, with a Hall coefficient and resistivity that are essentially temperature independent in the range of −78°C, is placed between the poles of the magnet in a Dewar flask that contains dry ice. A 10-ma current is supplied by a G-E constant-current source of the type used as a potentiometer power supply. The voltage, E_H, developed across a germanium plate of thickness t and Hall coefficient R, when the plate is placed in a field H and a current I is sent through the plate, is given by

$$E_H = \frac{RIH \times 10^{-8}}{t} .$$

For the plate used, the relationship between a change in magnetic field and a change in Hall voltage is

$$dE_H = 2 \times 10^{-6} \cdot dH .$$

The difference between the Hall voltage and a previously set reference voltage is applied through an RC network to the input of a Brown Electronic amplifier (Fig. 32). The pulsating output from the Brown amplifier controls a magnetic amplifier, the output of which is rectified, filtered, and applied to the magnet-control coils (Fig. 33).

The operation is as follows From previous calibration, the required voltage for any field is known. The desired reference voltage is set by use of a type-K2 potentiometer. The switches in the active circuit are closed. The motor-generator is turned on. The switch in the passive circuit (Fig. 31) is closed, and R_1 is adjusted

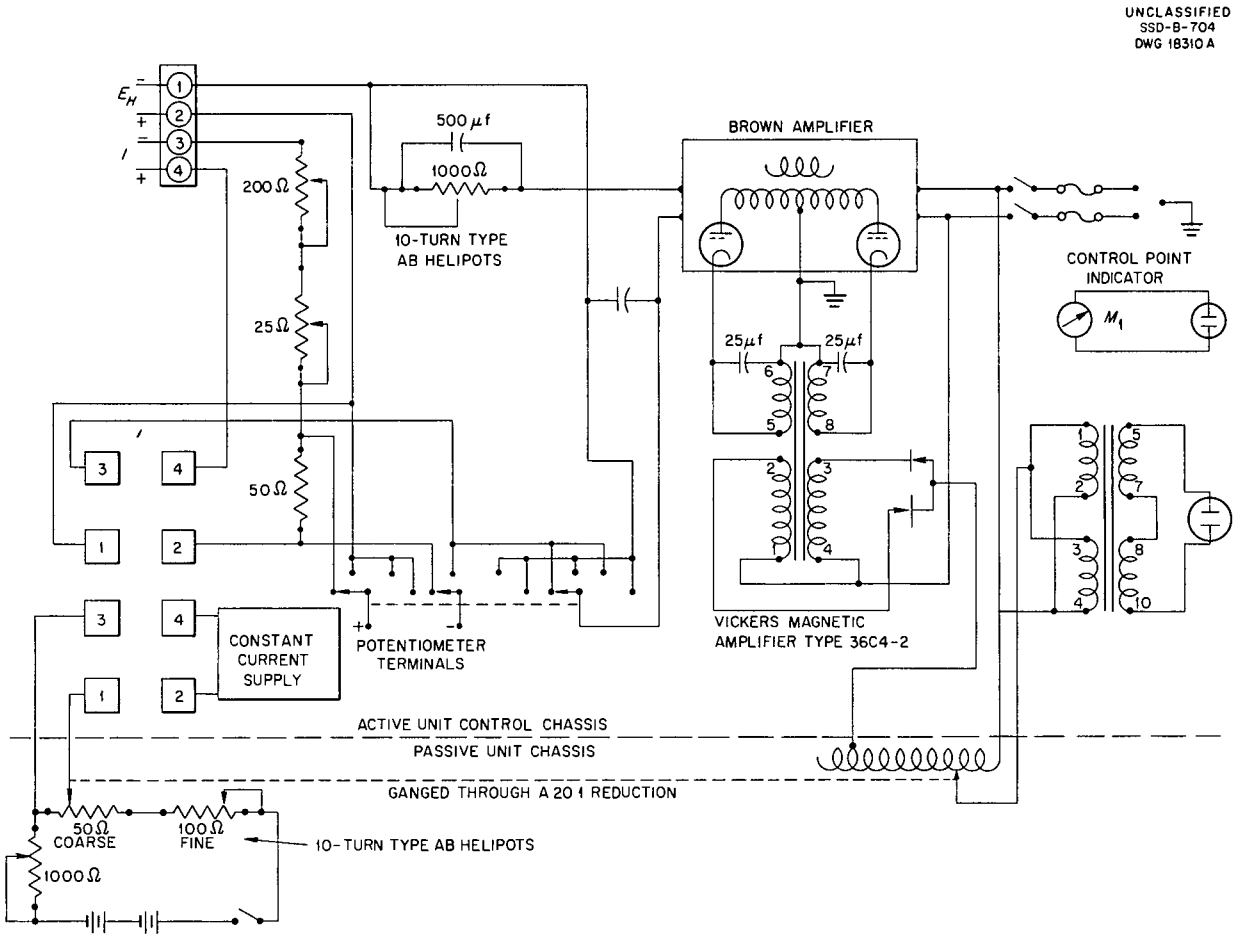

Fig. 32. ADL Magnet-Field Control, Active Element Control Circuit.

until M_1 (Fig. 32) is centered. The control circuits are then in operation.

In case drifts in the system cause the active circuit (Fig. 33) to saturate because the required output is either too high or too low, RL_1 or RL_2, as the case may be, will actuate a motor that adjusts a fine control, R_2, in the passive network (Fig. 31) and thus recenter M_1 (Fig. 32).

MAGNETIC SUSCEPTIBILITY OF GERMANIUM

D. K. Stevens

The program for developing and calibrating the equipment for determining the magnetic susceptibility of germanium continues and appears to be in its final stages. The copper-constantan thermocouples built into the liquid-nitrogen cryostat have been calibrated to 0.1°C at the liquid oxygen, dry ice, and ice points. Installation of a smaller coolant pump has resulted in the level of vibration being lowered below that which disturbs the balance when it is mounted on the magnet. A description of field-control devices installed during this quarter appears elsewhere in this report. These control units appear to hold the field constant to better than 0.05%, as is indicated when the balance is acted upon by the Gouy force exerted on an 0.008-in.-dia platinum wire suspended into the field. The reproducibility of a given field appears to be of the same order of magnitude.

The sensing element in the field control is an N-type germanium plate

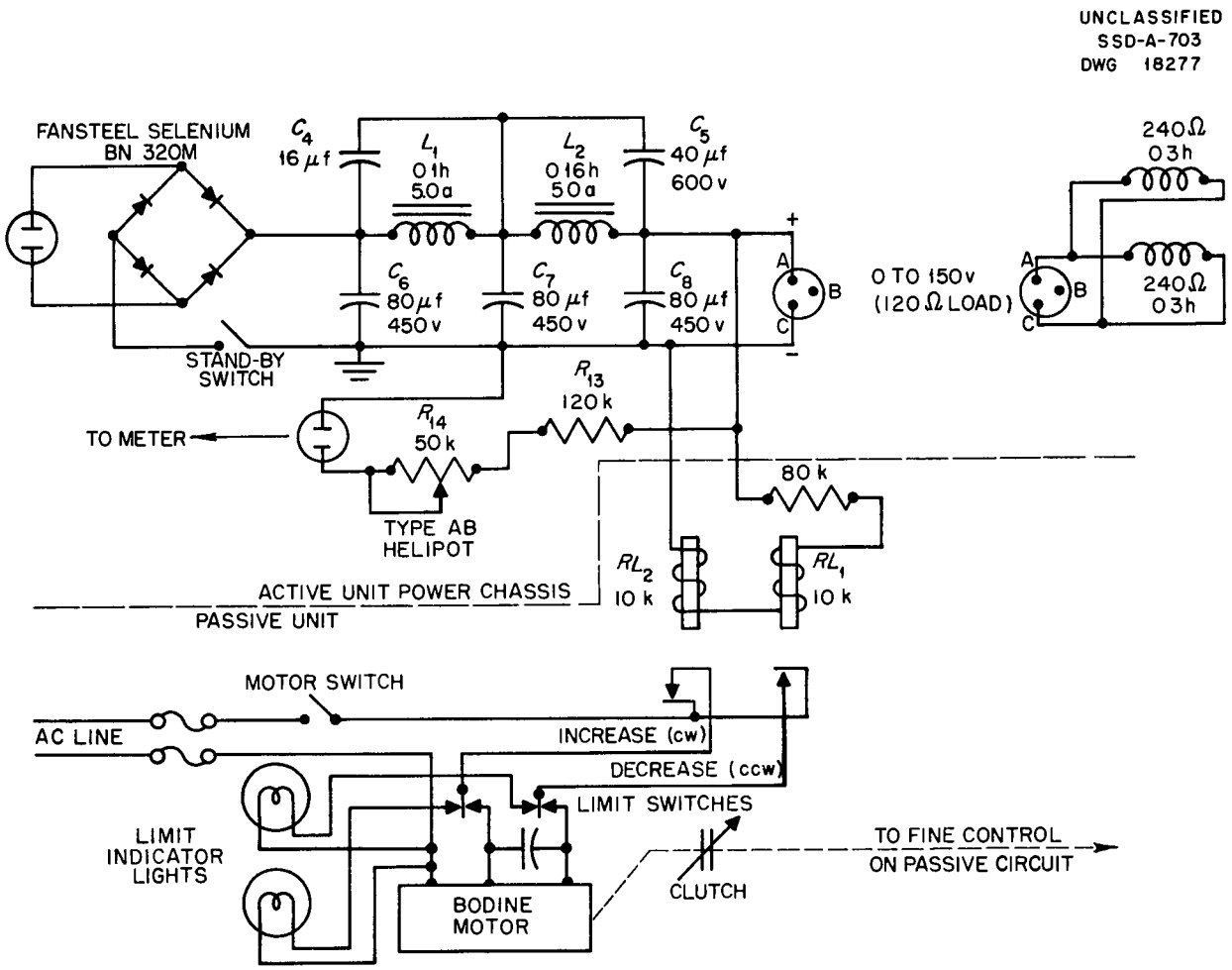

Fig. 33. ADL Magnet-Field Control, Active Control-Power Unit.

that has a resistivity of 3 ohm-centimeters. In the course of work on the control, it was noticed that the electrical resistance of the plate was strongly dependent upon magnetic field and that it changed from 125 ohms to approximately 154 ohms when the plate was placed in a magnetic field of approximately 22 kilogauss at room temperature.

One "dry run" has been made with the equipment on a 7.5×10^{-3} ohm-cm, N-type germanium cube in the range from room temperature to that of liquid nitrogen. Since corrections for ferromagnetic surface impurities were not made, the results will not be reported at this time. However, data that were self-consistent within 0.1% were obtained.

Samples will be suspended from the balance on 0.001-in.-dia molybdenum wire, and will thereby eliminate the need of a suspension correction to the data. The Gouy force on such a wire is less than 1 μg under the chosen conditions.

In order to eliminate problems of tedious positioning of samples in the field, of sample geometry, and of variation of $H\ \partial H/\partial Z$, the effective value of the latter quantity is determined at each measurement. When the sample is suspended in oxygen and in a

vacuum, the difference in forces acting upon the sample is related to the volume of the sample, volume susceptibility of O_2, and the value of $H\ \partial H/\partial Z$ by

$$F = V_s\ K_{O_2}\ H \frac{\partial H}{\partial Z}$$

Thus it is possible to determine $H\ \partial H/\partial Z$ for each suspended sample to the absolute accuracy to which the susceptibility of oxygen is known. Although the absolute accuracy to which the susceptibilities of other materials may be measured by this method is limited to the same degree, relative measurements do not suffer from this restriction.

RADIATION EFFECTS IN IONIC CRYSTALS

C. M. Nelson

A number of ionic-conductivity experiments have been completed on radiation-colored potassium chloride crystals at temperatures that range from 25 to 280°C. Annealing studies were made at constant temperature in an effort to establish the order of the annealing process. It appears that the situation is complicated and that several processes take place in the temperature range. In attempts to separate the different processes, it was observed that unirradiated potassium chloride crystals undergo some annealing when they are heated in vacuum at these temperatures. Since the latter effect was not noticed until the end of the period, the interpretation of this unexpected behavior and its effect on the previous results cannot be given yet.

The essential parts of the ionic-conductivity apparatus[5] used in the studies are shown in Fig. 34. Two 6-volt dry cells are used to give a

[5] C. M. Nelson, *Solid State Quar. Prog. Rep. Nov. 10, 1952*, ORNL-1429, p. 48.

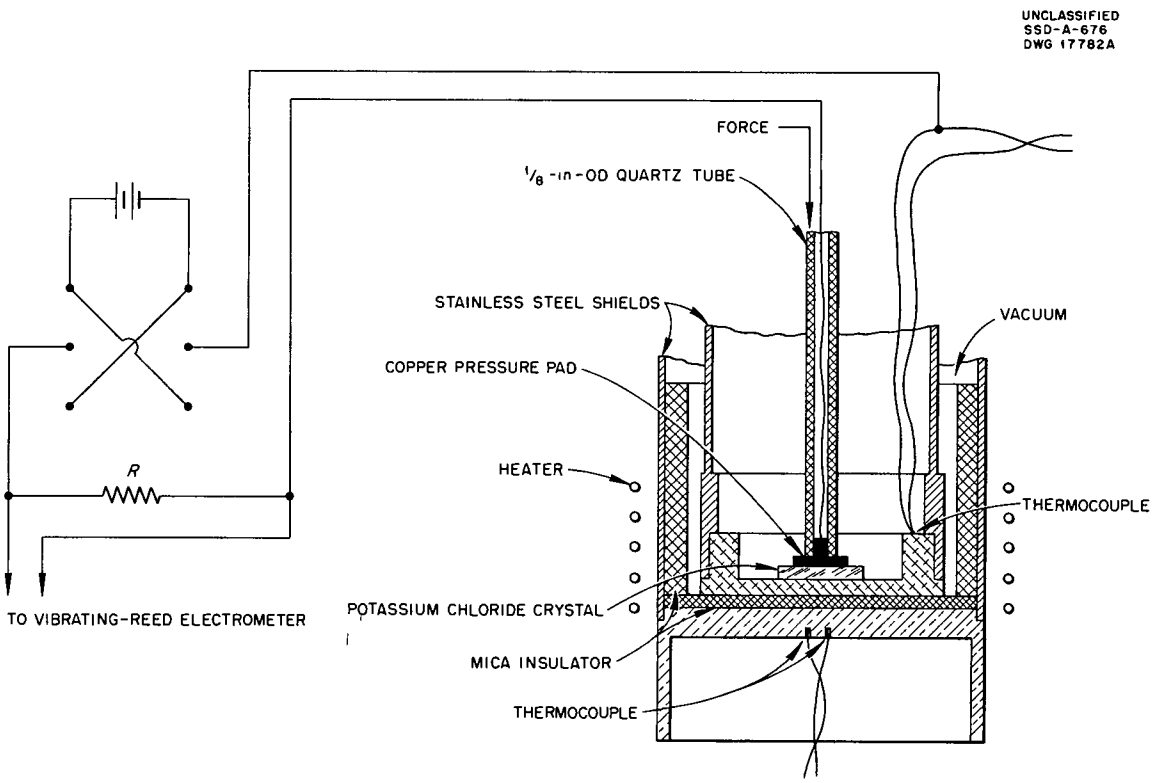

Fig. 34. Ionic Conductivity Apparatus.

potential of 12 volts across the crystal. The resistance, R, may have values of 10^8, 10^{10}, or 10^{12} ohms for these experiments.

Two typical plots that show the variation of conductivity with temperature for reactor-irradiated and Co^{60}-irradiated potassium chloride are given in Figs. 35 and 36. The dashed lines indicate that annealing is taking place. Unirradiated specimens with no color centers present yield a straight line over the entire temperature range. The over-all behavior of the ionic conductivity, σ, for potassium chloride after irradiation is in agreement with that obtained with a different apparatus and presented in a previous report.[6] Gamma irradiation reduces σ, presumably by reducing the number of effective potassium ions (K^+) by trapping holes in them. Long neutron irradiation enhances σ, presumably by creating K^+ vacancies. These qualitative conclusions will not be changed by the results of the annealing studies on unirradiated crystals, however, the studies are important in analyzing the kinetics of the annealing processes.

[6] R L Sproull and R S Caswell, *Solid State Quar Prog Rep Aug 10, 1952*, ORNL-1359, p 40

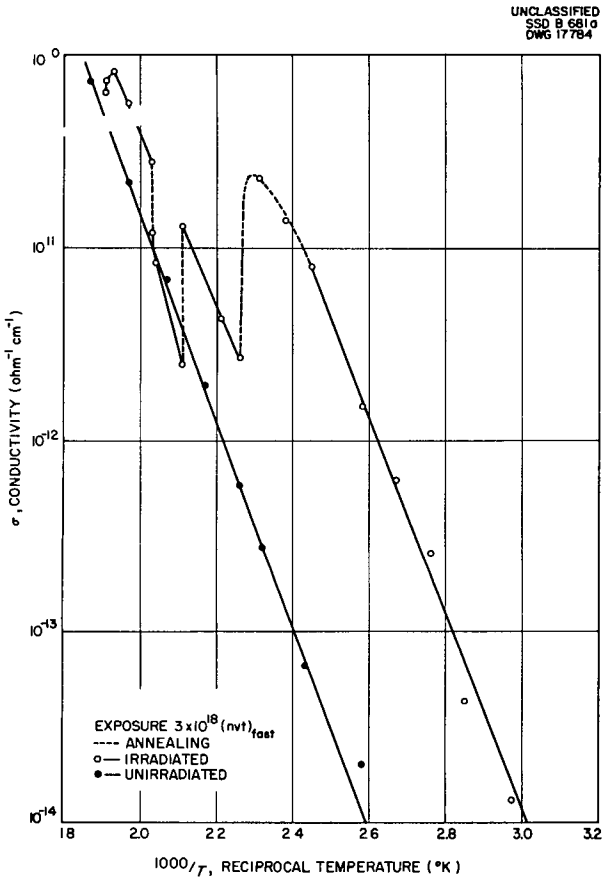

Fig. 35. Variation of Conductivity with Temperature for Reactor-Irradiated Potassium Chloride.

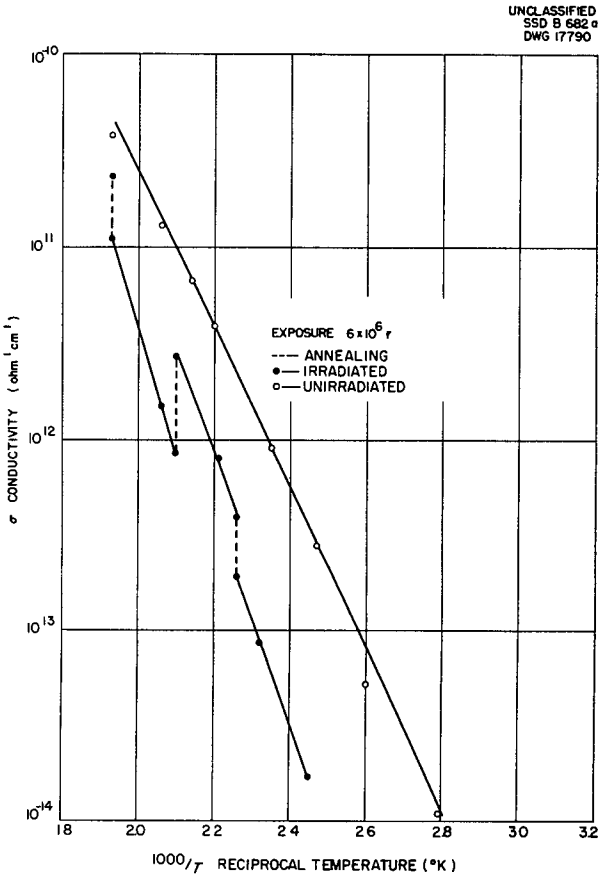

Fig. 36. Variation of Conductivity with Temperature for Co^{60} Irradiated Potassium Chloride.

ENGINEERING PROPERTIES

RADIATION STABILITY OF PLASTICS AND ELASTOMERS

C. D Bopp R. L. Towns
O. Sisman W. K. Kirkland

In order to determine the effect of radiation-intensity level on the amount of damage produced, elastomers were irradiated by a Co^{60} and by an Au^{198} source. The Au^{198} source gave a dose of 10^4 rep/hr, and the Co^{60} was used at appropriate distances in the canal to give intensities of the order of 10^6, 10^5, and 10^4 rep/hr. The average energy from Co^{60} is 1.25 Mev, and that from Au^{198} is 0 41 Mev Elongation was chosen as the property for study because it is very sensitive to radiation and therefore short exposure periods may be used. The results thus far are very preliminary, and the only conclusions that can be drawn are that, within a factor of three, there is no dependence of damage on dose rate or energy within the range studied.

The levels of intensity were measured by ionization chambers for which the calibration was calculated theoretically In order that the chambers could fit into a small irradiation space, the ionization chamber for measuring the Au^{198} radiation[1] was made rectangular in shape, with less spacing between electrodes than that in the chamber for Co^{60}, the chamber for Co^{60} was cylindrical. In both instances, a central electrode was 300 volts negative to the outside of the chamber, which was grounded. The chamber for Co^{60} was filled with argon at twice atmospheric pressure. The calculated calibration for a chamber similar to the chamber for Co^{60} checks dosimeter readings within 5% at a level of intensity of 10^3 rep/hr. The chamber for Co^{60} gives readings that are in agreement with a dosimetric method that employs the radiation-induced oxidation of Fe^{++} [2] Comparative measurements show agreement between the calculated calibrations of the chamber for Au^{198} and the chamber for Co^{60} at a level of intensity of 10^4 rep/hr Each chamber was placed, one at a time, in the same position in an air-filled pipe located in the canal. The location was 3 ft from the Co^{60} source and gave a level of intensity of about 10^4 rep/hr. It is planned to vary the voltage between the electrodes of the chambers at the 10^6-rep/hr level of intensity to determine whether the recombination of ions that occurs at the 300-volt operating voltage is sufficient to alter the calculated calibration.

The attack of ozone on most elastomers has always been a troublesome reaction, and is not well understood. It is known, however, that rubbers are damaged by ozone when in the stressed condition, but are unaffected when not stressed Ozone causes cracks to form in the surface of stretched rubber, and relieves the strain caused by stretching so that the material does not return to its original shape. Both the number of the cracks and the depth of the cracks are a function of ozone concentration and exposure (with the air circulation and elongation held constant). Because of merging of cracks, it is more accurate to estimate the extent of the damage by measuring the depth rather than the number of cracks.

Since ozone is formed in air in a radiation field, it is desirable to know the extent of damage by ozone, as well as radiation, on stressed rubbers that are irradiated in air A few preliminary tests have been made

(1) C D. Bopp, O Sisman, R. L Towns, and W K Kirkland, *Solid State Quar Prog Rep Aug. 10, 1952*, ORNL-1359, p 41

(2) C J Hochanadel, *J Phys. Chem* **56**, 587 (1952)

on a natural rubber formulation, and the results are shown in Fig. 37.[3] Specimens *a* and *b* show the cracking indicative of ozone attack on the sample that was stressed and irradiated in air. The circulation of air in the cans in which the rubber was irradiated is probably small, but it is apparently important since there is no attack on the side of the specimen that is partly shielded by the stretching jig. The concentration of ozone in the laboratory atmosphere was not sufficient to cause appreciable attack upon specimens that were stressed but were not irradiated (specimen *c*). No attack could be detected by measuring the depth of the cracks on specimens that were stretched and irradiated in a container filled with helium instead of circulating air during irradiation.

The generation of heat resulting from internal friction in synthetic rubber tires is an important consideration in design. It is planned to use a vibrating-reed method to study the effect of radiation on the dynamic properties of elastomers.[4] The frequency-amplitude relationship will be measured; then the dynamic modulus and the losses may be calculated.

(3) Compositions of rubber formulations are given in *Physics of Solids Institute Quar. Prog. Rep. April 30, 1951*, ORNL-1095, p. 96.

(4) A. W. Nolle, *J. Appl. Phys.* **19**, 753 (1948).

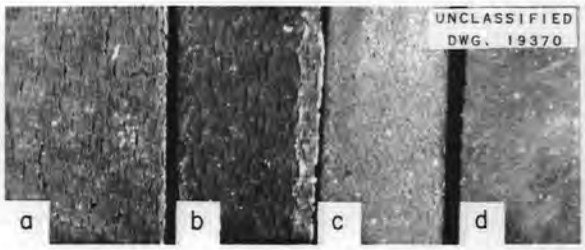

Fig. 37. Ozone-Induced Cracking of Natural Rubber Stressed During Irradiation. 10X.

a Stretched 25%, irradiated for exposure of 0.6×10^{18} nvt.

b Stretched 25%, irradiated in air for an exposure of 0.1×10^{18} nvt.

c Stretched 25%, not irradiated, exposed to laboratory atmosphere for same period as *a* was irradiated.

d Not stretched, but irradiated in air for same period as *a*.

CRYSTAL PHYSICS

DEFORMATION OF COPPER SINGLE CRYSTALS AT 300 AND 78°K

T. H. Blewitt R. E. Jamison
R. R. Coltman J. K. Redman

Single crystals of copper were grown from American Smelting and Refining Co. high-purity copper[1] by the Bridgman technique. From an activation analysis,[2] the results of which are shown in Table 11, it is clear that little, if any, impurity has been added during specimen preparations. The samples were grown, under high vacuum, in the shape of a standard ASTM tensile specimen. Figure 38 shows two specimens as grown in a split, AGOT-graphite mold.

The potential probes used to measure the electrical resistivity consisted of No. 36 magnet wire and were sintered to the sample. The sintering was achieved by allowing the weight of crystals to be supported by the No. 36 copper wire and then annealing the assembly at a high temperature (1030°C) for 3 hr at a pressure of 10^{-5} mm Hg, or less. The sintering technique

(1) T. H. Blewitt, R. R. Coltman, R. E. Jamison, and J. K. Redmond, *Solid State Quar. Prog. Rep. Aug. 10, 1952*, ORNL-1359, p. 47.

(2) G. W. Ledicotte and S. A. Reynolds, *Nucleonics* **8**, No. 3, 62 (1951).

TABLE 11. SEMIQUANTITATIVE ANALYSES OF IMPURITIES IN COPPER METAL

	IMPURITY (ppm)		
	Sample 175-B	Sample 182-B	Sample 182-A
Group I as Ag	<1*	<1*	<1*
Group IIa as As (As, Sc, Te, Mo, Ge)	1.5	2.0	4.5
Group IIb as Pt (Pt, Au)	0.15	0.20	0.10
Group IIc as Sb (Sb, Sn)	<0.003	<0.003	0.01
Group III as Fe (Fe, P, Ga, Zr, Hf, W, Ta, Cr, In, rare earths)	80	63	60
Group IV as Co (Co, Zn, Ni, Mn)	2.0	1.8	1.0
Group V as Ba (Ba, Sr, Ca, Mg)	<0.1	0.3	<0.1
Group VI as Na (K, Rb, Cs, Na)	200**	300**	200**

*Questionable - copper contaminated.

**Probably external contamination.

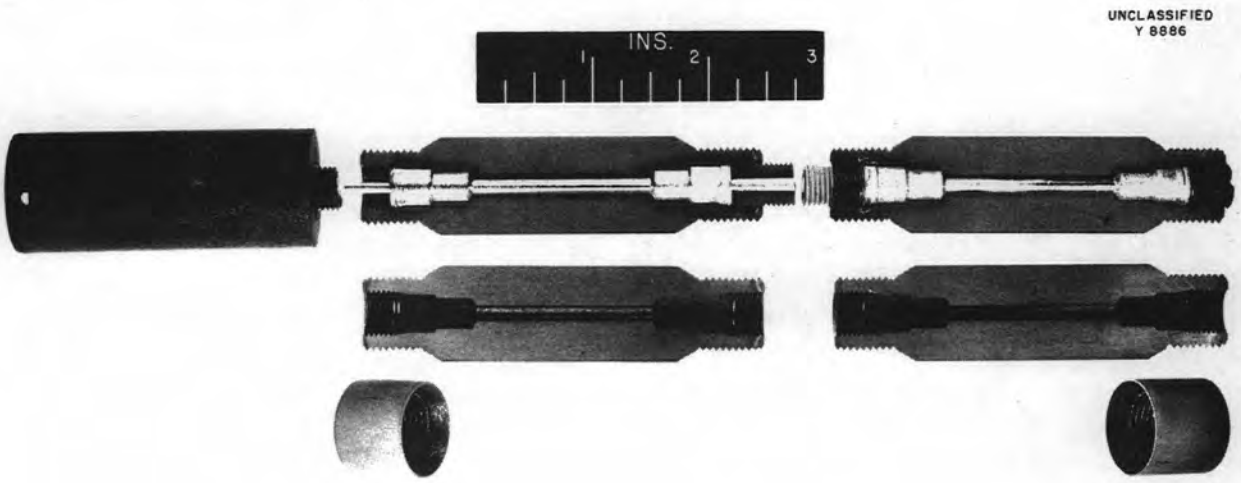

Fig. 38. Copper Single Crystals in Mold.

seemed to give a satisfactory bond, the cohesion was stronger than the wire. The sintering technique is better than welding or soldering because it reduces the possibility of the relatively fragile specimens being damaged and does not require the presence of a foreign material to secure a bond.

The samples were deformed in an Instron tensile machine. The machine was adapted for the deformation at low temperatures. In order to determine the reproducibility of data obtained by this technique, two samples of the same orientation were deformed at liquid-nitrogen temperature, and the resulting load-elongation curves were reproducible to ±1/2%. Although there is a very close agreement between the two curves, it should be noted that this does not imply that absolute values of strain are accurate to ±1/2%. When the cross-head motion is used to determine the elongation, the assumption is made that there is no deformation in the shoulders of the specimens. Determination of the elongation by direct means, compared with the results from the cross-head-motion method, indicates that shear strain is probably not in error by more than 0.04 anywhere on the stress-strain area.

Significant and somewhat surprising results of the temperature dependence of the rate of work hardening and the critical shear stress were noted. Figures 39 through 42 show the stress-strain curves of various pairs of copper crystals. In each figure the stress-strain relationships of two crystals of the same orientation are shown. One sample of each pair was deformed at 78°K, and the other was deformed at 300°K. In order to illustrate the transition from elastic to plastic strain, the stress-strain curve for both samples has been shown on an expanded scale for small strains. The curve over the entire range to the ultimate critical shear stress is also shown. In each of the figures, the points where duplex slip should occur are indicated by vertical arrows and, the points where resistance measurements were made are indicated by dashed lines.

From the data, summarized in Table 12, it would appear that the critical shear stress is independent of the temperature, at least in the region from 78 to 300°K, because (except for pair No. 182) each of the samples appears to have, within experimental limits, the same critical shear stress. In the case of the No. 182 pair of samples, No. 182B, which was deformed at 78°K, has the lower critical shear stress. It should be noted that if an activation energy were associated with deformation, the converse would be expected. It is not unreasonable that the apparent discrepancy arises, since

TABLE 12 EFFECTS OF TEMPERATURE ON CRITICAL SHEAR STRESS AND OF ORIENTATION ON THE RATE OF WORK HARDENING

SAMPLE NO	CRITICAL SHEAR STRESS (kg/mm^2)		INITIAL WORK HARDENING (kg/mm^2/unit strain)	RATIO OF CRITICAL SHEAR STRESS LATENT TO ACTIVE PLANE
	At 78°K	At 300°K		
142	0 219	0 218	12 84	0 5540
158	0 276	0 278	15 4	0 808
175	0 254	0 257	18 86	0 904
182	0 200	0 325	14 3	0 806

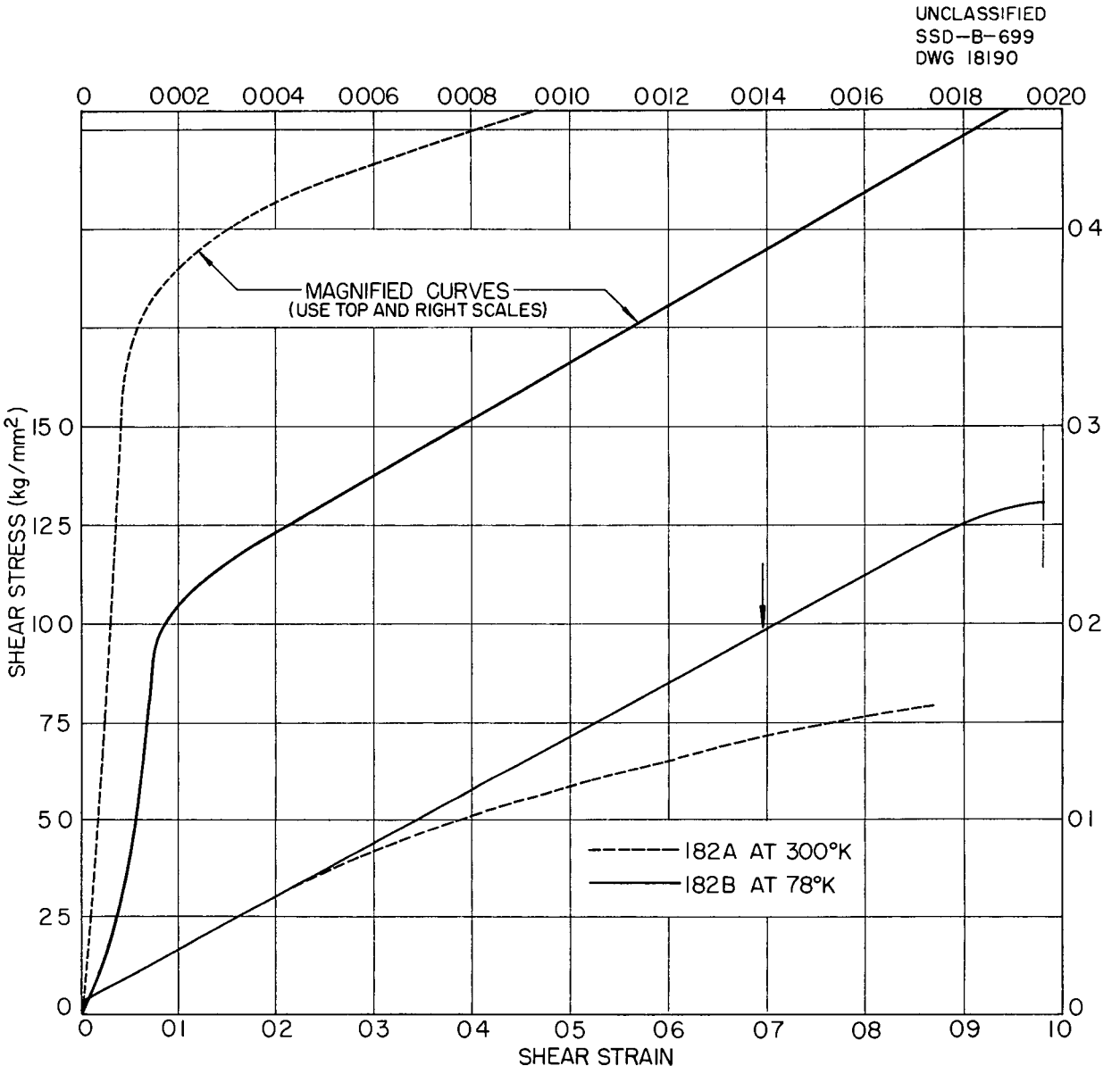

Fig. 39. Stress-Strain Curves of Copper Crystals 182A Deformed at 300°K and 182B Deformed at 78°K.

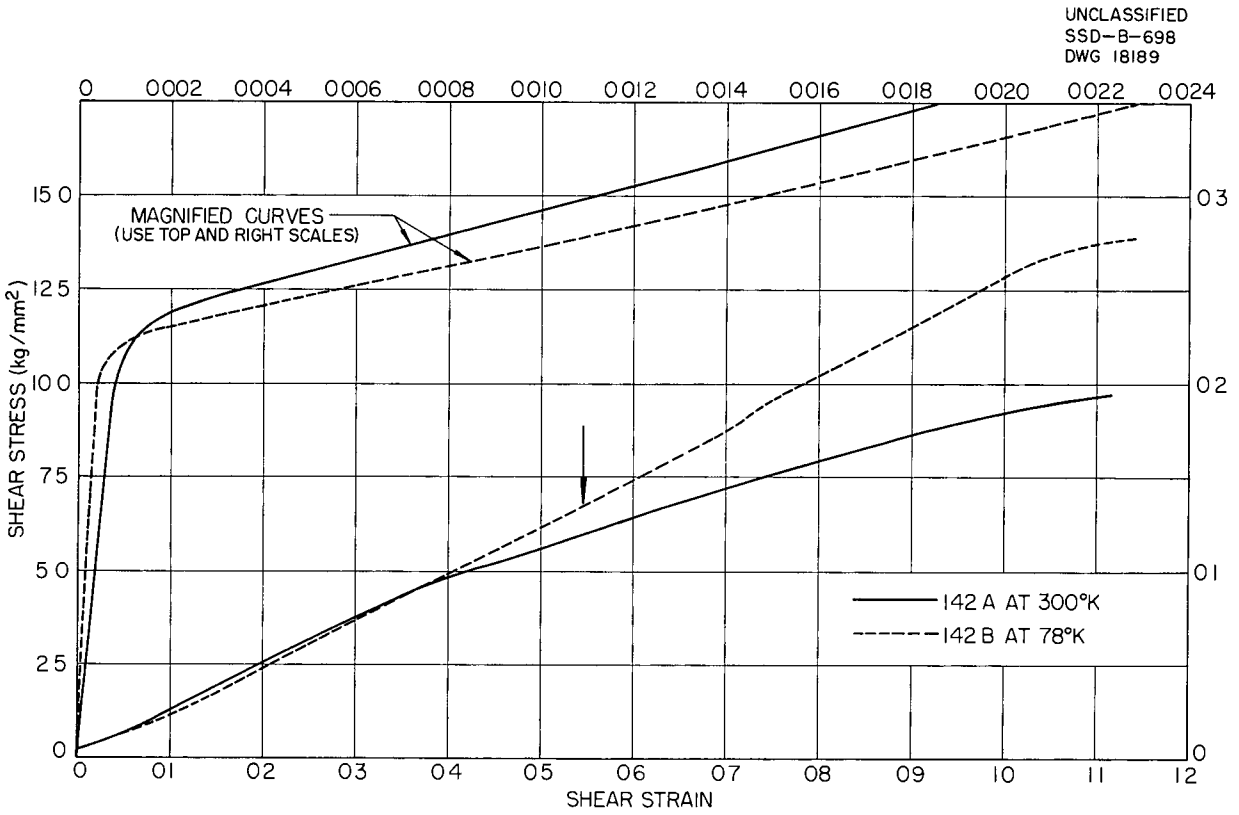

Fig. 40. Stress-Strain Curves of Copper Crystals 142A Deformed at 300°K and 142B Deformed at 78°K.

sample No. 182A was slightly deformed before the recorded deformation.

Evidence to support the viewpoint that the critical shear stress is independent of the temperature in the range from 78 to 300°K is apparent when the effect of temperature on the rate of work hardening is considered. From the data shown in Figs. 39 through 42 it is clear that the rate of work hardening is independent of temperature for shear strains less than 0.25. For strains greater than 0.25, the rate of work hardening is less at 300°K than at 78°K. The elongation at which the stress-strain curves diverge is independent of the onset of duplex slip, since the point in question occurs both prior to and after the onset of duplex slip. On the other hand, there seems to be a decided orientation effect on the rate of work hardening. When the orientation of the crystals shown in Fig. 43 and the data of Table 12 are considered, it appears that those crystals with the specimen axes nearest the dodecahedral plane have the highest rate of work hardening and the lowest ultimate shear stress and shear strain.[3]

It is reasonably clear that the critical shear stress is independent of temperature.[4] The results of

[3] G Masing and T Raffelsieper, *Z Metallkunde* **41**, 65 (1950), also reports an orientation dependence on the rate of work hardening in aluminum crystals

[4] The values reported are in close agreement with those reported by P W Neurath and J S Koehler, *J Appl Phys* **22**, 621 (1951) It should be noted, however, that even though the experimental technique was generally very different, the specimens were prepared from similar materials and in a similar manner

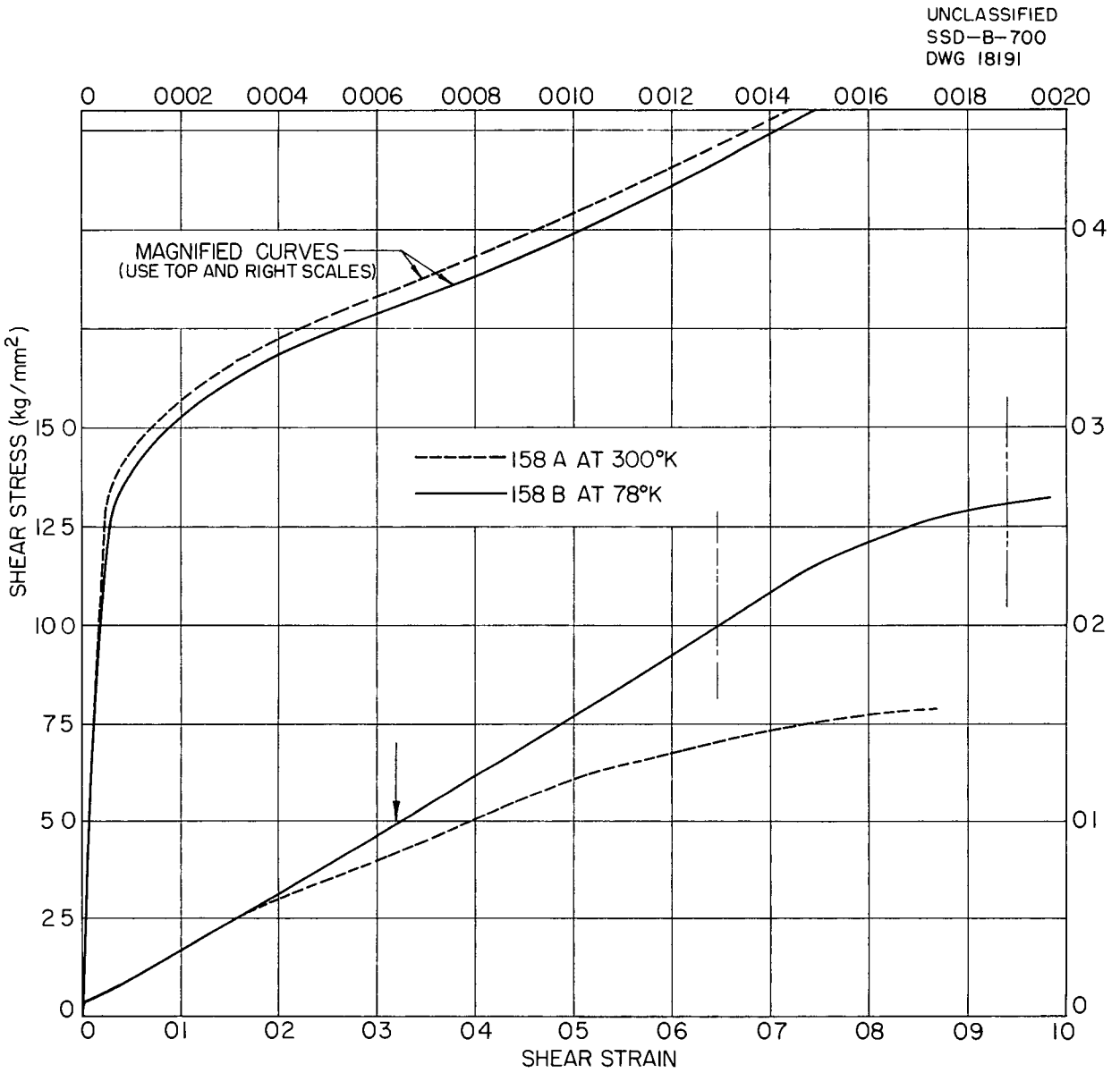

Fig. 41. Stress-Strain Curves of Copper Crystals 158A Deformed at 300°K and 158B Deformed at 78°K.

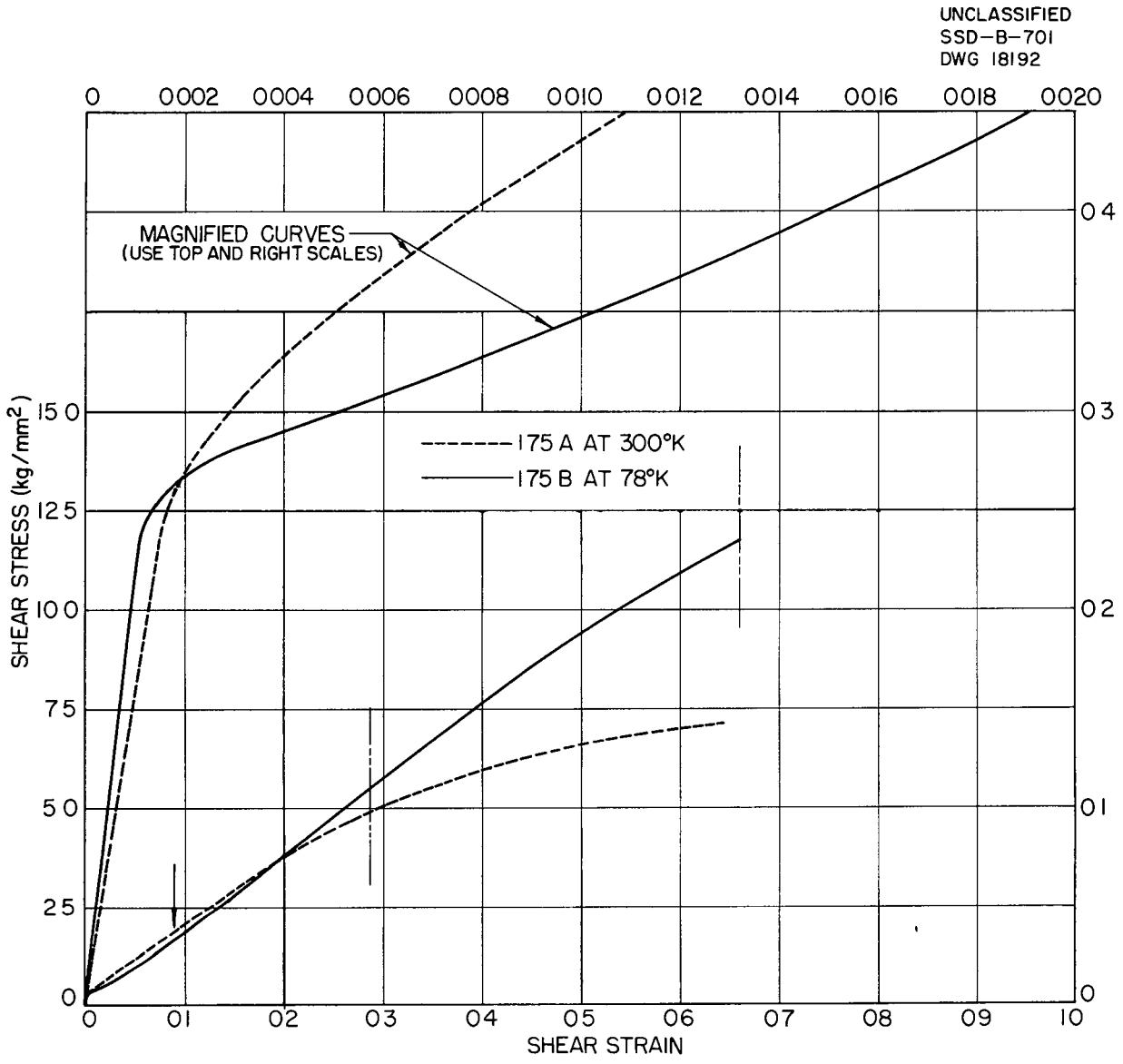

Fig. 42. Stress-Strain Curves of Copper Crystals 175A Deformed at 300°K and 175B Deformed at 78°K.

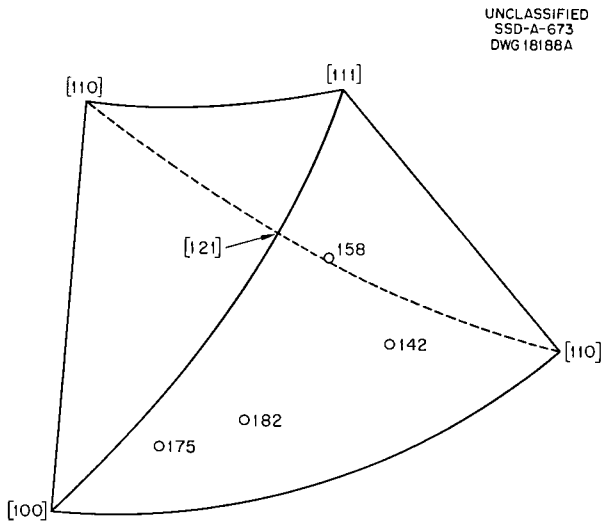

Fig. 43. Orientation of the Copper Single Crystals Before Deformation.

other investigators[5,6] seem to indicate that the critical shear stress has a definite dependence on temperature for both hexagonal and cubic metals. In fact, some effort has been made by Andrade[6] and by Kochendorfer[7] to explain the apparent temperature dependence. More recently, Mott,[8] by using the concept of the Frank-Read[9] spinning dislocation, has pointed out that only a slight temperature effect that is directly proportional to the temperature dependence of the bulk modulus for pure and annealed metals should be expected. Mott has further pointed out that impurity atoms would cause a hardening that would result from the formation of a Cottrell atmosphere in the vicinity of Frank-Read generators. This hardening is strongly temperature dependent[10] and the results of earlier investigators may have been the result of impurities. Experimentally, a strong temperature effect that seems to support the above viewpoint in some degree has been observed on the critical shear stress of reactor-irradiated copper crystals and MS 80 alpha-brass crystals.[11]

Electrical resistivity of the samples was determined by the potential-drop method.[1] All measurements were made while the sample was in the tensile machine. The samples were loaded in the tensile machine, then cooled in a bath of boiling nitrogen and plastically deformed. The load was then released, a 15-lb load was retained to ensure good electrical contact. The resistance was measured, the load released, and the sample allowed to warm to about 300°K. Following a 16-hr anneal, the samples were again cooled to 78°K, a tensile load of 15 lb was placed on the sample, and the resistance was again measured.

The data pertaining to the recovery of electrical resistance by annealing at 300°K are shown in Table 13. After the crystals were deformed at 78°K and annealed for 1 hr at 300°K, the electrical resistance at 78°K was reduced by an amount that is dependent on the amount of deformation. No change in resistance was apparent for strains less than 0.25. The recovery of the resistance is apparently not associated with the recovery of hardness because when the sample was reloaded at 78°K, an increase rather than a decrease in the yield point was observed. A discontinuity of small magnitude is

(5) E Schmid and W Boas, *Plasticity of Crystals*, F A Hughes Co , London, England, 1950

(6) E N da C Andrade, *Phil Mag* **43**, 1218 (1952)

(7) A Kochendorfer, *Plastiche Eigenschaften von Krystallen*, Julius Spunger, Berlin, 1941

(8) A F. Mott, *Phil Mag* **43**, 1151 (1952)

(9) F G Frank and T Read, p 44, *Symposium on the Plastic Deformation of Crystalline Solids*, Mellon Institute, Pittsburgh, May 19,20, 1950

(10) A H Cottrell and B A Bilby, *Proc Roy Soc (London)*, **A62**, (1949)

(11) Unpublished data of T H Blewitt, R R Coltman, and R E Jamison give the following values for the critical shear stress of copper crystals irradiated for 6 x 1018 neutrons/cm^2 317 kg/mm^2 at 300°K, 4 25 kg/mm^2 at 200°K, 6 30 at 78°K, and 7 78 kg/mm^2 at 4°K R E Jamison also reports the following values for MS 80 brass crystal 1 55 kg/mm^2 at 300°K and 3 07 kg/mm^2 at 78°K

TABLE 13 EFFECT OF ISOTHERMAL ANNEALING AT 300°K ON ELECTRICAL RESISTANCE OF COPPER CRYSTALS PLASTICALLY DEFORMED AT 78°K

SAMPLE NO	SHEAR STRAIN	SHEAR STRESS (kg/mm^2)	RESISTANCE (ohms x 10^6)		CHANGE IN RESISTANCE AT 78°K (%)	CHANGE IN RESISTIVITY (ohm-cm x 10^9)
			Before Anneal	After Anneal		
49	0 20		7 99	8 00	0	0
182	0 98	14 1	24 44	22 35	8 6	17 2
175	0 28	5 5	8 51	8 48	0 35	0 7
	0 66	11 7	12 80	12 30	3 7	7 4
158	0 65	10 2	12 07	11 89	1 5	3 0
	0 94	13 4	17 43	16 48	5 5	11 0

apparent when the yield point is examined on an expanded scale. Such results are illustrated in Figs. 44 and 45, where a definite strain-aging phenomenon is apparent. The strain aging was observed only in the regions where a recovery of electrical resistance was observed. If the test were stopped, the load released, the sample warmed, and then reloaded, the small maximum and the "easy flow" region for a strain less than 0.25 did not result. Similarly, in most cases following a rest period at 78°K, the anomolous yielding phenomenon was not observed. A yielding was observed for an annealing period at 78°K when the strain was very large and approached the ultimate strain.

The low-temperature recovery of the electrical resistance of plastically deformed metals has been associated with the motion of vacant lattice sites formed by deformation.[12] From the data of Table 13, it would appear that the number of vacancies formed is not proportional to the strain. If vacancies are formed by the interaction of a moving-screw dislocation with a dislocation that lies in another plane and if the number of vacancies does not vary with the strain, it would appear that a linear relationship between the strain and recoverable resistance should result. Unfortunately, there are not sufficient data,

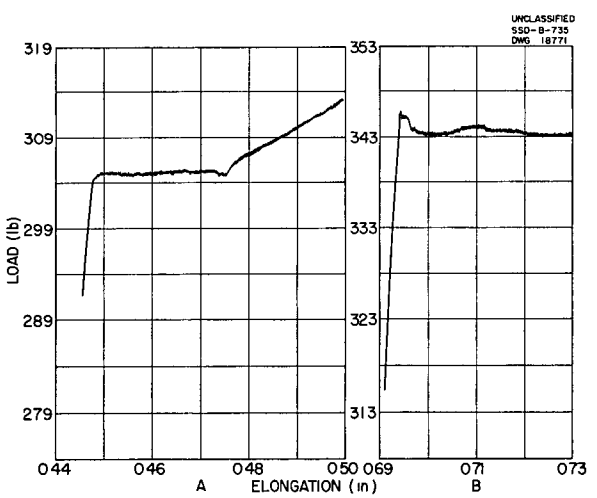

Fig. 44. Load-Elongation Curve of Copper Single Crystal Sample 158B after Reloading.

(12) This interpretation might be modified to some extent because of recent unpublished data that pertains to the reactor bombardment of disordered Cu_3Au R R Coltman and T. H Blewitt found that the defects, apparently vacancies formed by fast neutrons, failed to induce diffusion and ordering at an appreciable rate below 0°C It would appear that the activation energy for this process would certainly be no higher than that for the motion of defects in copper However, the defects that move at low temperatures in conformance with the earlier concepts will be arbitrarily termed vacancies, with the reservation that further evidence is necessary

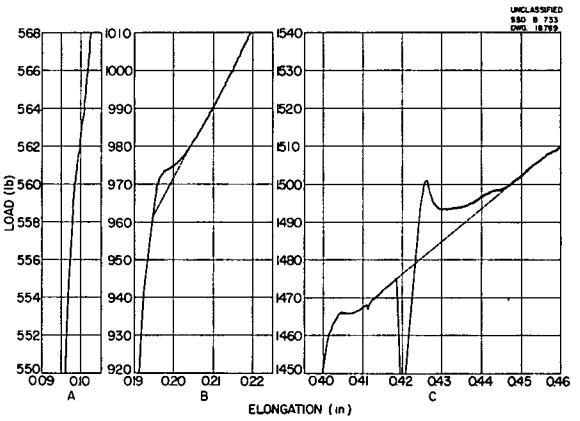

Fig. 45. Load-Elongation Curve of Copper Single Crystal Sample 200A after Reloading.

because of the orientation dependence of the stress-strain curves, for deciding the exact relationship between the strain and formation of vacancies. It is clear, however, that the recoverable resistance varies much more rapidly with the strain than the predicted linear relationship, this suggests that the distance between the generators and the barriers is not constant.

In addition, the proposal that the stress-strain relationship is dependent on the temperature might require some modification in the relatively low-temperature regions where normal self-diffusion cannot occur because it is quite apparent that the role attributed to vacant lattice sites in the hardening must be modified. If the defects have been annhilated, as perhaps is suggested by the reduction in resistance, then, following the annhilation or the motion of defects, an accompanying reduction in hardness would be expected. Instead, a small but definite increase in resistance to flow is observed, along with the characteristics associated with strain aging. It appears that the vacant lattice sites have sufficient mobility at 300°K to move to dislocations, and hardening occurs in the manner suggested by Cottrell.[13] It is tempting to assume, from the results in Figs. 39 through 42, that thermal fluctuations enable dislocations to break loose from the barriers, thus restricting their motion. It appears that the activation energy for this process is dependent on the localized stress, because a higher stress is required at lower temperatures. It may be that the mechanism proposed by Frank, which should be temperature-dependent to explain the passage of slip lines through grain boundaries, would be applicable. That is, based on Frank's work,[14] a stress concentration such as that in the vicinity of a dislocation pile-up might result in the activation of a new generator with the help of thermal energy. It is observed that the stress concentration must increase as the temperature decreases.

To confirm this theory, a pair of single crystals was deformed, one was deformed at 78°K and the other at 4.1°K. The results clearly substantiate the extrapolation to the zero point. The critical shear stress was the same in both samples, and the stress-strain curve at 4.1°K was linear so long as slip occurred, after an elongation of 75% (shear strain of about 1.50), the sample deformed by twinning, and finally fractured by cleavage after an elongation of about 120%. There was a sharp transition between slip and twinning. Thus it appears that the viewpoint that the stress-strain relationship of copper is linear at the zero point is amply demonstrated. The results are shown in Fig. 46.

---

(13) A H Cottrell, *Phys Soc (London)*, 30 (1948)

(14) F G Frank, *Pittsburgh Conference on the Plastic Deformation of Crystalline Solids*, 89 (1950)

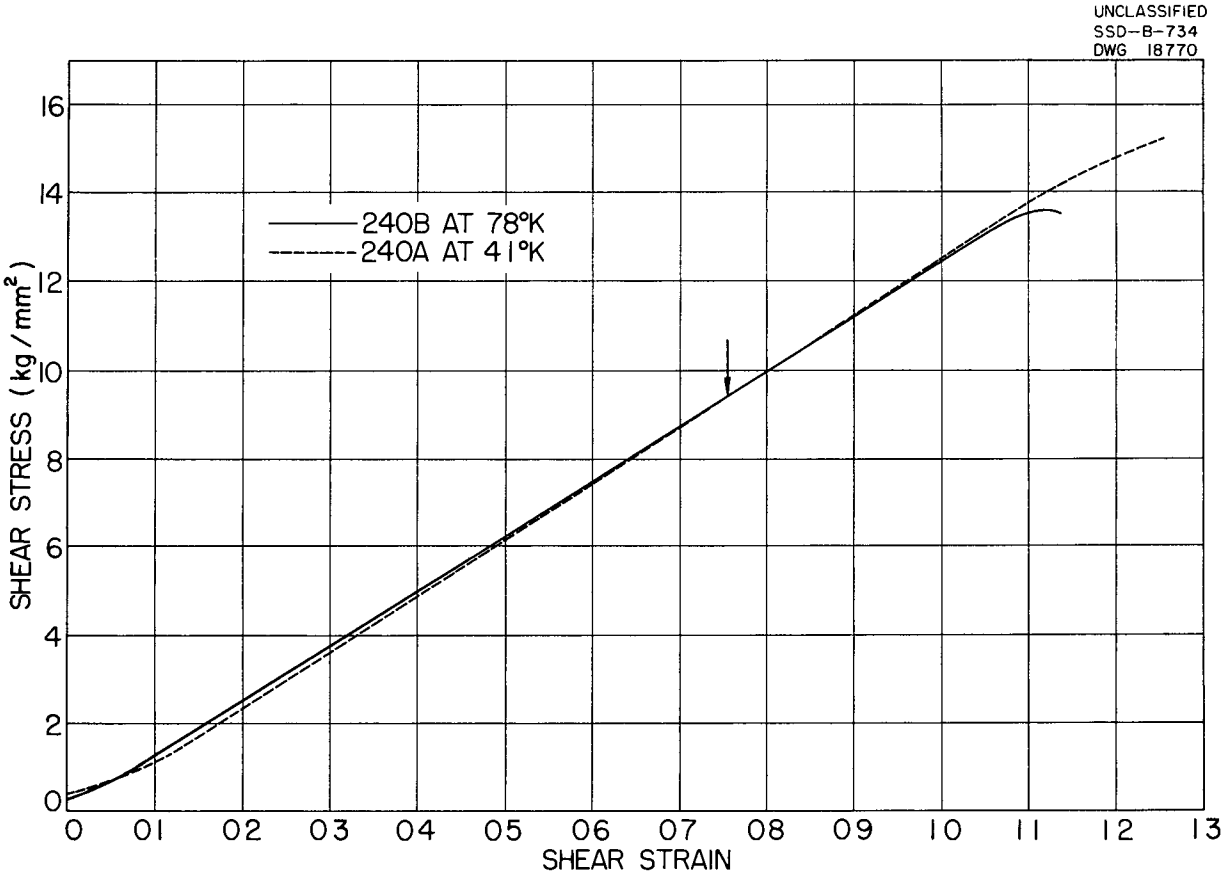

Fig. 46. Stress-Strain Curve of Copper Single Crystrals Deformed at 78 and 4.1°K.

SPECIAL PROJECTS

HALL AND MAGNETORESISTANCE EFFECTS IN METALS

R. H. Kernohan S. E. Dismuke

In the apparatus assembled by A. B. Lewis[1] during the summer of 1952, it was found difficult to obtain reproducibility of the very small magnetoresistance effect in copper because of variations in temperature of the metal being tested. To remedy this situation, a long, narrow, oil bath with a specimen holder was constructed in which the specimens could be oriented by rotating them in the bath that fitted between the poles of the ADL magnet. The oil bath has been tried and found to be partly successful. Some temperature variations remain, and new methods of decreasing the variations to less than 0.04°C will be attempted by revision of the oil-circulation system.

The wiring for the Hall and magnetoresistance apparatus has been permanently installed, and the electrical circuit is performing satisfactorily.

Several trial runs were made on the Hall-effect apparatus. Two determinations of the Hall constant for

[1] A B Lewis, *Solid State Quar Prog Rep Aug 10, 1952*, ORNL-1359, p 39

copper were made, agreement was within 3%. The average value for the constant, R, was -6.5×10^{-5} cm^3/coulomb, which agrees very well with published values.[2]

The Hall constant for beryllium-copper, one of the alloys of interest, was determined as -4.1×10^{-5} cm^3 per coulomb.

The electron mobility, μ, may be calculated from the product of the conductivity and Hall constant. From these results, μ = 38 cm^2/volt-sec for copper and μ = 4 cm^2/volt-sec for beryllium-copper.

---

[2] F. Seitz, *Modern Theory of Solids*, p. 183, McGraw-Hill, New York, 1940